

INTERMOLECULAR FORCE CALCULATIONS  
BASED ON THE EXP-6 PAIR POTENTIAL

A thesis submitted for the degree of  
Doctor of Philosophy of the University  
of London

by

Barry David Utting

of

The Department of Chemistry,  
Imperial College of Science and Technology,  
London S.W.7.

June, 1968.

Abstract

The EXP-6 pair potential has been incorporated into the cell theory of Lennard-Jones and Devonshire. The resulting EXP-6 cell model has been used in its quantum form to calculate various solid state properties of neon, argon, krypton and xenon. The appropriate values of the adjustable parameters in the pair potential are derived solely from zero point solid state data. The solution of the radial wave equation is through the WKB approximation, which has been adapted so that second derivatives of the energy levels with respect to volume may be evaluated. Similar calculations have been performed using the LJ 12:6 cell model. When calculated values of such properties as specific heat and entropy, which are considered too model sensitive to yield useful information, are ignored, the EXP-6 function exhibits some superiority in describing the solid state of argon, krypton and xenon. For solid neon, however, the LJ 12:6 function seems more suitable.

The effect of including triplet dispersion interactions in the static lattice energy on both the EXP-6 parameters and the EXP-6 solid state properties has also been investigated. For solid neon the effect of including triplet interactions is small. For the heavier inert gas solids, however, the values of the potential parameters and of the thermodynamic properties are changed appreciably by the inclusion of triplet interactions. Nevertheless, the conclusion that the EXP-6 function shows some superiority over the LJ 12:6 function in describing the heavier inert gas solids is

not altered. For all the substances considered the EXP-6 parameters derived by including triplet effects are more in line with those calculated from second virial data than are those derived from "pairwise additive" solid state calculations. For neon, argon and krypton the "triplet" parameters give better predictions of the second virial coefficient than do the "pairwise additive" ones.

Dedication

To Sue and Sarah

Acknowledgements

I should like to thank Dr. John Walkley for his guidance and encouragement in supervising the work described in this thesis during the two years prior to his emigration to Canada in 1966. I should also like to thank Dr. Neville Parsonage who kindly agreed to supervise my work on Dr. Walkley's departure. Dr. Parsonage's ready advice on a topic not directly related to his own interests has at all times been warmly appreciated.

The award of a research studentship by the Science Research Council which enabled this research to be completed and the use of the facilities of the University of London Institute of Computing Science are gratefully acknowledged.

Finally I offer special thanks to my many friends at Imperial College for making my career there a happy one and to Professor Buckingham of Bristol University for preventing my family from starving while this thesis was being written.

*B. D. Utting*

Contents

Chapter 1.	An Introduction to the Intermolecular Pair Potential . . . . .	7.
Chapter 2.	The Cell Theory as a Single Particle Model . . . . .	25.
Chapter 3.	The Quantum Cell Model and the Solution of the Radial Wave Equation . . . . .	45.
Chapter 4.	Pairwise Additive Cell Model Calculations for Solid Neon, Argon, Krypton and Xenon	66.
Chapter 5.	Triplet Interactions in the Inert Gas Solids and Some Considerations of the Second Virial Coefficient . . . . .	140.
Chapter 6.	Conclusion . . . . .	165.
References	. . . . .	169.
Appendix 1.	The Derivation of the Spherically Symmetric Cell Potential for the EXP-6 Potential . . . . .	175.
Appendix 2.	The "Exact" Finite Difference Solution of the Radial Wave Equation . . . . .	178.
Appendix 3.	The Numerical Characterisation of an n Parameter Potential Function from Zero Point Solid State Data . . . . .	181.

Contents (cont.)

Appendix 4.	Results of Pairwise Additive EXP-6 and LJ 12:6 Cell Model Calculations for Solid Neon, Argon, Krypton and Xenon . . . . .	183.
Appendix 5.	Experimental Data for Solid Neon, Argon, Krypton and Xenon . . . . .	189.
Appendix 6.	Results of EXP-6 Cell Model Calculations with Triplet Dispersion Interactions Included in the Static Lattice for Solid Neon, Argon, Krypton and Xenon . . . . .	195.
Appendix 7.	The Characterisation of an n Parameter Potential Function from Second Virial Data by Least Squares Refinement . . . . .	199.
Appendix 8.	Experimental and EXP-6 Calculated Values of the Second Virial Coefficients of Neon, Argon, Krypton and Xenon . . . . .	201.

Chapter 1An Introduction to the Intermolecular Pair Potential

The mutual potential energy of an isolated pair of molecules may be expressed as a function of their relative position and orientation with respect to one another. This function is called the intermolecular pair potential function.

This thesis is concerned solely with inert gas molecules, which are monatomic (i.e. in this case, the words "atom" and "molecule" may be used interchangeably), spherical and electronically saturated and, for these, the question of orientational dependence does not arise, so that the potential may be written as a function of only the centre to centre distance of the pair of molecules under consideration. Because of their simplicity, the inert gas molecules provide a useful testing ground for the fundamental theory of molecular interactions uncomplicated by orientation, electrostatic charge and permanent dipole effects.

There are two different lines of approach for the formulation of the pair potential. Either, with a knowledge of the physical properties of a macroscopic system we may attempt the inversion of the equations of statistical mechanics to give the pair function, or, by the consideration of an isolated pair of molecules we may attempt the derivation from first principles.



Let us consider first the interaction between an isolated pair of molecules. The mutual potential energy of a pair of inert gas molecules may be separated into two main parts:

- (1) short range repulsive forces, which dominate when electron overlap is large;
- (2) long range attractive forces, which dominate when electron overlap approaches zero.

The short range forces arise from a first order perturbation and consist of Coulombic and exchange terms. They are less well understood than the long range forces and most information as to their nature comes from the quantum mechanical study of specific interactions between electronically simple molecules. For instance, the helium-helium interaction has been widely studied (see, for example, Slater 1928, Rosen 1950, Griffing and Wehner 1955, Sakamoto and Ishiguro 1956, Phillipson 1962, Kestner and Sinanoglu 1966), but even in such a simple case as this, considerable approximations are needed to make the mathematics tractable. From calculations such as these, it seems that the short range potential energy varies in some exponential manner with distance, although, in general, the exact dependence is uncertain. For many purposes the repulsive energy is written in the highly simplified form:

$$\phi(r) = be^{-ar} \quad (1.1)$$

where  $r$  is the distance between molecular centres and  $a$  and  $b$  are constants.

The long range attractive forces are termed "dispersion" forces and arise from a second order perturbation. They were first treated theoretically by London (1930) who showed that the leading term in the dispersion energy varies as  $r^{-6}$  ( $r$  again being the intermolecular distance). This term represents the attraction of the dipole moments instantaneously induced in each molecule by the electronic motion in the other. Induced multipole interactions give rise to further terms varying as  $r^{-8}$ ,  $r^{-10}$  etc. (Margenau 1939a), but since these are small compared with the  $r^{-6}$  term, we may neglect them to a first approximation. London's expression for the induced dipole-induced dipole energy may be written as:

$$\phi(r)_{AB}^{dis} = -C^{AB}/r^6 \quad (1.2)$$

where  $C^{AB}$  is a positive coefficient, invariant to permutation of the molecules A and B, which depends on the energies and dipole oscillator strengths for the excitation of the molecules from their ground states to excited states. London approximated this coefficient by writing some of its terms as ionisation energies, but other workers (e.g. Slater and Kirkwood 1931, Margenau 1939b, Dalgarno and Kingston 1961, Bell and Kingston 1966) have calculated its value for various interactions from quantum mechanical first principles.

The theory of dispersion forces is for zero electron overlap. If overlap is allowed for in the second order perturbation, additional attractive forces called "second order exchange forces" appear

(see Margenau 1939b, McWeeny 1959, 1960, Murrell, Randic and Williams 1965, Salem 1965). Such interactions come into play at "intermediate" intermolecular separations and are most important for molecules without inner electron shells. As is the case with the short range repulsion, their evaluation is very difficult except for the simplest systems. From Margenau's calculations for helium, the second order exchange energy appears to show some sort of exponential dependence on intermolecular distance. For our purposes, however, second order exchange effects may be considered small and will not be discussed in any detail.

Let us now consider the second line of investigation, that of calculating the pair potential from the physical properties of a macroscopic system. To invert the equations of statistical mechanics to give the pair potential as an explicit function is an impracticable task and a very much simpler but more empirical approach is taken.

A pair potential function containing two or more adjustable parameters is proposed. The potential is "characterised" for the molecules under consideration by evaluating the parameters from suitable experimental data and tested by comparing values of physical properties predicted by the characterised function with experiment.

We may write the potential function for the interaction of a pair of inert gas molecules as:

$$\phi(r) = \phi(r)_{s.r.} + \phi(r)_{l.r.} \quad (1.3)$$

where  $\phi(r)_{s.r.}$  is the short range repulsive potential and  $\phi(r)_{l.r.}$  is the long range attractive potential. The function (1.3) has a minimum at some value of intermolecular distance,  $r_m$ .

Fig. 1. The mutual potential energy of a pair of inert gas molecules as a function of intermolecular distance

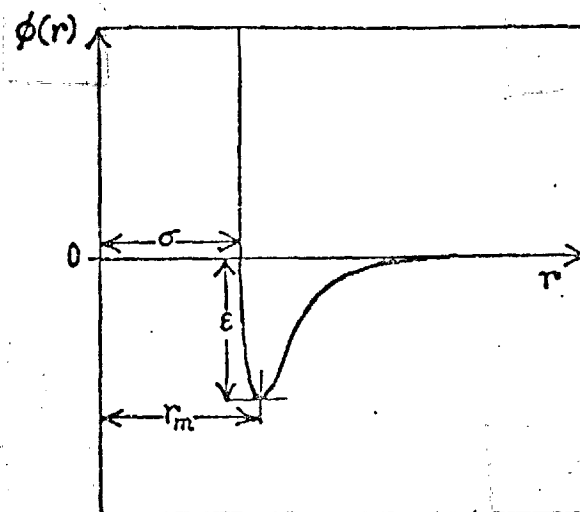


Fig. 1 is a sketch of the dependence of the pair potential on intermolecular distance given by an expression such as (1.3). Marked in the figure are:

- (1)  $\sigma$ , the value of  $r$  when  $\phi(r)$  is zero;
- (2)  $r_m$ , the value of  $r$  when  $\phi(r)$  is a minimum;
- (3)  $\epsilon$ , the depth of the potential minimum below zero.

A mathematical function suitable for the description of the inert gas pair interaction must give the general form shown in Fig. 1. The function is usually written in such a way that  $\epsilon$  and either  $\sigma$  or  $r_m$  are two of its adjustable parameters. Which of  $\sigma$  and  $r_m$  is chosen as a parameter is mainly a matter of convenience, since, for simple functions, there is

a mathematical relationship between them.

Many functions have been proposed for the inert gas pair potential. For examples of these the reader is referred to Hirschfelder, Curtiss and Bird 1954, p.31 et seq. Some of the functions are more realistic than others and some (e.g. the square well and Sutherland potentials) are gross approximations to what must be the true state of affairs. The reason for preferred use of one particular potential function rather than another is very often just mathematical expediency, especially if not too accurate results are required.

For example, the Mie-Lennard-Jones bireciprocal potential (Mie 1903, Lennard-Jones 1924) has been widely used in inert gas intermolecular force calculations, mainly because of its mathematical simplicity. It may be written as:

$$\phi(r) = C \left[ (\sigma/r)^m - (\sigma/r)^n \right] \quad (1.4)$$

where C is a constant given by

$$C = \left( \frac{m}{n} \right)^{\frac{n}{m-n}} \left( \frac{m}{m-n} \right)$$

and, in order to give the form required by (1.3),  $m > n$ .

The attractive term in this potential is in accordance with London's treatment of dispersion forces provided that  $n=6$ , but the mathematical form of the repulsion has no theoretical foundation whatever. Nevertheless, the function is very simple and lends itself to straightforward calculations of

macroscopic properties of assemblies of simple molecules.

The value of  $m$  giving the best representation of the LJ  $m:6$  potential for the inert gas pair interaction has been the subject of much discussion. For example, recent calculations by Zucker (1968 - but privately communicated to the author prior to publication) of solid state isotherms using solid state data alone to evaluate  $\epsilon$  and  $\sigma$  indicate that 12 is the best value of  $m$  for neon, argon and krypton and that  $m=11$  is most suitable for xenon. Also, calculations by Walkley and co-workers (Hillier and Walkley 1965, Jenkins and Walkley 1965) show that the use of the LJ 12:6 function gives a good picture of the solid state properties of solid argon and solid neon. These results agree with earlier ones from calculations by Corner (1948) for neon and argon, in which the potential was characterised using solid state experimental data and the best value of  $m$  was determined by predicting second virial coefficients and gas viscosities. However, they contradict the results of Horton and Leech (1963), who performed detailed calculations for the inert gas solids, neon, argon, krypton and xenon and found that 'no  $m=12$  calculation comes near to experiment'.

Other physical properties suggest other values for  $m$ . For example, Brown and Rowlinson (1960) using a thermodynamic discriminant satisfying a "Schwarz Inequality" suggest that  $m \geq 13.3$  for liquid argon near the triple point. This is in agreement with the suggestion by Rossi and Danon (1965) that a repulsion steeper than that given by  $m=12$  is necessary to account fully for the second virial coefficient

of the inert gases (see discussion of the Kihara core potential appearing on later pages of this chapter). On the other hand, the results of molecular scattering experiments performed by Amdur and Mason (1958) give repulsions considerably less steep than that given by  $m=12$ . Amdur's and Mason's values of  $m$  for the inert gases lie between 5 and 10, the "softest" repulsion being that of krypton ( $m=5.42$ ) and the "hardest" that of neon ( $m=9.99$ ). Since scattering experiments such as these are a direct measure of the repulsive energy at very small intermolecular distances where any attraction is negligible, insertion of these small  $m$  values in LJ  $m:6$  potentials cannot be expected to give reliable predictions of, for example, the solid state properties at normal pressures, which are sensitive to the region of the potential around the minimum. Indeed, substitution of  $m=5.42$  (the value for krypton) into an LJ  $m:6$  potential would lead to nonsensical results, since this gives a pair potential with the repulsion as a longer range force than the attraction, in direct contradiction to the basic and justifiable assumption that the repulsion is very short range in nature and that the attraction is reasonably long range. It is interesting to note, however, that the results of Amdur and Mason indicate that the repulsion softens considerably as very small intermolecular separations are reached.

We see therefore that the value of  $m$  giving the best representation of the inert gas pair interaction is not universal and, indeed, varies even for the prediction of different properties of the same substance. However, as we have seen, calculations

by Zucker point, in general, to a value of  $m=12$  for the best description of the solid state of the inert gases and, with  $m=12$  and  $n=6$ , (1.4) becomes:

$$\phi(r) = 4\epsilon \left[ \left( \frac{\sigma}{r} \right)^{12} - \left( \frac{\sigma}{r} \right)^6 \right] \quad (1.5)$$

which is the LJ 12:6 potential, the most commonly encountered bireciprocal function.

The LJ  $m:n$  function is a particular case of the Kihara core  $m:n$  potential (Kihara 1951, 1953, 1955). The Kihara core function is similar in form to the LJ 12:6 function, but involves a quantity  $\bar{\sigma}$ , which is the diameter of a spherical hard core situated around the centre of each molecule. It may be written:

$$\phi(r) = D\epsilon \left[ \left( \frac{\sigma - \bar{\sigma}}{r - \bar{\sigma}} \right)^m - \left( \frac{\sigma - \bar{\sigma}}{r - \bar{\sigma}} \right)^n \right] \quad (1.6)$$

where  $D$  is a constant depending only on  $m$  and  $n$  and  $m$  and  $n$  are usually assumed to be 12 and 6 respectively, as in the case of the LJ  $m:n$  function. If  $\bar{\sigma}=0$ , (1.6) becomes the LJ  $m:n$  potential, (1.4). Each term in an expression such as (1.6) may be written as a sum of terms given by the binomial expansion. The expansion of (1.6) for  $m=12$ ,  $n=6$  is:

$$\begin{aligned} \frac{\phi(r)}{D} &= \left( \frac{\sigma - \bar{\sigma}}{r} \right)^{12} \left[ 1 + 12 \left( \frac{\bar{\sigma}}{r} \right) + 78 \left( \frac{\bar{\sigma}}{r} \right)^2 + \dots \right] \\ &\quad - \left( \frac{\sigma - \bar{\sigma}}{r} \right)^6 \left[ 1 + 6 \left( \frac{\bar{\sigma}}{r} \right) + 21 \left( \frac{\bar{\sigma}}{r} \right)^2 + \dots \right] \quad (1.7) \end{aligned}$$

The Kihara core function was originally proposed to describe the behaviour of spherocylindrical molecules,



but, of late, it has found favour in the description of the spherical inert gas molecules. The attractive term in the 12:6 form is somewhat more realistic than that of the LJ 12:6 potential, in that, on expansion (see (1.7)), it gives terms in  $r^{-8}$ ,  $r^{-10}$  etc., in accordance with multipole considerations. It should be noted, however, that it also gives terms in  $r^{-7}$ ,  $r^{-9}$  etc., for which there is less theoretical justification in the case of spherical molecules, although it is known that, if the distance between two molecules is so great that retardation effects come into play, the  $r^{-6}$  dependence breaks down and the attraction varies as  $r^{-7}$  (Casimir and Polder 1948). The repulsion in the Kihara core 12:6 potential gives, on expansion (see (1.7)), a sum of terms varying as  $r^{-12}$ ,  $r^{-13}$ ,  $r^{-14}$  etc. Therefore, at small intermolecular distances, the repulsion is steeper than that of the LJ 12:6 potential, but is no less empirical as far as its mathematical form is concerned.

The hard core diameter,  $\delta$ , may be calculated in one of two ways. Either it may be considered as an adjustable parameter of the potential to be calculated from suitable experimental data - in this case the potential is a three parameter one - or it may be calculated using a formula derived by Danon and Pitzer (1962) - in this case the function is a two parameter one, as is the LJ potential.

Rossi and Danon (1965), using the latter procedure, have found that the Kihara core 12:6 function is far better than the LJ 12:6 function for the prediction of the second virial coefficient of argon, krypton and xenon over the whole temperature range

of experimental measurements, in spite of the fact that no extra flexibility is introduced by the inclusion of  $\bar{\sigma}$  as a third parameter. This work seems to indicate that a repulsion steeper than that given by  $m=12$  is required for an adequate description of the behaviour of the second virial coefficient, especially at low temperatures. Rossi and Danon also found that agreement between the value of the coefficient of  $r^{-6}$  calculated from quantum mechanical first principles and the value of the same coefficient given by the potential parameters evaluated by a consideration of the experimental second virial coefficient is far better for the Kihara core 12:6 than for the LJ 12:6 function. The corresponding values of the  $r^{-8}$  coefficient are also in fair agreement for the Kihara 12:6 potential.

On the other hand, work by Zucker (1968), which considers  $\bar{\sigma}$  as an adjustable parameter and which characterises the potential from solid state data only, shows that there is no significant improvement in the prediction of solid state isotherms when a Kihara core potential is used rather than a bireciprocal LJ form, in spite of the inclusion of the third parameter.

A function which is capable of very good predictions of the solid state properties of argon is that originally proposed by Guggenheim and McGlashan (1960) and later studied more thoroughly by McGlashan (1965). These authors took the step of dividing the pair potential into three parts:

- (1) the long range part where it is known that, to a first approximation, the function varies as  $r^{-6}$  and that the coefficient of this term is

calculable from quantum mechanics;

- (2) the part near the minimum of the curve, where the potential may be represented as an anharmonic oscillator:

$$\phi(r) = -\epsilon + k\left(\frac{r-r_m}{r_m}\right)^2 - \alpha\left(\frac{r-r_m}{r_m}\right)^3 + \beta\left(\frac{r-r_m}{r_m}\right)^4 - \dots \quad (1.8)$$

- (3) the short range part, of which the detailed mathematical form is uncertain. Guggenheim and McGlashan assumed that, since the potential in this range is very steep, it can be represented by an infinite cutoff at some value of intermolecular distance,  $d$ .

This "piece-wise" formulation of the potential is sensible from some points of view. The long range part of the function is in accordance with London's theory of dispersion forces and the formulation of the part near the minimum is perfectly general if  $\epsilon$ ,  $k$ ,  $\alpha$ ,  $\beta$ , etc. are all adjustable parameters. Guggenheim and McGlashan truncated the series after the four terms given in expression (1.8). This should give a good representation of the region of the curve near the minimum.

However, the repulsion is again highly empirical. In this case the repulsion is an even more gross approximation than that of the LJ potential. Since Guggenheim and McGlashan proposed this potential in order to predict only normal pressure solid argon properties, which are most sensitive to the region of potential around the minimum and relatively insensitive to the repulsion at small intermolecular

distances, the approximate form given by the infinite cutoff did not worry them unduly. Use of this potential for the prediction of properties sensitive to the repulsion cannot be expected to give good results, however. Also since the potential is mathematically defined only in three specific regions, parts of the potential lying outside these regions have to be guessed and, if the function is to be constructed over the whole range of intermolecular distance, the undefined parts have to be drawn freehand. As well as these points, the characterisation of the Guggenheim-McGlashan potential function requires the evaluation of six parameters. Although the use of functions involving too few parameters may place artificial restraints on the potential, the use of as many as six to predict only solid state properties confers so much flexibility that the function becomes almost "tailor made" for a specific interaction (in this case the argon-argon interaction), and using a potential form such as this makes it very difficult to say anything about the mathematical form of the general interaction between a pair of inert gas molecules.

Dymond, Rigby and Smith (1965) have forwarded the five term, two parameter function:

$$\phi(r) = \epsilon \left[ 0.331(r_m/r)^{28} - 1.7584(r_m/r)^{24} + 2.07151(r_m/r)^{18} - 1.74552(r_m/r)^8 - 0.39959(r_m/r)^6 \right] \quad (1.9)$$

as a representation of the inert gas pair interaction. This function is capable of giving a good description of the second virial coefficients and, if triplet

interactions are allowed for (see Chapter 5), of the crystal properties of neon, argon, krypton and xenon at 0°K. Once again, however, the repulsive terms in  $r^{-28}$  and  $r^{-18}$  are highly empirical. Also, Dymond, Rigby and Smith themselves admit that the five coefficients of the powers of  $1/r$  - obtained by a machine fit - have little physical meaning and that the  $r^{-24}$  attractive term is included only to give the breadth of potential well required by experiment. Nevertheless, the function does not suffer from the disadvantage of involving discontinuities and, further, contains only two adjustable parameters, thus avoiding unreasonable flexibility.

All the pair potential functions mentioned so far have the disadvantage of containing an unrealistic repulsive term. As we have seen, quantum mechanical calculations point to an exponential repulsion of some kind and, although the detailed nature of this repulsion is uncertain, it seems logical to cast it into an exponential form. With this in mind, perhaps the most realistic function which has been suggested to represent the inert gas interaction potential is that proposed by Buckingham and Corner (1947). This function may be written:

$$\phi(r) = b \exp\left[-\alpha(r/r_m)\right] - (cr^{-6} + c'r^{-8}) \exp\left[-4(r_m/r-1)^3\right] \quad r_m \geq r$$

$$\phi(r) = b \exp\left[-\alpha(r/r_m)\right] - (cr^{-6} + c'r^{-8}) \quad r \geq r_m \quad (1.10)$$

$$\text{where } b = \left[ -\frac{2}{3} + (1+\beta)cr_m^{-6} \right] \exp \alpha$$

$$c = \frac{2}{3} \alpha r_m^6 \left[ \alpha(1+\beta) - 6 - 8\beta \right]^{-1}$$

$$c' = \beta r_m^2 c$$

This is a two part potential with four parameters  $\xi$ ,  $r_m$ ,  $\alpha$ ,  $\beta$  and contains an exponential short range repulsive term in accordance with quantum mechanical indications. Also second order exchange forces are allowed for (somewhat arbitrarily admittedly) in the term  $(cr^{-6} + c'r^{-8}) \exp[-4(r_m/r-1)^3]$  and the induced quadrupole-induced dipole dispersion energy is included (in the  $r^{-8}$  term) as well as induced dipole-induced dipole energy (in the  $r^{-6}$  term). However, the gain in realism over other potentials has been accompanied by a considerable loss in simplicity and the function (1.10) is mathematically rather unwieldy.

Considerable simplification is effected by writing the potential as (see Kihara and Koba 1952):

$$\phi(r) = \frac{\alpha \xi}{\alpha - 6} \left[ \frac{6e^{\alpha}}{\alpha} \exp(-\alpha r/r_m) - (r_m/r)^6 \right] \quad (1.11)$$

which is the EXP-6 potential and involves three adjustable parameters  $\xi$ ,  $r_m$  and  $\alpha$ .  $\xi$  and  $r_m$  have their usual significance (see Fig. 1) and the value of  $\alpha$  is a measure of the steepness of the repulsive branch of the potential. This function contains an exponential repulsion and an  $r^{-6}$  attraction, both of which are quite realistic from a quantum mechanical point of view. Also the mathematical form of (1.11) is quite simple and the EXP-6 potential seems to offer the best compromise between realism and simplicity in the description of the inert gas pair interaction.

Although both terms in (1.11) are reasonable in themselves, their mathematical interaction gives rise to the appearance in the function of a spurious maximum at a small value of intermolecular distance ( $r_{\max}$ ). This is removed by writing the potential in

two parts, thus (see Hirschfelder, Curtiss and Bird 1954, p.33):

$$\phi(r) = \frac{A}{\alpha-6} \left[ \frac{6e^{\alpha}}{\alpha} \exp(-r/r_m) - (r_m/r)^6 \right] \quad r \geq r_{\max} \quad (1.12a)$$

$$\phi(r) = \infty \quad r \leq r_{\max} \quad (1.12b)$$

Generally the maximum occurs at such a small intermolecular distance that the potential is high enough on the repulsive branch for the assumption of an infinite cutoff to be valid. Indeed, for many purposes the potential energy at  $r_{\max}$  is so high that the maximum may be ignored completely. When working with the EXP-6 function, however, this anomaly should always be remembered and allowance made for it where necessary. A fuller discussion of the spurious maximum will be given in Chapter 4.

In spite of its realism and simplicity, the use of the EXP-6 potential has been rather limited in the past, mainly because calculations by Mason and Rice (1954) seemed to indicate that an exponential repulsion term predicts inert gas properties only marginally better than an inverse twelfth power repulsion.

Mason and Rice used measurements of zero point solid state properties, second virial coefficients and gas viscosities to characterise the EXP-6 function and they predicted only gas properties to test the potential. No test was made by performing detailed solid state calculations. Since the solid state data used has now been largely superseded and, for reasons which will become clear in later chapters, the use

of a mixture of solid state and gas properties to characterise and test a potential function must be viewed with some suspicion, their conclusions must be doubtful until further proof is available.

Characterisation of the EXP-6 function for the inert gases argon, krypton and xenon by a consideration of the second virial coefficient alone shows that this potential gives far better predictions of this property than does the LJ 12:6 potential (Sherwood and Prausnitz 1964). It should be pointed out, however, that the Kihara core 12:6 potential, assuming  $\bar{\sigma}$  to be an adjustable parameter, is capable of predicting the second virial coefficients of these gases to the same accuracy as the EXP-6 function (Sherwood and Prausnitz 1964) and, therefore, the better representation of the interaction may be due to the inclusion of three parameters rather than two. On the other hand, we should remember that Rossi's and Danon's work shows that the Kihara core potential, treated as a two parameter function, is also more capable of predicting the second virial coefficient of the heavier inert gases, than is the LJ 12:6. Whatever the reason for the markedly superior prediction of the second virial coefficient by these more complicated functions, there seems little doubt that a function so simple as the LJ 12:6 is not adequate for the description of this property. Nevertheless, we have seen that the LJ potential is capable of giving a fair picture of at least some of the solid state properties of some of the inert gases; and that comparison with the results given by the Kihara core shows that little improvement is apparent with this more complicated function, as far as the prediction of solid state isotherms is



concerned. However, detailed calculations of solid state properties based on the EXP-6 pair potential have not been performed and the LJ 12:6 function awaits comparison with the EXP-6 as far as its ability to predict the properties of the inert gas crystals is concerned.

Detailed EXP-6 calculations of the solid state properties of neon, argon, krypton and xenon have therefore been undertaken. Some second virial coefficient calculations have also been performed. Later chapters of this thesis describe these calculations, and present and attempt to interpret their results. Some comparison is made with results calculated from the LJ 12:6 pair function.

## Chapter 2

### The Cell Theory as a Single Particle Model

#### The many body problem

If we consider any macroscopic system, we need to calculate the system partition function before the equations of statistical mechanics can be used to calculate the thermodynamic properties of the assembly.

In the classical formulation of statistical mechanics the canonical partition function may be written:

$$Z_{NC1} = \frac{1}{N!} \left( \frac{2\pi mkT}{h^2} \right)^{3N/2} \int \dots \int \exp\{-W(\underline{R}_1, \underline{R}_2, \dots, \underline{R}_N)/(kT)\} d\underline{R}_1 d\underline{R}_2 \dots d\underline{R}_N \quad (2.1)$$

where  $m$  is the mass of each molecule in the system,  $N$  is the number of molecules present,  $T$  is the temperature,  $W(\underline{R}_1, \underline{R}_2, \dots, \underline{R}_N)$  is the potential energy of the configuration of the system represented by the position vectors  $\underline{R}_1, \underline{R}_2, \dots, \underline{R}_N$  of the molecules,  $k$  and  $h$  are the Boltzmann and Planck constants respectively and the integration is carried out over all phase space. The expression:

$$Q = \frac{1}{N!} \int \dots \int \exp\{-W(\underline{R}_1, \underline{R}_2, \dots, \underline{R}_N)/(kT)\} d\underline{R}_1 d\underline{R}_2 \dots d\underline{R}_N \quad (2.2)$$

is called the configurational integral of the system.

Using quantum statistical mechanics, the partition function may be written as the sum over states expression:

$$Z_{NQu} = \sum_j \exp\{-E_j/(kT)\} \quad (2.3)$$

where  $E_j$ , the  $j$ th energy state of the system, is given by the Schroedinger equation:

$$\sum_{i=1}^N \nabla_i^2 \Psi_j(R_1, R_2, \dots, R_N) + \frac{8\pi^2 m}{h^2} [E_j - W(R_1, R_2, \dots, R_N)] \times \Psi_j(R_1, R_2, \dots, R_N) = 0 \quad (2.4)$$

It should be noted at this point that here and elsewhere in the this thesis, unless otherwise stated, the term "quantum statistical mechanics" refers to Boltzmann statistics, which takes account of the quantum mechanical concept of energy taking discrete values, but takes no account of molecular spin, as do Fermi-Dirac and Bose Einstein statistics.

It is very difficult to elicit an real information from expressions (2.1) and (2.3) which depend on complicated potential functions depending on the co-ordinates of all the molecules of the system. Therefore, considerable simplifications have to be made before useful results can be obtained. A way of simplifying the expressions for a molecular assembly at high density is to use the cell theory of Lennard-Jones and Devonshire (1937, 1938). In its original form this theory was for classical systems interacting according to an LJ 12:6 potential. It is, however, straightforwardly extended to quantum systems (see Levelt and Hurst 1960, Hillier and Walkley 1964) and

to other potential functions, provided that they are not too complicated. In our work we extended it to the EXP-6 function.

The cell theory of Lennard-Jones and Devonshire(LJD)

The LJD cell theory formulates an equation of state and thermodynamic properties of molecular systems for which three assumptions are valid. These assumptions are:

- (1) that the volume available to the system may be divided into identical cells, each cell being occupied by one molecule;
- (2) that the centres of the cells lie on a regular lattice;
- (3) that each molecule moves independently of all others in the system.

These assumptions mean that we may write the expression for the potential energy of a system of  $N$  molecules at vector displacements  $\underline{R}_1, \underline{R}_2, \dots, \underline{R}_N$  from their cell centres as a sum of terms, each of which depends on the vector displacement  $\underline{R}_i$  of a single molecule  $i$  from its cell centre. Thus:

$$W(\underline{R}_1, \underline{R}_2, \dots, \underline{R}_N) = W(0) + \sum_{i=1}^N \overline{w(\underline{R}_i)} \quad (2.5)$$

where  $W(\underline{R}_1, \underline{R}_2, \dots, \underline{R}_N)$  is the total potential energy of the configuration,  $W(0)$  the potential energy when all molecules are at their cell centres and  $\overline{w(\underline{R}_i)}$  the change in the potential field experienced by a molecule  $i$  when it is displaced from its cell centre by a vector  $\underline{R}_i$  with all other molecules remaining at their cell centres.

Substitution of the potential energy given by (2.5) in the configurational integral (2.2) gives an expression in terms of the co-ordinates of one particle only. The configurational integral may now be written:

$$Q = \exp[-W(0)/(kT)] v_f^N \quad (2.6)$$

$v_f$  is called the "free volume integral" of a molecule and is given by:

$$v_f = \int_{\Delta} \exp[-w(\underline{R})/(kT)] d\underline{R} \quad (2.7)$$

where  $\int_{\Delta}$  denotes integration over the interior of the cell occupied by the molecule.

Use of (2.5) also allows the sum over states expression (2.3) to be written in terms of the energy levels of a single particle of the system, thus:

$$Z_{NQu} = \exp[-W(0)/(kT)] \left\{ \sum_j g_j \exp[-\lambda_j/(kT)] \right\}^N \quad (2.8)$$

where  $\lambda_j$ , the  $j$ th molecular energy level, has a degeneracy  $g_j$  and is given by the single particle Schroedinger equation:

$$\nabla^2 \psi_j(\underline{R}) + \frac{8\pi^2 m}{h^2} \left[ \lambda_j - w(\underline{R}) \right] \psi_j(\underline{R}) = 0 \quad (2.9)$$

where  $\psi_j(\underline{R})$  falls to zero when the end of the vector  $\underline{R}$  falls outside the boundary of the cell.

Therefore, the LJD cell theory, in both its classical and quantum forms, requires the formulation

of the "cell potential",  $\overline{w(\mathbf{R})}$ , which depends only on the co-ordinates of a single molecule of the system. The  $3N$  dimensional problem has now been reduced to one of 3 dimensions, but  $\overline{w(\mathbf{R})}$  is still a complicated function of all three co-ordinates of a particle in its cell and further simplification is necessary in order to make the evaluation of (2.7) and the solution of (2.9) possible.

If the lattice occupied by the cell centres is face centred cubic (f.c.c.) - the structure under normal conditions of all the inert gas crystals except helium - each molecule at its lattice point is surrounded by 12 nearest neighbours at the vertices of a dodecahedron. Lennard-Jones and Devonshire approximated the potential in this dodecahedral cell by assuming the neighbours to be uniformly distributed over a sphere centred on the lattice site of the central molecule and of radius  $a_1$ , the nearest neighbour distance.

For a spherically symmetric environment the cell potential,  $\overline{w(\mathbf{R})}$ , may be written as a function of  $|\mathbf{R}|$  ( $=R$ ) only, provided that "pairwise additivity" is assumed - i.e. that the potential field experienced by the central molecule is the sum of all pair interactions between it and all the molecules on the sphere. The "sphericalised" cell potential is given by:

$$\overline{w(\mathbf{R})} = z_1 \left\{ \frac{1}{2} \int_0^\pi \left[ \phi(\sqrt{a_1^2 + R^2 - 2Ra_1 \cos\theta}) \sin\theta d\theta - \phi(a_1) \right] \right\} \quad (2.10)$$

where  $\phi$  is the pair potential function,  $R$  is the distance of the central molecule from its lattice point,  $a_1$  is the nearest neighbour distance and  $z_1$  is the number of near-

est neighbours.

Consideration of further neighbours gives the expression:

$$\overline{w(R)} = \sum_i z_i \left\{ \frac{1}{2} \int_0^\pi \left[ \phi(\sqrt{a_i^2 + R^2 - 2Ra_i \cos\theta}) \right] \sin\theta d\theta - \phi(a_i) \right\} \quad (2.11)$$

where  $a_i$  is the distance of the  $i$ th shell of neighbours from the central lattice site and  $z_i$  is the number of neighbours in the  $i$ th shell.

For the f.c.c. lattice structure:

$$a_i/a_1 = i^{\frac{1}{2}} \quad (2.12)$$

and values of  $z_i$  have been tabulated by Kihara and Koba (1952) for  $i=1,2,\dots,65$ . For this structure, the volume,  $V$ , of a system of  $N$  molecules is related to the nearest neighbour distance,  $a_1$ , by:

$$V = Na_1^3/2^{\frac{1}{2}} \quad (2.13)$$

and the length of the side of the crystallographic unit cell (the cell constant) is given by:

$$a_0 = 2^{\frac{1}{2}} a_1 \quad (2.14)$$

The volume of a cell of the system is equal to the volume per molecule of the system. The cell radius,  $R_c$ , is the radius of the sphere whose volume is equal to the volume per molecule. By virtue of (2.13),  $R_c$  for a f.c.c. lattice is given as:

$$R_c = \left( \frac{3}{4\pi 2^{\frac{1}{2}}} \right)^{\frac{1}{3}} a_1$$

$$\text{or } R_c = 0.55267a_1 \quad (2.15)$$

Now that the cell potential depends only upon the displacement  $R$ , we may transform expression (2.7) for the free volume and the single particle Schroedinger equation, (2.9), to spherical polar co-ordinates and separate out the angular dependence to give equations depending only on  $R$ .

The classical free volume integral becomes:

$$v_f = 4\pi \int_0^{R_c} \exp\{-w(R)/(kT)\} R^2 dR \quad (2.16)$$

The upper limit of integration is  $R=R_c$  because the cell theory requires that each molecule is confined to its cell and, therefore, the furthest distance that a molecule can move from its lattice site is  $R_c$ . This upper limit is more correct than  $R=0.5a_1$ , which was used by Lennard-Jones and Devonshire in their original paper, although, at high densities, the integrand in (2.16) is effectively zero at distances greater than  $0.5a_1$ .

In the quantum mechanical formulation, the energy levels are now given by the radial wave equation:

$$\frac{d^2 S_{1,n}(R)}{dR^2} + \left[ \frac{8\pi^2 m}{h^2} \lambda_{1,n} - \frac{1(1+1)}{R^2} - \frac{8\pi^2 m w(R)}{h^2} \right] S_{1,n}(R) = 0 \quad (2.17)$$

where  $S_{1,n}(R) = R U_{1,n}(R)$ ,  $U_{1,n}(R)$  being the radial component of the wave function corresponding to quantum numbers  $l$  and  $n$ . Since  $U_{1,n}(R)$  must be finite everywhere and since each particle is confined



to its cell, the boundary conditions on (2.17) are:

$$S_{l,n}(0) = S_{l,n}(R_c) = 0 \quad (2.17a)$$

$n$  and  $l$  are the principal and azimuthal quantum numbers respectively for the eigenvalue  $\lambda_{l,n}$  and may independently take any integer value,  $0, 1, 2, 3, \dots$  etc. Each energy level is  $(2l+1)$  degenerate by virtue of the magnetic quantum number  $m$ , which may take values  $-l, -(l-1), \dots, 0, \dots, (l-1), l$  for each value of  $l$ . Thus the sum over states expression (2.8) becomes:

$$Z_{NQu} = \sum_{l,n} (2l+1) \exp[-\lambda_{l,n}/(kT)]^N \exp[-W(0)/(kT)] \quad (2.18)$$

The calculation of the equation of state and thermodynamic properties of the system is now possible provided that the integration in (2.11) may be performed for the chosen pair potential  $\phi$ . Both the integration required for the calculation of classical thermodynamic properties and the solution of the radial wave equation (2.17) in the quantum case can be carried out, but, even with the simplified cell potential, numerical and/or approximate methods need to be used. The evaluation of the  $W(0)$  term is effected by assuming pairwise additivity and performing a lattice sum over all pairs of particles in the system.  $W(0)$  may thus be written:

$$W(0) = Nw(0)/2 \quad (2.19)$$

where  $w(0)$  is given by:

$$w(0) = \sum_i z_i \phi(a_i) \quad (2.20)$$

### Reduced quantities

Before we consider the cell model in more detail, it is convenient to introduce the concept of "reduced variables", the use of which considerably simplifies many of the expressions derived in the course of intermolecular force calculations.

As we have seen in Chapter 1, the pair potential may be written in terms of a characteristic energy parameter,  $\xi$ , and a characteristic length parameter,  $d$ , which is usually one of the two quantities  $\sigma$  and  $r_m$  (see Fig. 1). The parameters  $\xi$  and  $d$  enable molecular quantities and bulk properties to be reduced to dimensionless form.

By making the transformation,  $r^*=r/d$ , the pair intermolecular distance  $r$  is reduced to the dimensionless quantity  $r^*$  and the pair potential  $\phi(r)$  may be replaced by  $\phi(r^*)$ , where the functional dependence is now upon  $r^*$  rather than upon  $r$ . Similarly,  $\overline{w(R)}$  may be replaced by  $\overline{w(R^*)}$ , where  $R^*=R/d$ .

The pair potential can be written in dimensionless form, thus:

$$\phi^*(r^*) = \phi(r^*)/\xi \quad (2.21)$$

so that the LJ 12:6 ((1.5)) and the EXP-6 ((1.10a) and (1.10b)) functions may be written in terms of reduced variables as:

$$\phi^*(r^*) = 4(r^{*-12} - r^{*-6}) \quad (2.22)$$

and

$$\phi^*(r^*) = \frac{\alpha}{\alpha-6} \left[ \frac{6e^{\alpha} \exp(-\alpha r^*)}{\alpha} - r^{*-6} \right] \quad r^* \geq r_m^* \quad (2.23a)$$

$$\phi^*(r^*) = \infty \quad r_m^* \geq r^* \quad (2.23b)$$

respectively, where  $d=\sigma$  in the case of the LJ 12:6 function and  $d=r_m$  in the case of the EXP-6 function.

Expression (2.11) may be written in reduced form as:

$$\overline{w^*(R^*)} = \sum_i z_i \left\{ \frac{1}{2} \int_0^\pi \phi^*(\sqrt{a_i^{*2} + R^{*2} - 2R^*a_i^* \cos\theta}) \sin\theta d\theta - \phi^*(a_i^*) \right\} \quad (2.24)$$

where  $\overline{w^*(R^*)} = \overline{w(R^*)}/\epsilon$  and  $a_i^* = a_i/d$ .

Reduction of the free volume integral (2.16) gives:

$$v_f^* = 4\pi \int_0^{R_c^*} \left[ \exp \left[ -\overline{w^*(R^*)}/T^* \right] \right] R^{*2} dR^* \quad (2.25)$$

where  $v_f^* = v_f/d^3$ ,  $R_c^* = R_c/d$  and  $T^* = kT/\epsilon$ .

The sum over states expression may be written in terms of reduced variables, thus:

$$Z_{NQu} = \sum_{1,n} (2l+1) \exp(-\lambda_{1,n}^*/T^*) \int_0^{R_c^*} \exp \left[ -Nw^*(o)/2T^* \right] \quad (2.26)$$

where  $\lambda_{1,n}^* = \lambda_{1,n}/\epsilon$ ,  $w^*(o) = w(o)/\epsilon$   
and  $\lambda_{1,n}^*$  is given by the radial wave equation (2.17) expressed in reduced variables:

$$\frac{d^2 S_{1,n}^*(R^*)}{dR^{*2}} + \left[ \frac{8\pi^2 \lambda_{1,n}^{*2}}{\Lambda^{*2}} - \frac{1(1+1)}{R^{*2}} - \frac{8\pi^2 \overline{w^*(R^*)}}{\Lambda^{*2}} \right] S_{1,n}^*(R^*) = 0 \quad (2.27)$$

together with the boundary conditions:

$$S_{1,n}^*(0) = S_{1,n}^*(R_c^*) = 0 \quad (2.27a)$$

$\Lambda^*$  is called the quantum parameter and is given by:

$$\Lambda^* = \frac{h}{(mc)^2 d} \quad (2.28)$$

$w^*(o)$  is given by the reduced lattice sum:

$$w^*(o) = \sum_i z_i \phi^*(a_i^*) \quad (2.29)$$

which for the LJ 12:6 function may be written:

$$w^*(o) = 4 \left[ \frac{S(12)}{a_1^{*12}} - \frac{S(6)}{a_1^{*6}} \right] \quad (2.30)$$

where:

$$S(n) = \sum_i z_i (a_i^*/a_1^*)^{-n} \quad (2.31)$$

and for the EXP-6 function:

$$w^*(o) = \frac{\alpha}{\alpha^{-6}} \left[ \frac{6e^{\alpha} R(0)}{\alpha} - \frac{S(6)}{a_1^{*6}} \right] \quad (2.32)$$

where  $S(6)$  is given by (2.31) and  $R(0)$  by:

$$R(n) = \sum_i z_i (a_i^*/a_1^*)^n \exp(-\alpha a_i^*) \quad (n=0) \quad (2.33)$$

As mentioned at the beginning of this section, bulk

properties may be expressed as reduced, dimensionless quantities. Examples of commonly encountered bulk properties expressed as reduced quantities are given below.

- (1) Volume  

$$V^* = V / (Nd^3) \quad (2.34a)$$
- (2) Helmholtz Free Energy  

$$F^* = F / (N\epsilon) \quad (2.34b)$$
- (3) Internal Energy  

$$U^* = U / (N\epsilon) \quad (2.34c)$$
- (4) Specific heat at constant volume or constant pressure  

$$C^* = C / (Nk) \quad (2.34d)$$
- (5) Entropy  

$$S^* = S / (Nk) \quad (2.34e)$$
- (6) Pressure  

$$p^* = pd^3 / \epsilon \quad (2.34f)$$
- (7) Volume expansivity  

$$\beta^* = \beta k / \epsilon$$

where  $\beta = (1/V) (\partial V / \partial T)_p$  (2.34g)
- (8) Isothermal compressibility  

$$\chi_T^* = \chi_T / d^3 \quad (2.34h)$$

where  $\chi_T = -(1/V) (\partial V / \partial p)_T$
- (9) Second virial coefficient  

$$B^* = B / (Nd^3) \quad (2.34i)$$

Reduced quantities will appear often in this thesis and will always be denoted by a superscripted star.

The sphericalised reduced cell potential,  $\overline{w^*(R^*)}$   
for the LJ 12:6 and EXP-6 functions

Use of the reduced LJ 12:6 function (2.22) as the pair potential function  $\phi^*$  in the expression for the reduced cell potential (2.24) leads to a straightforward integration if we make the transformation,  $x = (a_1^{*2} + R^{*2} - 2R^*a_1^* \cos\theta)^{1/2}$ . With this transformation, the integrands in the cell potential corresponding to the attractive and repulsive terms in the pair potential are inverse 11th and inverse 5th powers of  $x$  respectively, giving  $\overline{w^*(R^*)}$  as:

$$\overline{w^*(R^*)} = \frac{1}{R^*a_1^*} \left[ \frac{T(10)}{5} {}_{12} - \frac{T(4)}{2} {}_6 \right] - \frac{4S(12)}{a_1^{*12}} + \frac{4S(6)}{a_1^*6} \quad (2.35)$$

where  $S(n)$  is given by (2.31) and  $T(n)_m$  by:

$$T(n)_m = \sum_{i=1}^m \sum_{j=1}^m (a_i^*/a_j^*)^{(n-m+1)} \left[ (a_i^* - R^*)^{-n} - (a_i^* + R^*)^{-n} \right] \quad (2.36)$$

Expressions (2.23a), (2.23b) and (2.24) give the reduced EXP-6 cell potential as:

$$\overline{w^*(R^*)} = \frac{\alpha}{\alpha - 6} \left\{ \frac{6e^\alpha}{\alpha^2} \left[ \frac{A \sinh(\alpha R^*)}{R^*} - \frac{R(-1) \cosh(\alpha R^*)}{a_1^*} \right] - \frac{T(4)_6}{8a_1^*R^*} - \frac{6e^\alpha R(0)}{\alpha} + \frac{S(6)}{a_1^{*6}} \right\} R^*_{\max} \geq R^* \quad (2.37a)$$

$$\overline{w^*(R^*)} = \infty, R^* \geq R^*_{\max} \quad (2.37b)$$

where  $R(n)$  is given by (2.33),  $T(n)_m$  by (2.36),  $S(n)$  by (2.31) and  $A$  by:

$$A = \frac{R(0) + R(-1)}{a_1^* \alpha} \quad (2.38)$$

$R^*_{\max}$  is the reduced distance from the cell centre of the spurious maximum in the cell potential corresponding to the one at  $r^*_{\max}$  in the EXP-6 pair potential.

As we shall see later (Chapter 4), inert gas densities for which the cell model is valid give a cell potential maximum well beyond the cell radius for physically reasonable values of  $\alpha$ , and therefore can generally be ignored. Nevertheless, the reduced EXP-6 potential should properly be expressed in terms of the two parts given by (2.37a) and (2.37b).

The integration required to obtain the expression (2.37a) is more complicated than that required to derive the reduced LJ 12:6 cell potential (2.35), but is still readily effected by making the transformation,  $x = (a_1^{*2} + R^{*2} - 2R^*a_1^* \cos\theta)^{\frac{1}{2}}$ , as before. Integration by parts gives the cell potential term corresponding to the repulsive term in the EXP-6 pair function and the integrand corresponding to the attractive term is an inverse fifth power of  $x$ , as in the case of the LJ 12:6 treatment. The detailed derivation of the reduced EXP-6 cell potential is given in Appendix 1.

For some purposes it is convenient to cast  $\overline{w^*(R^*)}$  into open form by expanding it as an infinite Taylor series. Because of the sphericalisation procedure used in the derivation of  $\overline{w^*(R^*)}$ , only even powers of  $R^*$  appear in the expansion, which may be written:

$$\overline{w^*(R^*)} = \sum_{k=1}^{\infty} C_{2k}^* R^{*2k} \quad (2.39)$$

where the coefficients  $C_{2k}^*$  ( $k=1,2,\dots$ ) are functions only of nearest neighbour distance (and therefore of density) and of the pair potential parameters other than  $\sigma$  and  $d$ . Since the first term in the expansion of  $\frac{1}{2} \int_0^\pi \phi^* (a_1^{*2} + R^{*2} - 2R^*a_1^* \cos\theta) \sin\theta d\theta$  is identically

equal to  $\phi^*(a_1^*)$ , no constant term appears in (2.39). (2.39) represents the potential experienced by an anharmonic oscillator. The first term in  $R^*{}^2$  represents the harmonic contribution to the cell field and higher terms represent anharmonic contributions.

The coefficients  $C_{2k}^*$  ( $k=1,2,\dots$ ) for the LJ 12:6 and EXP-6 potentials are:

$$C_{2k}^* = 4 \left[ \frac{(2k+10)! S(2k+12)}{10! (2k+1)! a_1^{*(2k+12)}} - \frac{(2k+4)! S(2k+6)}{4! (2k+1)! a_1^{*(2k+6)}} \right] \quad (2.40)$$

and

$$C_{2k}^* = \frac{\alpha}{\alpha - 6} \left[ \frac{6e^{-\alpha} (2k-2)}{(2k)!} \left[ \frac{\alpha A}{2k+1} - \frac{R(-1)}{a_1^*} \right] - \frac{(2k+4)! S(2k+6)}{4! (2k+1)! a_1^{*(2k+6)}} \right] \quad (2.41)$$

respectively, where  $S(n)$  is given by (2.31),  $R(n)$  by (2.33) and  $A$  by (2.38).

### The cell theory as a model of the solid state

Having derived the simplified spherically symmetric cell potential for molecules interacting according to an LJ 12:6 pair potential, Lennard-Jones and Devonshire derived an equation of state by the use of classical statistical mechanics. They considered only nearest neighbour interactions in the formulation of the cell potential and for the static lattice energy term they used the expression given by Lennard-Jones and Ingham (1925), viz:

$$w^*(o) = 6(1.0109V^*{}^{-4} - 2.4090V^*{}^{-2})$$



As originally conceived, the cell theory was intended to formulate an equation of state and thermodynamic properties of the liquid and dense gas states of simple molecules. In support of this, Lennard-Jones and Devonshire found that the LJ 12:6 classical cell theory predicted the existence of both "condensed" and "gaseous" phases at low temperatures and also the existence of a critical isotherm. For substances whose intermolecular pair potential might be expected to follow a dependence such as the LJ 12:6 (e.g. the inert gases) the calculated densities and boiling points of the condensed phase were reasonably close to the experimental properties of the liquid. They were, however, even closer to the solid properties. The temperature of the critical isotherm was close to that given by experimental measurements on suitable substances, but the critical density and pressure differed considerably from their experimental values.

Barker (1963, p.56 et seq.), by a detailed comparison of the experimental properties of solid and liquid argon at and around the triple point with those predicted by the LJ 12:6 classical cell model, has clearly shown that the cell model is more properly a theory of the solid rather than of the liquid and gas states. He interprets the critical isotherm as pertaining to solid-expanded solid transition rather than to a liquid-gas transition, as originally supposed by Lennard-Jones and Devonshire, and explains (p.75 et seq.) how the applicability of the model to the solid state follows directly from the assumptions on which it is based. The conclusion that the cell model is really a description of the solid state was in fact indicated by the

later work of Lennard-Jones and Devonshire (Lennard-Jones and Devonshire 1939a, b, Devonshire 1940, Corner and Lennard-Jones 1941), who propounded an order-disorder theory of melting to explain the difference between the solid and liquid states.

Briefly, the reason we cannot apply the cell theory, as presented in this chapter, to the liquid state is that the lattice concept inherent in the cell model gives long range order in the system, a property typical of the solid, but not of the liquid, in which we expect to find short range order but long range disorder around any representative molecule. To make the picture of the liquid state more clear, let us compare the molecular behaviour of an ideal gas with that of an ideal crystal. In an ideal gas the whole volume of the system is available to any molecule in the system - the molecules are "delocalised" - and this leads to a "communal entropy" term of value  $Nk$  in the description of the assembly. In the ideal crystal, on the other hand, where the molecules are localised around their lattice sites (the situation given by cell theory), the communal entropy is zero, since the volume available to a molecule is equal to the volume per molecule. Somewhere between these extremes lies the liquid state. It has been suggested (Eyring 1936) that multiplication of the partition function of a lattice by a factor  $e^N$  could give a better description of the liquid state, but this gives the communal

entropy of an ideal gas and it is more likely that this term appears gradually as we move from the solid, through the liquid, to the gas state (Alder 1962).

Various workers have attempted to account for the communal entropy, either by employing a cell model in which the cells are allocated in such a way that they may be occupied by more than one molecule (Janssens and Prigogine 1950, Pople 1951, Barker 1955, 1956, 1957), or by considering the behaviour of molecules in clusters of cells (de Boer 1954, Cohen, de Boer and Salsburg 1955, 1957, Salsburg, Cohen, Reithmeyer and de Boer 1957, Cohen and Reithmeyer 1958). Such treatments, however, involve many approximations and the problem of communal entropy in the liquid remains largely unsolved.

The cell model, then, represents a system of molecules in restricted oscillatory motion about a set of lattice points and is therefore a model of the solid state. Further, it is a model which is capable of taking explicit account of anharmonicity in the molecular vibrations (see (2.39)). However, even as a description of the solid state, it is still an approximation by virtue of the assumption of independent molecular motion - the Einstein approximation (Einstein 1907, 1911a, b) - and the sphericalisation procedure required to make the cell potential spherically symmetric.

The error introduced by sphericalisation has been studied by Barker (1956). He calculated the classical free volume given by the correct three dimensional cell potential and compared it to that given by the

sphericalised cell potential. He found that the error passes through a maximum ( $v_f(\text{correct})/v_f(\text{sphericalised})=1.4$ ) in the region of the critical density and that, on proceeding to high densities, the sphericalisation procedure becomes progressively more exact, until, in the limit of high density, the correct and sphericalised cell potentials become identical. He therefore came to the conclusion that the error introduced by sphericalisation is negligible at solid state densities.

The Einstein approximation of independent molecular motion undoubtedly leads to some error in the calculation of thermodynamic properties. These would be expected to be most pronounced in such properties as specific heat and entropy, which are independent of the static lattice energy (see following chapter) and therefore particularly sensitive to the molecular motion in the solid. Correlation of molecular motion in classical statistics may be allowed for by the method of Barker (1955, 1956), who considered binary and ternary correlations. A more rigorous approach is the lattice dynamical method pioneered by Born and von Karman (1912, 1913), which considers the motion of the complete lattice in quantum statistics. The lattice dynamical method is, however, mathematically complicated, even in the simplest case of harmonic lattice vibrations (see Montroll 1942, 1943, Montroll and Peaslee 1944). The complexity of the lattice dynamical treatment of an anharmonic crystal is greater still and, although there exists a formal framework for the treatment of anharmonic lattice vibrations to any degree of accuracy (Cowley 1963), the difficulties of the mathematics are so great that, to date, detailed

theory has been developed only for first order anharmonic effects (see Leibfried and Ludwig 1961). In consequence, even the most modern lattice dynamical calculations (see, for example, Feldman and Horton 1967) take account of only such effects. Further, lattice dynamical calculations usually consider only nearest neighbour interactions, although some workers (Wallace 1963, Reissland 1965) have attempted to allow for more distant neighbours.

On the other hand, with the use of an Einstein model such as the cell model, it is comparatively simple to take explicit account of even high order anharmonic effects, as well as interactions between non-nearest neighbours. From the point of simplicity, then, the cell model has much to recommend it and it is felt that it can be used to good effect, so long as suitable care is taken not to stretch the theory beyond its limits.

Chapter 3The Quantum Cell Model and the Solution of the Radial Wave EquationQuantum effects in the inert gas solids

Although classical statistics may serve as a convenient approximation at high temperatures, any model purporting to give a complete description of the solid state of any substance right down to absolute zero temperature must involve the use of quantum statistical methods. Indeed, it is well known that classical methods, no matter how refined, fail completely to give even qualitatively correct results for the low temperature values of such non-static lattice dependent properties as specific heat and entropy; and it was not until Einstein (1907, 1911a,b) used the concept of "quantised oscillators" to explain the experimentally observed decrease in the specific heat of solid substances from the classical Dulong-Petit value of  $C_v = 3R \text{ mole}^{-1}$  at high temperature to  $C_v = 0$  in the limit of absolute zero temperature, that a realistic picture of the temperature variation of these properties could be obtained. It has been mentioned in Chapter 2 that such properties as specific heat and entropy would be expected to be particularly sensitive to the model used to represent the solid state and, indeed, Einstein's theory, with its assumption of independent molecular motion, was found to lead to errors in the low temperature values of specific heat. Similar errors would be expected from the use

of the cell model, which is simply an Einstein model which makes allowance for anharmonic effects. They may be removed by allowing for correlated molecular motion (Debye 1912, Born and von Karman 1912, 1913).

Properties expected to be less model sensitive are those, such as free energy and molar volume, depending strongly on the static lattice energy, which is unaffected by the vibrational motion of the crystal. By virtue of the purely classical nature of the static lattice, these properties are also less sensitive to quantum effects and their low temperature behaviour can be described, at least qualitatively, in terms of classical statistics.

Quantum effects in the static lattice dependent properties are governed by the value of the zero point vibrational energy,  $E_0$ , and a simple and convenient way of judging their relative importance in the inert gas solids is to compare, for each substance, how much  $E_0$  contributes to  $F_0$ , the total free energy of the crystal at 0°K.

A method of estimating the zero point energy of a crystal from experimental data is to use the relation:

$$E_0 = (9/8)R\theta_{D,0} \quad (3.1)$$

which is derived from a Debye model of the solid (Debye 1912) in which  $\theta_{D,0}$  is taken to be the limiting high temperature value,  $\theta_{D,\infty}$ . The use of (3.1) was originally proposed by Domb and Salter (1952) who showed that, whereas the previously accepted expression involving the T=0 value of  $\theta_D$

led to a substantial error in the evaluation of  $E_0$ , the replacement of  $\Theta_D$  by  $\Theta_{D,0}$  in a Debye solid reproduced exactly the second moment of the correct frequency distribution as given by the lattice dynamical methods of Born and von Karman (1912, 1913) and, consequently, led to a value of  $E_0$  in very close agreement with the correct one. For the f.c.c. lattice, which is the one pertinent to the present work, nearest neighbour considerations revealed the value of the zero point energy as given by (3.1) to be a mere 0.5% different from the correct value, while the use of the  $T=0$  value of  $\Theta_D$  leads to a result some 15% in error. The use of an Einstein model of the solid leads to a value of  $E_0$  ~3% different from that given by (3.1).

An objection that might be raised against the use of (3.1) in the context of the inert gas solids is that it is based on the assumption that the zero point vibrations of the crystal are harmonic. Now, while this may be assumed valid for the heavier inert gases, this is not the case for molecules as light as those of neon (see Reissland 1965). However, since at the moment we are not concerned with an evaluation of  $E_0$  for its own sake but wish only to demonstrate the effects of quantum behaviour, we take (3.1) to be a convenient approximation even when anharmonic effects are present and in such a situation assume that  $\Theta_{D,0}$  defines an effective harmonic lattice corresponding to the anharmonic one.

An experimental value of  $\Theta_{D,0}$  for any solid can be derived either from the temperature variation of the specific heat or from the elastic constants of the solid, and  $E_0$  is simply given by the negative of



the value of the sublimation energy extrapolated to absolute zero temperature. Using the data quoted by Pollack (1964) it is found that  $E_0$  expressed as a percentage of  $F_0$  (paying no regard to positive and negative signs) has values of 34, 10, 5 and 3 for neon, argon, krypton and xenon respectively. It is clear that quantum deviations are apparent in the  $0^\circ\text{K}$  free energies (and, by inference, in the  $0^\circ\text{K}$  values of other static lattice dependent properties) of all the inert gas solids. As expected from molecular weight considerations, they are most pronounced in solid neon and least in solid xenon, but even in the case of the latter substance the zero point energy is readily detectable in the total free energy.

Another way of looking at quantum effects in the static lattice dependent properties of the inert gas solids is in terms of the quantum parameter,  $\Lambda^*$ , previously mentioned in Chapter 2 and given by expression (2.28). This quantity is the reduced de Broglie wave length corresponding to an energy of  $\xi$ , the depth below zero of the minimum in the pair potential, and, as its name implies, is directly related to quantum behaviour. It was first introduced into the theory of intermolecular forces by de Boer (1948) who considered the classical and quantum statistical behaviour of pairwise additive systems of molecules interacting according to a two parameter potential function of the type  $\phi = \xi f(r/d)$ . He showed that, if classical statistics are obeyed, then the reduced thermodynamic properties of such systems may be expressed as universal functions of reduced volume  $V^*$  and reduced temperature  $T^*$ . Thus for any property:

$$X^*_{\text{classical}} = X^*(V^*, T^*) \quad (3.2)$$

and for the equation of state:

$$p_{\text{classical}}^* = p^*(V^*, T^*) \quad (3.3)$$

If, on the other hand, quantum statistics are obeyed, the reduced thermodynamic properties are now universal functions of  $\Lambda^*$  as well as of  $V^*$  and  $T^*$ , so that (3.2) and (3.3) become:

$$X_{\text{quantum}}^* = X^*(V^*, T^*, \Lambda^*) \quad (3.4)$$

and

$$p_{\text{quantum}}^* = p^*(V^*, T^*, \Lambda^*) \quad (3.5)$$

respectively. These revert to their classical analogues when  $\Lambda^*=0$ .

It is clear that values of the reduced thermodynamic properties at  $0^\circ\text{K}$  and zero pressure of systems for which (3.4) and (3.5) hold may be calculated as functions of  $\Lambda^*$  only. Such calculations have been widely undertaken (e.g. by de Boer and Blaisse 1948, Salter 1954, Dugdale and MacDonald 1954, Bernardes 1960, Hurst and Levelt 1961, Zucker 1961) with particular reference to the inert gas solids. Calculations of this type generally make use of the LJ 12:6 potential and a simple quantum model of the solid state to give plots of  $0^\circ\text{K}$ , zero pressure values of such properties as reduced free energy, reduced volume and reduced isothermal compressibility as functions of  $\Lambda^*$ . Such plots give substantial agreement with experimental data (see Figs.2 and 3 below), but comparison of the experimental points with  $\Lambda^*=0$  (i.e. classical) values of the properties shows that such agreement is possible only if quantum behaviour is accounted for. This is the case even for xenon, which comes closest

to classical behaviour.

Fig.2. Reduced equilibrium volume at  $0^{\circ}\text{K}$  and zero pressure ( $V_0^*$ ) as a function of the quantum parameter ( $\Lambda^*$ ) for the LJ 12:6 pair potential (after Zucker 1961).

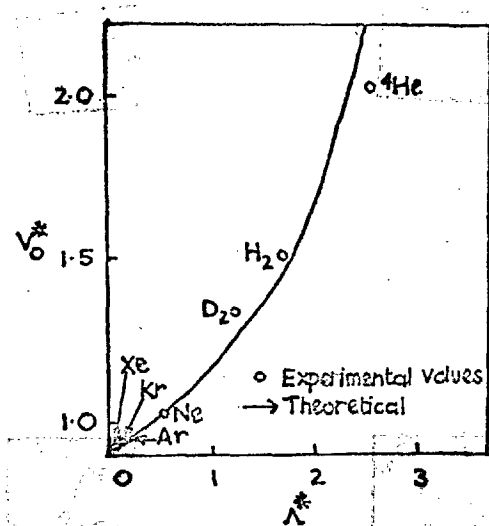
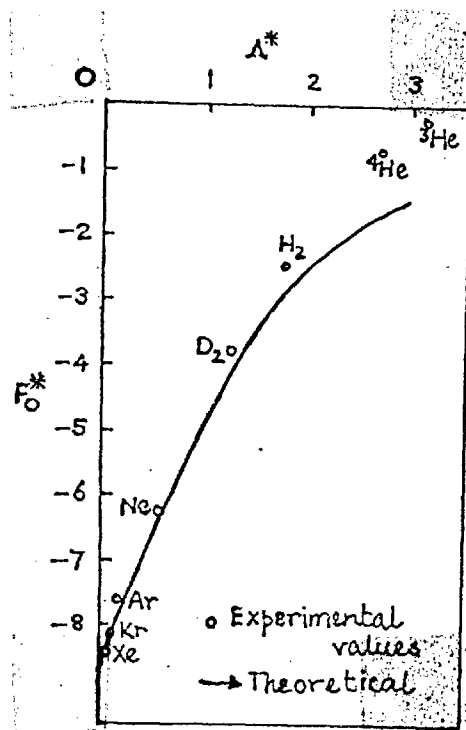


Fig.3. Reduced crystal free energy at  $0^{\circ}\text{K}$  and zero pressure ( $F_0^*$ ) as a function of the quantum parameter ( $\Lambda^*$ ) for the LJ 12:6 pair potential (after Zucker 1961).



It is quite clear then that the use of a quantum statistical model is essential, even from the point of view of the static lattice dependent properties, if a realistic picture of the low temperature thermodynamics of the inert gas solids is to be obtained. The incorporation of quantum statistics into the LJD cell model has been covered in principle in Chapter 2. The practical application of the theory is described in the second section of the present chapter.

The thermodynamic properties of a quantum cell model system and the solution of the radial wave equation.

As we have seen in Chapter 2, the quantum form of the cell theory of Lennard-Jones and Devonshire gives the partition function of an N particle, pair-wise additive lattice, at a reduced temperature of  $T^*$  (and an implied reduced volume of  $V^*$ ), as the sum over states expression (2.26):

$$Z_{NQu} = \left[ \sum_{l,n} (2l+1) \exp(-\lambda_{l,n}^*/T^*) \right]^N \exp[-Nw^*(o)/(2T^*)]$$

where  $w^*(o)$  is the reduced potential energy experienced by a representative particle in the static lattice; and the quantities  $\lambda_{l,n}^*$  ( $l=0,1,2,\dots$ ;  $n=0,1,2,\dots$ ) are reduced single particle energy levels, corresponding to the sphericalised cell field,  $\overline{w(R)}$ , and determined by the radial wave equation (2.27):

$$\frac{d^2 S_{l,n}^*(R^*)}{dR^{*2}} + \left[ \frac{8\pi^2 \lambda_{l,n}^*}{\Lambda^{*2}} - \frac{l(l+1)}{R^{*2}} - \frac{8\pi^2}{\Lambda^{*2}} \overline{w^*(R^*)} \right] \times S_{l,n}^*(R^*) = 0$$

under the conditions (2.27a):

$$S_{l,n}^*(0) = S_{l,n}^*(R_c^*) = 0$$

$R_c^*$  being the reduced cell radius.

From the partition function, the bulk thermodynamic properties follow directly by use of standard statistical mechanical relations. For example, the Helmholtz free energy, internal energy, specific heat at constant volume and entropy are given in reduced

form as:

$$F^* = \frac{-T^* \ln Z_{NQU}}{N} = -T^* \ln [\Sigma(1)] + \frac{w^*(0)}{2} \quad (3.7a)$$

$$U^* = \frac{T^{*2}}{N} \left( \frac{\partial \ln Z_{NQU}}{\partial T^*} \right)_{V^*} = \frac{\Sigma(\lambda_{l,n}^*)}{\Sigma(1)} + \frac{w^*(0)}{2} \quad (3.7b)$$

$$\begin{aligned} C_V^* &= \frac{2T^*}{N} \left( \frac{\partial \ln Z_{NQU}}{\partial T^*} \right)_{V^*} + \frac{T^{*2}}{N} \left( \frac{\partial^2 \ln Z_{NQU}}{\partial T^{*2}} \right)_{V^*} \\ &= \frac{1}{T^{*2}} \left\{ \frac{\Sigma(\lambda_{l,n}^*; \lambda_{l,n}^*)}{\Sigma(1)} - \left[ \frac{\Sigma(\lambda_{l,n}^*)}{\Sigma(1)} \right]^2 \right\} \quad (3.7c) \end{aligned}$$

$$\begin{aligned} S^* &= \frac{\ln Z_{NQU}}{N} + \frac{T^*}{N} \left( \frac{\partial \ln Z_{NQU}}{\partial T^*} \right)_{V^*} \\ &= \ln [\Sigma(1)] + \frac{1}{T^*} \left[ \frac{\Sigma(\lambda_{l,n}^*)}{\Sigma(1)} \right] \quad (3.7d) \end{aligned}$$

where  $\Sigma(a; b; c; \dots) = \sum_{l,n} (2l+1) \chi_{abc\dots} \exp(-\lambda_{l,n}^*/T^*)$

and  $\Sigma(1) = \sum_{l,n} (2l+1) \exp(-\lambda_{l,n}^*/T^*)$

In the same notation the reduced equation of state is given by:

$$p^* = \frac{-T^*}{N} \left( \frac{\partial \ln Z_{NQU}}{\partial V^*} \right)_{T^*} = -\frac{\Sigma(\lambda_{l,n}^{*'})}{\Sigma(1)} - \frac{w^*(0)'}{2} \quad (3.7e)$$

and reduced isothermal compressibility and reduced volume expansivity by:

$$\chi_{T^*}^* = -\frac{1}{V^*} \left( \frac{\partial V^*}{\partial p^*} \right)_{T^*} = \frac{1}{V^* \left\{ -\frac{\Sigma(\lambda_{l,n}^{*''})}{\Sigma(1)} + \frac{1}{T^*} \left[ \frac{\Sigma(\lambda_{l,n}^* \lambda_{l,n}^{*'})}{\Sigma(1)} - \frac{\Sigma(\lambda_{l,n}^{*'})^2}{\Sigma(1)^2} \right] + \frac{w^*(0)''}{2} \right\}} \quad (3.7f)$$

and

$$f_p^* = \frac{1}{V^*} \left( \frac{\partial V^*}{\partial T^*} \right)_p = \frac{1}{V^*} \frac{\left[ \frac{\Sigma(\lambda_{1,n}^* \lambda_{1,n}^{*'})}{\Sigma(1)} - \frac{\Sigma(\lambda_{1,n}^*) \Sigma(\lambda_{1,n}^{*'})}{\Sigma(1)^2} \right]}{\left\{ -\frac{\Sigma(\lambda_{1,n}^{*''})}{\Sigma(1)} + \frac{1}{T^*} \left[ \frac{\Sigma(\lambda_{1,n}^* \lambda_{1,n}^{*''})}{\Sigma(1)} - \frac{\Sigma(\lambda_{1,n}^{*'})^2}{\Sigma(1)^2} \right] - \frac{W^*(0)}{2} \right\}} \quad (3.7g)$$

where a single prime denotes single differentiation and a double prime double differentiation with respect to  $V^*$ . The reduced specific heat at constant pressure is given by substituting expressions (3.7c), (3.7f) and (3.7g) into the reduced thermodynamic relation:

$$C_p^* = C_v^* + \frac{\beta^{*2} T^* V^*}{\chi_T^*} \quad (3.7h)$$

Although, in general, because of the complexity of the function,  $\overline{w^*(R^*)}$ , the radial wave equation (2.27) cannot be solved analytically, it can be solved "exactly" - in the sense that the eigenvalues can be evaluated to any prescribed degree of accuracy - by use of either a series expansion or finite difference technique.

The former approach was adopted by Levelt and Hurst (1960) who wrote the functions  $S_{1,n}^*(R^*)$ , (related to  $U_{1,n}^*(R^*)$ , the radial component of the total wave function, by  $S_{1,n}^*(R^*) = R^* U_{1,n}^*(R^*)$ , see Chapter 2), as a power series in  $R^*$ . On substituting this function into the radial wave equation and equating terms involving like powers of  $R^*$ , Levelt and Hurst found half the coefficients of the expansion to be identically zero and the others to be related by simple recursion relations, involving the eigenvalue  $\lambda_{1,n}^*$ , the quantum number 1 and the coefficients

$C_{2k}^*$  ( $k=1,2,3,\dots$ ) of the series expansion of  $w^*(R^*)$ , (see (2.31) in Chapter 2). They determined the eigenvalues of energy iteratively by causing  $S_{1,n}^*(R^*)$  to fall to zero at the cell radius in accordance with the boundary condition,  $S_{1,n}^*(R_c^*)=0$ . The other boundary condition,  $S_{1,n}^*(0)=0$ , is implicit in the method.

Although this method proved reasonably successful in treating molecules of high  $\Lambda^*$ , e.g. hydrogen and deuterium (which, in spite of their lack of spherical symmetry, may, for many purposes, be considered in the same context as the inert gas molecules), it is very cumbersome and time consuming for heavier molecules. In a later paper, Hurst and Levelt (1961) estimated that, for argon, over 1000 terms would be required in the series representation of the wave function for a reasonably accurate value of the lowest energy level to be obtained.

The more versatile finite difference method given by Hillier, Islam and Walkley (1965) transforms the radial wave equation into four simultaneous, first order, linear differential equations which may be integrated in a stepwise manner, using a Runge-Kutta numerical technique. Because of the behaviour of the term  $l(l+1)/R^{*2}$  at  $R^*=0$ , the initial point of the integration is chosen as  $R^*=10^{-5}R_c^*$  and the initial values of the function  $S_{1,n}^*(R^*)$  and the various derivatives required by the method are calculated using the series expansion of Levelt and Hurst, which is rapidly convergent for such a small value of  $R^*$ . The eigenvalues are calculated by iteration such that

the boundary condition at  $R^*=R_c^*$  is satisfied.

Although this technique is of somewhat faster application than that of Levelt and Hurst, it still requires considerable computing time and suffers from a further defect common to both exact methods. This is that neither provides a direct way of determining the volume derivatives of the eigenvalues and, therefore, the evaluation of such properties as pressure, isothermal compressibility and volume expansivity (see (3.7e), (3.7f), (3.7g)) is not possible without recourse to numerical differentiation, either of the eigenvalues themselves or of the logarithm of the partition function. Now, of all mathematical operations, differentiation is perhaps the most awkward to treat by numerical methods, in that a single reasonable evaluation of a derivative requires highly accurate calculations of the quantity to be differentiated at many closely spaced values of the differentiating variable. Such a procedure is both cumbersome and very time consuming and, in the present context, must be considered unsuitable, especially when it is remembered that the calculation of exact eigenvalues is in itself a slow process.

Nevertheless, "exact" methods are useful in testing how well approximate methods evaluate the eigenvalues and the thermodynamic properties not dependent on volume derivatives and, since the finite difference technique has been used for this purpose in this work, a complete treatment of this method is given in Appendix 2.



In the majority of the solid state calculations described in this thesis, the solution of the radial wave equation has been effected through the semi-classical Wentzel-Kramers-Brillouin (WKB) approximation. This method allows rapid evaluation of a large number of energy levels and reasonably straightforward calculation of their volume derivatives. Its application to the quantum cell model was developed in these laboratories by Hillier and Walkley (1964) and was later used by them and others (Hillier, Islam and Walkley 1965, Hillier and Walkley 1965, Jenkins and Walkley 1965) in detailed calculations based on the LJ 12:6 potential. A similar method has been used by Henderson and Reed (1964). The approach taken here is similar to that of Hillier and Walkley, but with modifications which make for greater numerical efficiency and also allow the second volume derivatives of the energy levels to be calculated.

The full treatment of the WKB approximation is covered in most quantum mechanical texts (for example, see Schiff 1955, p.185 et seq.) and only an outline is given here. Briefly then, the WKB approximation, as applied to one dimensional systems, expands the exponential of  $i/h$  ( $h$  is Planck's constant) times the wave function as a power series in  $h$ . On neglecting terms beyond the second in this expansion, the solution of the Schroedinger equation gives eigenfunctions which are valid in regions of positive and negative kinetic energy far removed from classical turning points of the motion. Approximate solutions for the two regions are then found that are

reasonably accurate at a turning point and, at the same time, have the correct asymptotic behaviour. The turning point is assumed linear and the solutions connected across it. For a particle moving in a potential well, the asymptotic forms of the solutions arising from the two turning points of the motion are matched in the interior of the well to give a determining equation for the energy levels:

$$\int_{x_1}^{x_2} \frac{2\pi}{h} \left\{ 2m [\lambda_n - V(x)] \right\}^{\frac{1}{2}} dx = (n + \frac{1}{2})\pi \quad (3.8)$$

( $n = 0, 1, 2, \dots$ )

where  $m$  and  $\lambda_n$  are the mass and  $n$ th energy level respectively of the particle,  $V(x)$  is the potential field and  $x_1$  and  $x_2$  ( $x_2 > x_1$ ) are the classical turning points of the motion (i.e. the points where  $\lambda_n = V(x)$ ).

Equation (3.8) is straightforwardly extended to three dimensional radial systems by replacing  $x$  by  $r$ ,  $\lambda_n$  by  $\lambda_{l,n}$  and  $V(x)$  by  $V(r) + h^2(l + \frac{1}{2})^2 / (2mr^2)$ . In our notation, the equation determining the reduced energy levels  $\lambda_{l,n}^*$  corresponding to the reduced cell potential  $\overline{w^*(R^*)}$  may be written:

$$\int_{R_1^*}^{R_2^*} Q^{*\frac{1}{2}} dR^* = (n + \frac{1}{2})\pi \quad (3.9)$$

where

$$Q^* = \frac{8\pi^2}{\Lambda^{*2}} \lambda_{l,n}^* - \frac{(l + \frac{1}{2})^2}{R^{*2}} - \frac{8\pi^2}{\Lambda^{*2}} \overline{w^*(R^*)} \quad (3.9a)$$

and  $R_1^*$  and  $R_2^*$  ( $R_2^* > R_1^*$ ) are the positive roots of the equation:

$$Q^*(R^*) = 0 \quad (3.9b)$$

The replacement of  $l(l+1)$  by  $(l+\frac{1}{2})^2$  in the centrifugal part of the kinetic energy of the three dimensional system is necessary to fulfil the boundary condition  $S_{1,n}^*(0)=0$  (Langer 1937), and is equivalent to causing the solution of the radial wave equation, written in terms of  $S_{1,n}(R)$ , to behave in the same way at  $R=0$  as does that of the one dimensional Schroedinger equation at  $x=-\infty$ . The other boundary condition,  $S_{1,n}^*(R_c^*)=0$ , is not fulfilled in the WKB approximation; instead  $S_{1,n}^*(R^*) \rightarrow 0$  as  $R^* \rightarrow \infty$ . This is in direct contrast with the 'exact' methods, in which the satisfaction of this condition is inherent in the solution of the wave equation. Nevertheless, as far as the substances considered here are concerned, the use of the WKB formula (3.9) is justified by virtue of  $R_c^*$ 's being sufficiently large in comparison with  $R_2^*$  for the points  $R^*=R_c^*$  and  $R^*=\infty$  to be considered equivalent.

With this in mind, the use of (3.9) in calculating the low lying energy levels is justified by the similarity between  $\overline{w}(R)$  at small displacements and the harmonic potential  $V=C_2R^2$  (see the expansion (2.39) in Chapter 2), for which particular case the WKB approximation gives the energy levels exactly (Froman and Froman 1965, p.120 et seq.). (3.9) is also valid for the high energy levels by virtue of the asymptotic nature of the approximation, which makes it generally applicable only when the classical turning points of the motion are well separated.

The numerical accuracy with which the WKB method gives the energy levels of an LJ 12:6 cell model system was initially studied by Hillier and Walkley (1964) who compared the WKB values of the energy levels with the

"exact" finite difference values for hydrogen and deuterium at various values of  $V^*$ . The inaccuracies arising from the use of the WKB method were found to be small and, for the substances considered here, which, due to their higher molecular weight more nearly approach harmonic behaviour, the inaccuracies in the LJ 12:6 energy levels would be expected to be even smaller. Although there is no a priori reason to doubt that the WKB approximation is also applicable to EXP-6 calculations, we felt it advisable to verify that this is indeed the case and this was done in the course of the calculations reported in the next chapter.

Strictly speaking, the use of the WKB approach is preferable to methods which treat a particle in an Einstein lattice as a harmonic oscillator perturbed by anharmonic terms (Henkel 1955, Zucker 1964) because of its ability to take accurate account of all anharmonic terms in the evaluation of the high energy levels where molecular displacements are large. Perturbation methods, on the other hand, are accurate only in the evaluation of energy levels for which mean excursions of the molecules from their lattice points are small enough to render valid the truncation of the series expansion of the potential field after a small number of terms (two in the treatment of Henkel and three in that of Zucker). However, it should be pointed out that, even at the triple points of the substances considered here, the partition function should not be sensitive enough to the very high energy levels for the second order perturbation treatment of Zucker to lead to serious inaccuracies in the evaluation of the thermodynamic properties and the author's preference for

the WKB approximation is only marginal.

Since, for an f.c.c. lattice,  $V^* = a_1^{*3}/2^{\frac{1}{2}}$  (see Chapter 2), the first and second reduced volume derivatives of  $\lambda_{1,n}^*$  are given by:

$$\frac{d\lambda_{1,n}^*}{dV^*} = \left( \frac{2^{\frac{1}{2}}}{3a_1^{*2}} \right) \left( \frac{d\lambda_{1,n}^*}{da_1^*} \right) \quad (3.10)$$

and

$$\frac{d^2\lambda_{1,n}^*}{dV^{*2}} = \frac{2}{9a_1^{*4}} \left( \frac{d^2\lambda_{1,n}^*}{da_1^{*2}} - \frac{2}{a_1^*} \frac{d\lambda_{1,n}^*}{da_1^*} \right) \quad (3.11)$$

respectively.

In the WKB approximation expressions for  $d\lambda_{1,n}^*/da_1^*$  and  $d^2\lambda_{1,n}^*/da_1^{*2}$  are given by differentiation, under certain conditions, of (3.9) with respect to  $a_1^*$ . Although both  $R_1^*$  and  $R_2^*$  are both dependent on  $a_1^*$ , the fact that, by definition,  $Q^*$  (and therefore  $Q^{*\frac{1}{2}}$ ) is zero at these points allows the first derivatives to be obtained by straightforward differentiation under the integral sign. This gives:

$$\frac{d\lambda_{1,n}^*}{da_1^*} = \frac{\int_{R_1^*}^{R_2^*} \frac{\partial W^*(R^*)}{\partial a_1^*} Q^{*-\frac{1}{2}} dR^*}{\int_{R_1^*}^{R_2^*} Q^{*-\frac{1}{2}} dR^*} \quad (3.12)$$

Although this expression, somewhat rearranged, has been used to good effect in the calculations of Walkley and co-workers, in view of the fact that the presence of  $Q^{*-\frac{1}{2}}$  leads to infinities in the integrands at  $R_1^*$  and  $R_2^*$ , it is felt that further comment is required as to its validity.

Let us consider the behaviour of the function  $Q^{*-1/2}$  in the region of the turning points  $R_1^*$  and  $R_2^*$ . Expansion of  $Q^*$  about each turning point shows that  $Q^{*-1/2}$  varies as  $(R^*-R_1^*)^{-1/2}$  for  $R^*$  near  $R_1^*$  and as  $(R_2^*-R^*)^{-1/2}$  for  $R^*$  near  $R_2^*$ . (We note as an aside that, if this were not the case, the two turning points would not be linear and the WKB method would not be applicable anyway). Also, since the leading term in each of the expansions of  $\frac{\partial w^*(R^*)}{\partial a_1^*}$  about  $R_1^*$  and  $R_2^*$  are independent of  $R^*$ , the variation of  $\left[\frac{\partial w^*(R^*)}{\partial a_1^*}\right] Q^{*-1/2}$  with  $R^*$  in the regions near the turning points is the same as that of  $Q^{*-1/2}$ . Since the integration of functions varying as  $(R^*-R_1^*)^{-1/2}$  and  $(R_2^*-R^*)^{-1/2}$  leads to ones varying according to the corresponding positive powers, the contribution of the parts of the integrals arising from the regions close to the turning points approach a limiting value of zero. Therefore, in spite of the presence of the infinities in the integrands, the integrals themselves are finite and the use of (3.12) is justified.

However, even though (3.12) is valid in itself, the presence of the infinities in the integrands makes it impossible to obtain the second derivative  $d^2 \lambda_{1,n}^* / da_1^{*2}$  by straightforward differentiation of this expression. Differentiation of (3.12), as it stands, would require that we find:

$$\frac{d}{da_1^*} \int_{R_1^*}^{R_2^*} \left[ \frac{\partial w^*(R^*)}{\partial a_1^*} \right] Q^{*-1/2} dR^* \quad (3.13)$$

and

$$\frac{d}{da_1^*} \int_{R_1^*}^{R_2^*} Q^{*-1/2} dR^* \quad (3.14)$$

Let us consider the second of these quantities, (3.14).

Carrying out the differentiation we should obtain:

$$\begin{aligned} \frac{d}{da_1^*} \int_{R_1^*}^{R_2^*} Q^{*-1/2} dR^* &= -\frac{1}{2} \left( \frac{8\pi^2}{\Lambda^{*2}} \right) \int_{R_1^*}^{R_2^*} \left[ \frac{d\lambda_{1,n}^*}{da_1^*} - \frac{\partial W^*(R^*)}{\partial a_1^*} \right] Q^{*-3/2} dR^* \\ &+ \frac{dR_1^*}{da_1^*} [Q^{*-1/2}]_{R^*=R_1^*} + \frac{dR_2^*}{da_1^*} [Q^{*-1/2}]_{R^*=R_2^*} \end{aligned} \quad (3.15)$$

Since  $R_1^*$  and  $R_2^*$  are the zeros of  $Q^*$ , the second and third terms in this expression are immediately seen to be of infinite absolute value. The first term is also ill behaved, by virtue of the appearance of  $Q^{*-3/2}$  in the integral, which in contrast to integrals involving  $Q^{*-1/2}$ , has infinite rather than zero contributions in the regions of the turning points. Similarly, formal differentiation in (3.14) leads to terms of infinite value and we conclude that the use of (3.12) must lead to an undefined value for  $d^2\lambda_{1,n}^*/da_1^{*2}$ .

In view of this, we make use of a suggestion by Munn (private communication) that application of Gauss-Mehler quadrature (see Kopal 1955, p.381 et seq.) to the evaluation of the integrals appearing in (3.12) avoids consideration of infinities in the integrands. Accordingly we make the substitution:

$$R^* = \frac{(R_2^* - R_1^*)}{2} \cos \theta + \frac{(R_2^* + R_1^*)}{2} \quad (3.16)$$

(3.14) now becomes:

$$\frac{d\lambda_{1,n}^*}{da_1^*} = \frac{\int_0^\pi \left[ \frac{\partial W^*(R^*)}{\partial a_1^*} Q^{*-1/2} \right]_{R^*=A^*c+B^* \sin \theta} d\theta}{\int_0^\pi \left[ Q^{*-1/2} \right]_{R^*=A^*c+B^* \sin \theta} d\theta} \quad (3.17)$$

where, for convenience,  $A^*$  has been written for  $(R_2^* - R_1^*)/2$ ,  $B^*$  for  $(R_1^* + R_2^*)/2$  and  $c$  for  $\cos \theta$ . The first non-vanishing terms in the expansions about  $\theta = 0$  and  $\theta = \pi$  of both the integrands in (3.17) are independent of  $\theta$  and, therefore, both functions are finite at the limits of the integration. Further, the substitution (3.16) does not give rise to infinities at any other point in the range of integration. Now, differentiation of (3.17) with respect to  $a_1^*$  gives a defined expression for  $d^2 \lambda_{1,n}^* / da_1^{*2}$ . This is:

$$\begin{aligned} \frac{d^2 \lambda_{1,n}^*}{da_1^{*2}} = & \left\{ \frac{1}{2} \int_0^\pi \left[ \frac{d\lambda_{1,n}^*}{da_1^*} - \frac{\partial W^*(R^*)}{\partial a_1^*} \right]_{R^*=A^*c+B^*} \right\} \left\{ \frac{\partial^2 W^*(R^*)}{\partial a_1^{*2}} + 2 \frac{\partial W^*(R^*)}{\partial a_1^*} \frac{\partial (A^*c+B^*)}{\partial a_1^*} \right\} \\ & - \frac{\partial^2 W^*(R^*)}{\partial a_1^{*2}} \left[ Q^{*-3/2} \right]_{R^*=A^*c+B^*} \int_0^\pi d\theta \\ & + \int_0^\pi \left[ \frac{\partial}{\partial a_1^*} \left[ \frac{\partial W^*(R^*)}{\partial a_1^*} \right]_{R^*=A^*c+B^*} \right] \left[ Q^{*-1/2} \right]_{R^*=A^*c+B^*} \sin \theta d\theta \\ & \times \left\{ \int_0^\pi \left[ Q^{*-1/2} \right]_{R^*=A^*c+B^*} \sin \theta d\theta \right\}^{-1} \end{aligned} \quad (3.18)$$

where the quantities  $\frac{\partial}{\partial a_1^*} \left[ W^*(R^*) \right]_{R^*=A^*c+B^*}$  and

$\frac{\partial}{\partial a_1^*} \left[ \frac{\partial W^*(R^*)}{\partial a_1^*} \right]_{R^*=A^*c+B^*}$  are given by:

$$\frac{\partial}{\partial a_1^*} \left[ W^*(R^*) \right]_{R^*=A^*c+B^*} = \left[ \frac{\partial W^*(R^*)}{\partial a_1^*} \right]_{R^*=A^*c+B^*} + \frac{\partial (A^*c+B^*)}{\partial a_1^*} \left[ \frac{\partial W^*(R^*)}{\partial R^*} \right]_{R^*=A^*c+B^*} \quad (3.18a)$$



and

$$\frac{\partial}{\partial a_1^*} \left[ \frac{\partial W^*(R^*)}{\partial a_1^*} \right]_{R^*=A^*C+B^*} = \left[ \frac{\partial^2 W^*(R^*)}{\partial a_1^{*2}} \right]_{R^*=A^*C+B^*} + \frac{\partial(A^*C+B^*)}{\partial a_1^{*2}} \left[ \frac{\partial W^*(R^*)}{\partial R^*} \right]_{R^*=A^*C+B^*} \quad (3.18b)$$

Since:

$$\frac{\partial(A^*C+B^*)}{\partial a_1^*} = \left( \frac{dR_2^*}{da_1^*} - \frac{dR_1^*}{da_1^*} \right) \cos \theta + \left( \frac{dR_2^*}{da_1^*} + \frac{dR_1^*}{da_1^*} \right)$$

we also require the formulation of  $dR_1^*/da_1^*$  and  $dR_2^*/da_1^*$ .

Remembering that  $R_1^*$  and  $R_2^*$  are the solutions of:

$$Q^* = \frac{8\pi^2 \lambda_{1,n}^*}{\Lambda^{*2}} - \frac{(1 + \frac{1}{2})^2}{R^{*2}} - \frac{8\pi^2 \overline{W^*(R^*)}}{\Lambda^{*2}} = 0$$

the derivatives are given by:

$$\frac{dR_t^*}{da_1^*} = \frac{8\pi^2 \left\{ \left[ \frac{\partial W^*(R^*)}{\partial a_1^*} \right]_{R^*=R_t^*} - \frac{d\lambda_{1,n}^*}{da_1^*} \right\}}{\left\{ \frac{2(1 + \frac{1}{2})^2}{R_t^{*3}} - \frac{8\pi^2 \left[ \frac{\partial W^*(R^*)}{\partial R^*} \right]_{R^*=R_t^*}}{\Lambda^{*2}} \right\}} \quad (t=1,2) \quad (3.18c)$$

In view of the substitution (3.16) required to give a usable expression for  $d^2 \lambda_{1,n}^* / a_1^{*2}$ , in the calculations described here, all the integrals required have been evaluated using the Gauss-Mehler quadrature formula:

$$\int_0^\pi f(\cos \theta) d\theta = \frac{\pi}{N} \sum_{j=1}^n f \left[ \cos \left( \frac{2j-1}{2n} \pi \right) \right] \quad (3.19)$$

where  $2n$  is the number of intervals over which integration is performed.

Since  $\sin \theta = (1 - \cos^2 \theta)^{\frac{1}{2}}$ , the integrals appearing in (3.17) and (3.18) are clearly in the form required for the application of formula (3.19). To transform (3.9) to the correct form we again make use of the

substitution (3.16) to give:

$$\int_0^{\pi} [Q^{* \frac{1}{2}}]_{R^* = A^* \zeta + B^*} \sin \theta d\theta = (u + \frac{1}{2})\pi \quad (3.20)$$

Now, numerical solution of this equation gives the value of  $\lambda_{1,n}^*$  for the chosen pair potential  $\phi$  and any given values of  $l$ ,  $n$ ,  $a_1^*$  and  $\Lambda^*$ . Use of this value of  $\lambda_{1,n}^*$  in (3.17) leads to the value of  $d\lambda_{1,n}^*/da_1^*$  and substitution of the calculated quantities  $\lambda_{1,n}^*$  and  $d\lambda_{1,n}^*/da_1^*$  in (3.18) gives the value of  $d^2\lambda_{1,n}^*/da_1^{*2}$ . Further details of the numerical procedure used are left until Chapter 4.

Chapter 4Pairwise Additive Cell Model Calculations for Solid Neon,  
Argon, Krypton and XenonThe evaluation of characteristic parameters

Before we can perform detailed calculations of the physical properties of the inert gases, we require reliable values of the adjustable parameters appearing in the pair interaction,  $\phi(r)$ , for each gas. In the absence of a unique determination of  $\phi(r)$  by the second virial coefficient of the gas alone (Keller and Zumino 1959), it appears necessary to turn to a consideration of the solid state itself if unambiguous values of the parameters suitable for solid state investigations are to be obtained. This is especially the case if we wish to study, for example, the variation of the lattice constant of the solid with temperature, which is so small that the values of the parameters used become almost critical (Hilliier and Walkley 1965, Jenkins and Walkley 1965, Jenkins 1966).

In contrast to the second virial coefficient, which by definition represents the interaction of only two molecules outside the perturbing field of all others in the system, the properties of the solid state are multiparticle in nature and require some assumption as to the additivity of the potential in their calculation. The assumption generally made is that the total potential of the system can be taken as the sum of all pair interactions, and it is on this basis that the cell model treatment described in

Chapter 2 is developed. For the purposes of the present chapter, we take this assumption to be valid, but recognise that its use in the evaluation of potential parameters probably leads to an effective  $\phi(r)$ , which reflects the influence of non-additive effects in the solid, rather than a true pair function. Since we test this effective function by calculations performed under the same assumption, our approach is at least self consistent and, so long as multibody effects are not overbearing, the use of such an approach would be expected to provide a fair indication of how well a chosen potential function represents the true inert gas pair interaction. The test of whether this is the case or not comes in the following chapter, where the influence of many body effects in the inert gas solids is subjected to greater scrutiny. For the present, we remark only that, if solid state data is to be used at all for characterisation purposes, it is considered desirable that such data should be used on its own rather than in conjunction with second virial and other gaseous data (for examples of such an approach, see Corner 1948, Mason and Rice 1954). In view of the comments made above, not only is the use of such a mixture of solid state and gaseous data inconsistent in itself, but also precludes the consideration of non-additivity in the solid by comparing solid state parameters with second virial parameters (see Chapter 5).

The solid state data most commonly used for characterisation purposes are  $L_0(0)$ , the crystal sublimation energy at  $0^\circ\text{K}$  and effectively zero pressure and  $a_{00}(0)$ , the lattice constant (or, equivalently,  $V_0(0)$  the molar volume) of the crystal at the same temperature and pressure (Corner 1948, Mason and Rice 1954, Zucker 1956, Hillier,

Islam and Walkley 1965). For two parameter potentials, such as the LJ 12:6, these suffice to determine the interaction completely, the two appropriate equations being:

$$-L_o(0)/(N\xi) = \left[ \lambda_{o,o}^* + \frac{1}{2}w^*(o) \right]_{a_o^*=a_{oo}^*(0)} \quad (4.1)$$

and

$$0 = \left[ d\lambda_{o,o}^*/da_1^* + \frac{1}{2}(dw^*(o)/da_1^*) \right]_{a_o^*=a_{oo}^*(0)} \quad (4.2)$$

(4.1) is given by setting  $-L_o(0)$  equal to  $F_o$ , the crystal free energy at  $0^\circ\text{K}$  for  $a_o = a_{oo}(0)$  and transforming to reduced variables. (4.2) is given by partial differentiation of  $F_o$  with respect to volume at constant temperature, followed by setting  $(\partial F_o/\partial V)_T (= -p_o)$  to zero for  $a_o = a_{oo}(0)$ , substituting  $Na_1^3/2^{3/2}$  for  $V$  (see (2.13)) and transforming to reduced variables. It is remembered that  $a_o$  is related to  $a_1$ , the nearest neighbour distance in the crystal, by  $a_o/2^{1/2} = a_1$  (see (2.14)).

For the EXP-6 function, with its three parameters,  $\xi$ ,  $r_m$  and  $\alpha$ , a third property is required in addition to  $L_o(0)$  and  $a_{oo}(0)$  for a complete characterisation. In the light of recent single crystal, X-ray determinations of the isothermal compressibility  $(\chi_T = -(1/V)(\partial V/\partial p)_T)$  of solid neon, argon and krypton by Simmons and co-workers - in the first place these results were privately communicated to us, but have since been published (Peterson, Batchelder and Simmons 1966, Batchelder, Losee and Simmons 1967, Urvas, Losee and Simmons 1967) - it was decided to use  $\chi_{T_0}(0)$ , the  $0^\circ\text{K}$ , zero pressure value of this quantity, as the third property for these substances. Using  $L_o(0)$ ,  $a_{oo}(0)$  and  $\chi_{T_0}(0)$ ,  $\xi$ ,  $r_m$

and  $\alpha$  are given by (4.1) and (4.2), together with:

$$\frac{r_m^3}{\chi_{T_0}(0)\epsilon} = \left\{ \frac{2^{\frac{1}{2}}}{9a_1^*} \left[ \frac{d^2 \lambda_{0,0}^*}{da_1^{*2}} + \frac{1}{2} \frac{d^2 w^*(o)}{da_1^{*2}} \right] \right\}_{a_0^* = a_{00}^*(0)} \quad (4.3)$$

(4.3) is obtained by double differentiation of  $F_0$  with respect to volume at constant temperature, followed by multiplication by  $V$  and putting  $V(\partial^2 F_0 / \partial V^2)_{T_0} = -V(\partial p_0 / \partial V)_{T_0} = 1/\chi_{T_0}(0)$  for  $a_0 = a_{00}(0)$ . The equation is written in terms of  $a_1^*$  by substituting  $V = Na_1^3/2^{\frac{1}{2}}$ , transforming to reduced variables and putting:

$$\frac{2^{\frac{1}{2}}}{3a_1^{*2}} \left[ \frac{d \lambda_{0,0}^*}{da_1^*} + \frac{1}{2} \frac{dw^*(o)}{da_1^*} \right] = \frac{-p_0 r_m^3}{\epsilon} = 0 \text{ for } a_0 = a_{00}(0)$$

For xenon, we turned to the bulk density  $p$ - $V$  measurements of Packard and Swenson (1963) for a suitable third property. This data allows a value of  $\chi_{T_0}(0)$  to be derived, but, owing to the lower accuracy of the experimental method and the fitting procedure used to obtain  $\chi_{T_0}(0)$ , this does not approach the accuracy of the single crystal values for neon, argon and krypton. Therefore, we used the zero point isotherm of xenon and chose, as the third property,  $a_{00}(p_0)$ , the value of the lattice constant at  $0^\circ\text{K}$  and the highest pressure,  $p_0 (=20\text{kbar})$ , under which measurements were carried out. In this case the appropriate equations are (4.1), (4.2) and:

$$(-p_0 r_m^3)/\epsilon = \left\{ \left( \frac{2^{\frac{1}{2}}}{3a_1^{*2}} \right) \left[ \frac{d \lambda_{0,0}^*}{da_1^*} + \frac{1}{2} \frac{dw^*(o)}{da_1^*} \right] \right\}_{a_0^* = a_{00}^*(p_0)} \quad (4.4)$$

where  $p_0=20\text{kbar}$ . (4.4) is the non-zero pressure equivalent of (4.2).

A complete list of the various experimental data which we used is given in Table 1.

Table 1

Experimental zero point data used for characterisation purposes

Substance	$L_0(0)$ (cal mole <sup>-1</sup> )	$a_{00}(0)$ (Å)	$\chi_{To}(0)$ (cm <sup>2</sup> dyne <sup>-1</sup> )x10 <sup>11</sup>	$a_{00}(20\text{kbar})$ (Å)
Neon	448 <sup>a)</sup>	4.4637 <sup>d)</sup>	9.0 <sup>d)</sup>	-
Argon	1846 <sup>b)</sup>	5.3111 <sup>e)</sup>	3.75 <sup>e)</sup>	-
Krypton	2666 <sup>b)</sup>	5.6459 <sup>f)</sup>	2.91 <sup>f)</sup>	-
Xenon	3828 <sup>c)</sup>	6.13 <sup>g)</sup>	-	5.658 <sup>h)</sup>

- a) Clusius, Flubacher, Piesbergen, Schleich and Sperandio (1960);  
 b) Beaumont, Chihara and Morrison (1961);  
 c) Whalley and Schneider (1955);  
 d) Batchelder, Losee and Simmons (1967);  
 e) Peterson, Batchelder and Simmons (1966);  
 f) Urvas, Losee and Simmons (1967);  
 g) quoted by Pollack, (1964) from the results of Sears and Klug (1962) and Bolz and Mauer (unpublished work);  
 h) Packard and Swenson (1963).

The results in d), e) and f) were communicated to us prior to their publication.

For the solution of each appropriate set of simultaneous equations, we used the extended Newton-Raphson technique described in Appendix 3. In conjunction with the WKB approximation for the evaluation of  $\lambda_{0,0}^*$  and its derivatives, this provides a simple and rapid method of evaluating the parameters to any desired degree of accuracy, so long as reasonable first guesses at the values of the parameters are possible. It is eminently suitable for machine computation and has been programmed by the author for the characterisation of both the LJ 12:6 function, using (4.1) and (4.2), and of the EXP-6 function, using either (4.1), (4.2) and (4.3) or (4.1), (4.2) and (4.4).

A brief outline of the numerical procedure used by the programs is as follows. The values of the appropriate experimental zero point properties, the first guesses at the parameters and the molecular weight of the substance under investigation are input as data. This data is used to calculate the first approximation to the quantum parameter  $\Lambda^*$  (see (2.28)) and the reduced nearest neighbour distance  $a_1^*$  corresponding to the value of  $a_{00}(0)$ . From this value of  $a_1^*$ , values of  $w^*(0)$ ,  $dw^*(0)/da_1^*$  and, if necessary,  $d^2w^*(0)/da_1^{*2}$  are calculated. For the LJ 12:6 function, expression (2.30) is used for this purpose, together with the values of  $S(12)$  and  $S(6)$  given by Kihara and Koba (1952). For the EXP-6 function, the appropriate expression is (2.32), the terms corresponding to attraction in  $\phi(r)$  being calculated using the same value of  $S(6)$  as that used for the LJ 12:6 function and those corresponding to repulsion by summing over sufficient shells of neighbours to give a specified



accuracy.

The next step is the calculation of  $\lambda_{0,0}^*$ ,  $d\lambda_{0,0}^*/da_1^*$  and, if necessary,  $d^2\lambda_{0,0}^*/da_1^{*2}$  for the value of  $a_1^*$  corresponding to  $a_0 = a_{00}(0)$ . In these calculations,  $\overline{w^*(R^*)}$  and its derivatives are calculated for a number of shells of neighbours specified in the input data, the expressions used to give  $\overline{w^*(R^*)}$  for the LJ 12:6 and EXP-6 functions being (2.35) and (2.37a) respectively. Using a first approximation to  $\lambda_{0,0}^*$ , either read in as data or calculated in the program through the harmonic approximation, the turning points  $R_1^*$  and  $R_2^*$  are roughly located by scanning the function  $Q^*$  (see (3.9a) and (3.9b)), noting where it changes sign and applying the method of "similar triangles". The values of  $R_1^*$  and  $R_2^*$  are then refined to a specified accuracy by applying a Newton-Raphson iterative technique to the solution of equation (3.9b). Using the refined values of the turning points, a better value of  $\lambda_{0,0}^*$  is calculated by the application of a Newton-Raphson technique to equation (3.20). The necessary integrations are carried out using the Gauss-Nehler quadrature formula (3.19) for some specified number of intervals. The values of the turning points appropriate to the new value of  $\lambda_{0,0}^*$  are calculated from the old values of  $R_1^*$  and  $R_2^*$  by again applying a Newton-Raphson technique to equation (3.9b). The new values of  $R_1^*$  and  $R_2^*$  are then employed in the calculation of an even better value of  $\lambda_{0,0}^*$ . The procedure is repeated until  $\lambda_{0,0}^*$  is iterated to some specified accuracy.  $d\lambda_{0,0}^*/da_1^*$  is then calculated using (3.17) and, if required,  $d^2\lambda_{0,0}^*/da_1^{*2}$  using (3.18), the necessary integrations being performed in the same manner as those in the

calculation of  $\lambda_{o,o}^*$ . In the case of the characterisation of the EXP-6 function for xenon,  $dw^*(o)/da_1^*$  and  $d\lambda_{o,o}^*/da_1^*$  are then calculated in the same way as before, but for the value of  $a_1^*$  corresponding to  $a_o = a_{oo}$  ( $p_o = 20\text{kbar}$ ).

Now - making use of the notation used in Appendix 3 - the quantities  $F_i(P_{1o}, \dots, P_{no})$  ( $i=1, \dots, n$ ) are calculated for the appropriate set of equations. By adjusting in turn the first guess at each parameter and repeating the calculations, the difference quotients  $(\Delta F_i / \Delta P_j)_o$  ( $i=1, \dots, n; j=1, \dots, n$ ) are evaluated and, thence, by the solution of equations (A.3.4), better values of the parameters obtained. The whole procedure is repeated until the parameters have been iterated to a specified accuracy.

In our calculations the parameters were iterated such that each one was accurate to at least  $10^{-2}\%$ . The iteration accuracy for the evaluation of the turning points  $R_1^*$  and  $R_2^*$  was  $10^{-3}\%$  and that for the evaluation of  $\lambda_{o,o}^*$ ,  $10^{-2}\%$ . The integrals required were calculated using 10 Gauss-Mehler quadrature intervals, which proved capable of giving  $\lambda_{o,o}^*$  to an accuracy of  $10^{-3}\%$ . The calculation of  $\overline{w^*(R^*)}$  was for three shells of neighbours, it being found that the use of "three shell" parameters in the "three shell" calculation of thermodynamic properties (see following section but one) leads to results insignificantly different from calculations involving more distant neighbours. In the characterisation of the EXP-6 function, the repulsive

parts of the static lattice terms were calculated to an accuracy of not less than  $10^{-2}\%$ .

The results of the calculations for the EXP-6 function are given in Table 2 and those for the LJ 12:6 function in Table 3.

Table 2

EXP-6 parameters derived from the pairwise additive consideration of the solid state at 0°K

Substance	$\epsilon(\text{erg}) \times 10^{15}$	$r_m(\text{\AA})$	$\alpha$	$\Lambda^* = h / [(m\epsilon)^{\frac{1}{2}} r_m]$
Neon	5.462	3.090	16.13	0.5012
Argon	17.14	3.808	14.23	0.1632
Krypton	23.89	4.062	14.84	0.08946
Xenon	32.77	4.444	13.55	0.05578

Table 3

LJ 12:6 parameters derived from the pairwise additive consideration of the solid state at 0°K

Substance	$\epsilon(\text{erg}) \times 10^{15}$	$\sigma(\text{\AA})$	$\Lambda^* = h / [(m\epsilon)^{\frac{1}{2}} \sigma]$
Neon	5.015	2.774	0.5826
Argon	16.50	3.401	0.1862
Krypton	22.75	3.636	0.1024
Xenon	31.98	3.960	0.06337

The EXP-6 and LJ 12:6 potentials given by these parameters are plotted as the full and dashed curves respectively in Figures 4, 5, 6, 7.

Fig.4. Neon - pair potential energy,  $\phi$ , divided by Boltzmann constant,  $k$ , as a function of intermolecular distance,  $r$ .

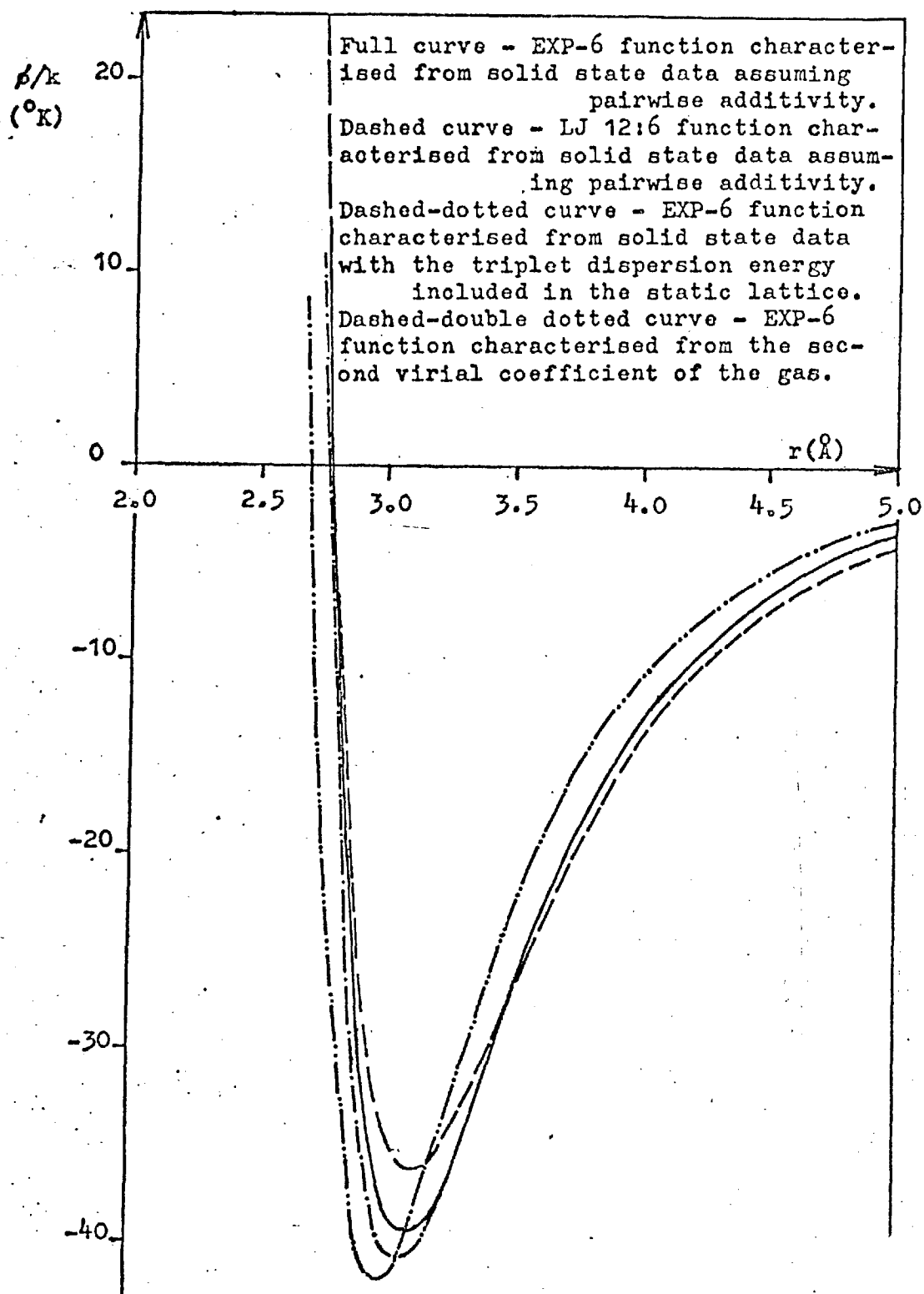


Fig.5. Argon - pair potential energy,  $\phi$ , divided by Boltzmann's constant,  $k$ , as a function of intermolecular distance,  $r$ .

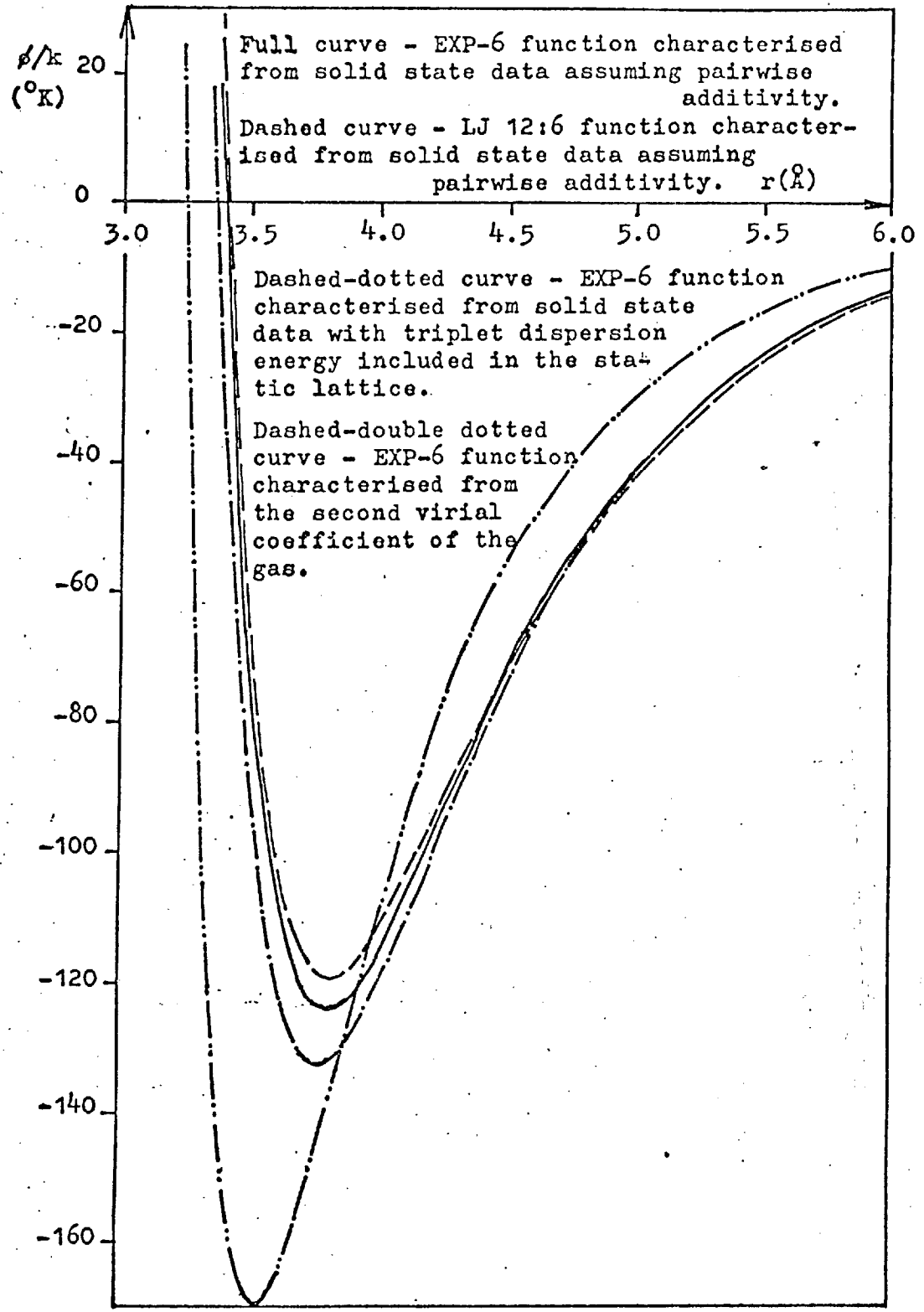


Fig. 6. Krypton - pair potential energy,  $\phi$ , divided by Boltzmann's constant,  $k$ , as a function of intermolecular distance,  $r$ .

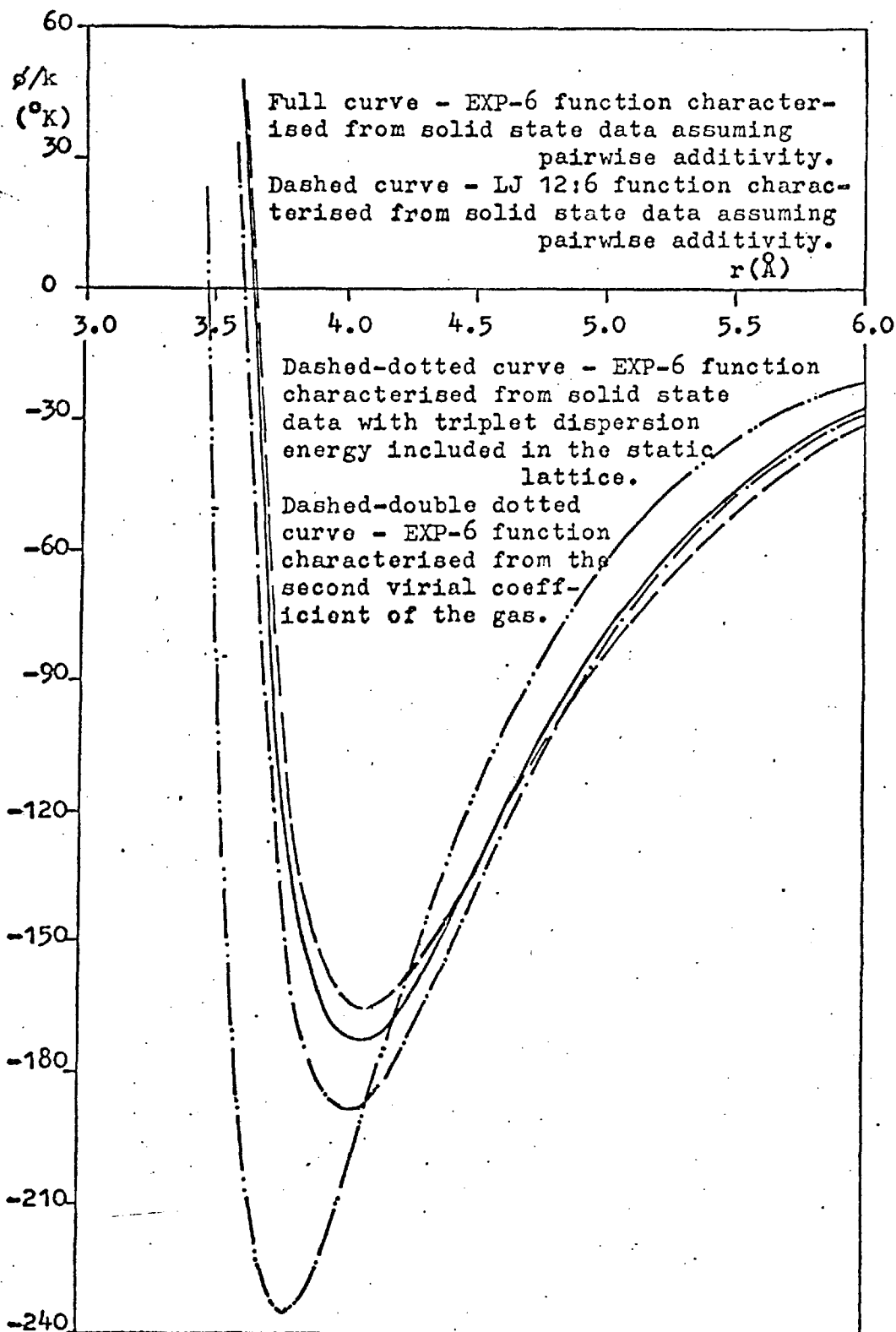
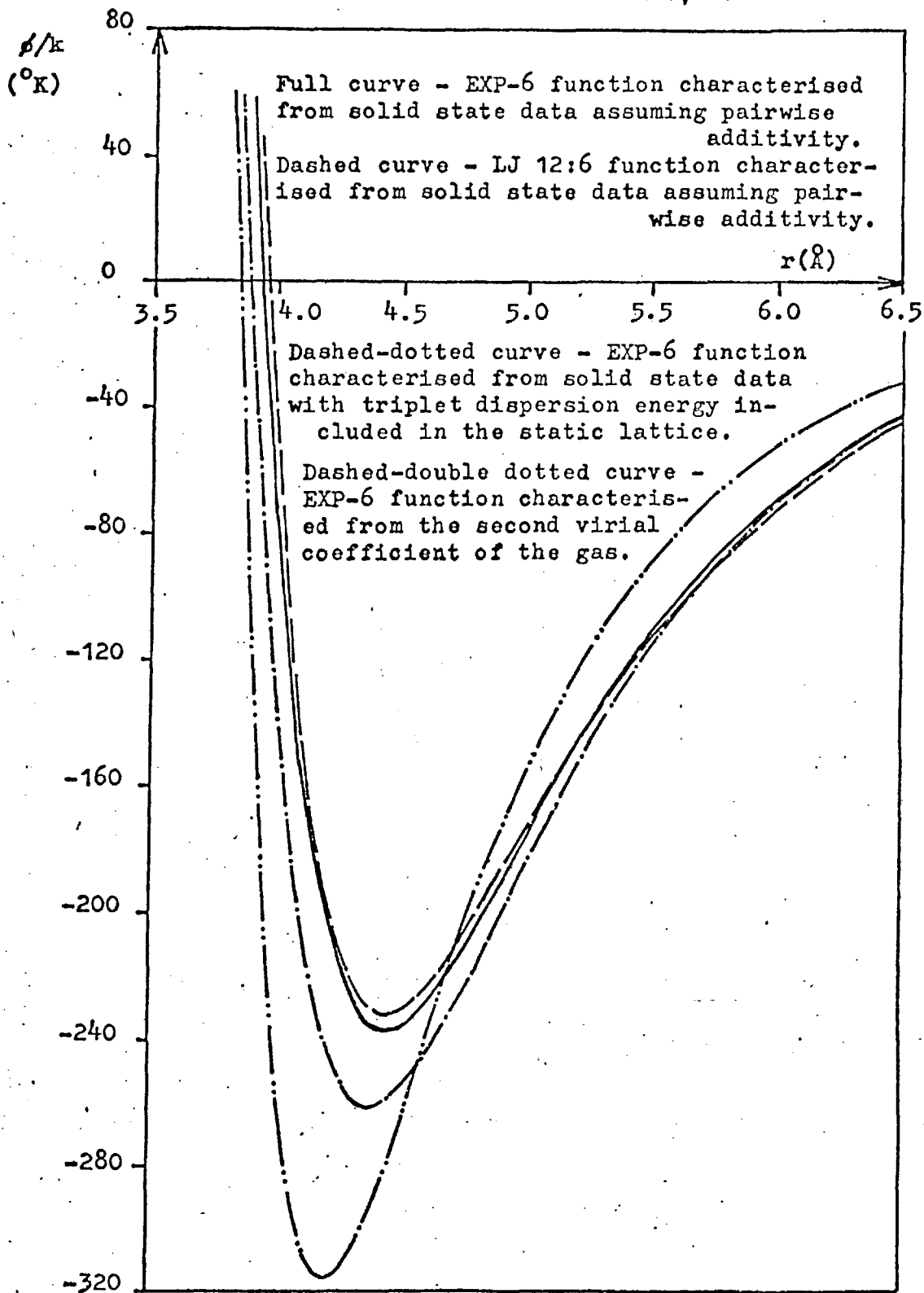


Fig. 7. Xenon - pair potential energy,  $\phi$ , divided by Boltzmann's constant,  $k$ , as a function of intermolecular distance,  $r$ .



It is seen that, in the case of each of the substances considered here, the pair potential given by the EXP-6 function characterised by solid state data has a somewhat lower, slightly narrower bowl than that given by the corresponding LJ 12:6 function.

### The spurious maximum in the EXP-6 potential

In Chapter 2 it was pointed out that, due to the spurious maximum in the EXP-6 pair potential at  $r^*=r^*_{\max}$ , there is a similar anomaly in the reduced cell potential,  $\overline{w^*(R^*)}$ , at some reduced distance,  $R^*=R^*_{\max}$ . For this reason,  $\overline{w^*(R^*)}$  is written in two parts given by (2.37a) and (2.37b), in direct analogy with the description of  $\phi^*(r^*)$  by (2.23a) and (2.23b):

For any given value of  $\alpha$ ,  $r^*_{\max}$  is given by the smaller root of the transcendental equation:

$$-e^{\alpha} \exp(-\alpha r^*) + r^{*-7} = 0 \quad (4.5)$$

the larger root,  $r^*=1$ , being the position of the minimum of  $\phi^*(r^*)$ . (4.5) is straightforwardly solved by numerical methods and values of  $r^*_{\max}$  and  $\phi^*(r^*_{\max})$ , the reduced pair energy at the maximum, have been tabulated for physically realistic values of  $\alpha$  by Hirschfelder, Curtiss and Bird (1954), p.34. Their results are reproduced in Table 4.



Table 4

The position and energy of the spurious maximum in the EXP-6 potential

$\alpha$	$r_{\max}^*$	$\phi^*(r_{\max}^*)$
12.0	0.30247	1705
12.5	0.27304	3518
13.0	0.24697	7110
13.5	0.22382	14115
14.0	0.20319	27585
14.5	0.18476	53170
15.0	0.16825	101222

From this table we see that  $r_{\max}^*$  decreases and  $\phi^*(r_{\max}^*)$  increases with increasing  $\alpha$ , but that, even at the lowest value of  $\alpha$  quoted (i.e. 12), the value of  $r_{\max}^*$  represents an intermolecular distance much less than the equilibrium separation and the maximum appears well up on the repulsive branch of the potential. Consequently we should expect that the presence of the maximum in  $\overline{w^*(R^*)}$ , if it is to have any effect at all, would influence the calculation of only the higher lying energy levels. For this reason the zero point calculations described in the previous section were performed under the assumption that the maximum could be ignored.

The value of  $R_{\max}^*$  is given by the largest root of:

$$\frac{\partial w^*(R^*)}{\partial R^*} = \frac{\alpha}{\alpha - 6} \left\{ \frac{6e^\alpha}{\alpha^2} \left[ \frac{A}{R^*} \cosh(\alpha R^*) - \frac{\sinh(\alpha R^*)}{R^*} \right] - \frac{\alpha R^* (-1) \sinh(\alpha R^*)}{a_1} + \frac{T(4)_6}{8a_1 R^{*2}} - \frac{T'(5)_6}{2a_1 R^*} \right\} = 0 \quad (4.6)$$

where (4.6) is given by differentiation of (2.37a), A being defined by (2.38),  $R(n)$  by (2.33),  $T(4)_6$  by (2.36) and  $T'(5)_6$  by:

$$T'(5)_6 = \sum_i z_i (a_i^*/a_1^*)^{-1} [(a_i^* - R^*)^{-5} - (a_i^* + R^*)^{-5}] \quad (4.7)$$

The value of  $R_{\max}^*$  depends on two variables,  $\alpha$  and  $a_1^*$ . However, for any fixed value of  $a_1^*$ , we should expect, from the results in Table 4, that the values of  $R_{\max}^*$  and  $\overline{w^*(R_{\max}^*)}$  would increase with increasing  $\alpha$  and, consequently, we restrict our attention to the lowest value of  $\alpha$  relevant to the present work. Using  $\alpha = 13.55$  (see Table 2), the rough solution of (4.6) for  $a_1^* = 0.8$  gives  $R_{\max}^* \simeq 0.61$  and  $\overline{w^*(R_{\max}^*)} \simeq 5 \times 10^3$  and, for  $a_1^* = 1.15$ ,  $R_{\max}^* \simeq 0.98$  and  $\overline{w^*(R_{\max}^*)} \simeq 3 \times 10^3$ . Since all the solid state densities appropriate to the present calculations lie between those represented by  $a_1^*$  values of 0.8 and 1.15 and since, for fixed  $\alpha$ , both  $R_{\max}^*$  and  $\overline{w^*(R_{\max}^*)}$  prove to be monotonic functions of  $a_1^*$ , these values may be considered as extreme limits. We see that in both cases the value of  $R_{\max}^*$  is well beyond the reduced cell radius,  $R_c^*$  ( $= 0.55267a_1^*$  - see Chapter 2), and the energy at the maximum is so high as to be well above the highest energy level that could ever be required for an accurate evaluation of the partition function,  $Z_{NQu}$ . In view of this we felt it quite safe to ignore the maximum in  $\overline{w^*(R^*)}$  altogether and all our solid state calculations have been performed regarding  $\overline{w^*(R^*)}$  to be given solely by (2.37a).

The only problem that this approach introduced was the purely numerical one of correctly locating the turning points  $R_1^*$  and  $R_2^*$  by scanning the function

$Q^*$ . For the EXP-6 function,  $Q^*$ , instead of changing sign only twice as it should do, has a further zero beyond  $R_2^*$  caused by the maximum in  $\overline{w^*(R^*)}$ . Now, it is possible, if the choice of the scanning interval is too large, that the first turning point  $R_1^*$  can be missed altogether and the turning points taken to be  $R_2^*$  and the position of the anomalous zero. This possibility was ruled out by programming the scanning sequence in such a way that the zeros of  $Q^*$  obtained are taken to be  $R_1^*$  and  $R_2^*$  only if the changes of sign across them are correct, i.e. a change from negative to positive across  $R_1^*$  and from positive to negative across  $R_2^*$ . If this is not the case, the interval is automatically increased in the program and the scanning process repeated until the correct turning points are obtained.

In the static lattice terms, there is no possibility of the spurious maximum affecting the calculations. For the densities appropriate to our calculations, the nearest neighbour distance in the crystal is always sufficiently large for the maximum to be ignored completely.

### The thermodynamic properties

Having calculated the values of the parameters appearing in the LJ 12:6 and EXP-6 pair interactions and having assured ourselves that the spurious maximum in the EXP-6 function may be safely ignored in solid state calculations, the thermodynamic properties of solid neon, argon, krypton and xenon were calculated through the expressions (3.7a) - (3.7h).

Since the expressions (3.7a) - (3.7h), as they stand, assume volume and temperature to be the independent variables, whereas experimental measurements are invariably made at fixed pressure and temperature, comparison between theory and experiment requires the solution of (3.7e) for  $V^*$  at fixed  $p^*$  and  $T^*$ . Use of this value of  $V^*$  together with the appropriate value of  $T^*$  then gives other thermodynamic properties. The solution of (3.7e) for  $V^*$  may be performed graphically (Hillier and Walkley 1965, Jenkins 1966), but in the work described here use was made of a Newton-Raphson iterative technique. This allows the calculations to be performed completely by machine and to any desired degree of accuracy. The iteration formula may be written:

$$V_{k+1}^* = V_k^* \left\{ 1 + \chi_T^*(V_k^*, T^*) [p^* - p^*(V_k^*, T^*)] \right\} \quad (4.8)$$

where  $V_k^*$  and  $V_{k+1}^*$  are, respectively,  $k$ th and  $(k+1)$ th approximations to the reduced volume  $V^*$  corresponding to a reduced pressure  $p^*$  and a reduced temperature  $T^*$ , and  $p^*(V_k^*, T^*)$  and  $\chi_T^*(V_k^*, T^*)$  are calculated through (3.7e) and (3.7f) for a reduced volume  $V_k^*$  and reduced temperature  $T^*$ .

The numerical procedure for the calculation of the thermodynamic properties was incorporated in the same computer programs as were used for the determination of the potential parameters. It is briefly summarised below.

The values of  $p^*$  and  $T^*$  for which calculations are to be performed are input as datum numbers, together

with an approximate value of  $V^*$ , the value of the quantum parameter  $\Lambda^*$  and, in the case of EXP-6 calculations, the value of the parameter  $\alpha$ . After calculating the value of  $a_1^*$  corresponding to the input value of  $V^*$ , the static lattice terms,  $w^*(o)$ ,  $dw^*(o)/da_1^*$  and  $d^2w^*(o)/da_1^{*2}$  are evaluated from whichever of (2.30) and (2.32) is appropriate, using a similar approach to that employed for the calculation of the static lattice terms in the characterisation procedure. Following this, the derivatives of  $w^*(o)$  with respect to  $a_1^*$  are converted to those with respect to  $V^*$  by use of relations of the same form as (3.10) and (3.11).

Now the reduced energy levels  $\lambda_{1,n}^*$  ( $l=0,1,2,\dots$ ;  $n=0,1,2,\dots$ ) and their first and second derivatives with respect to  $V^*$  are calculated for the value of  $a_1^*$  corresponding to the input value of  $V^*$ , using whichever of (2.35) and (2.37a) is appropriate for the evaluation of  $\overline{w^*(R^*)}$ , this quantity being calculated for a number of shells of neighbours specified in the input data. For any  $(l,n)$ , the values of  $\lambda_{1,n}^*$ ,  $d\lambda_{1,n}^*/da_1^*$  and  $d^2\lambda_{1,n}^*/da_1^{*2}$  are calculated through the WKB relations (3.20), (3.17) and (3.18), using the same iteration procedure for the solution of (3.20) and the same method of quadrature as was employed for the calculation of the  $l=0, n=0$  energy level terms in the determination of the potential parameters. The derivatives of  $\lambda_{1,n}^*$  with respect to  $a_1^*$  are transformed to the corresponding ones with respect to  $V^*$  by use of (3.10) and (3.11).

The organisation of the computation of the energy level terms is such that calculations are performed

for  $n=0,1,2,\dots$  etc. keeping  $l$  constant at  $0,1,2,\dots$  etc. in turn. An approximate value of  $\lambda_{0,0}^*$  is either input as a datum number or calculated in the program using the harmonic approximation. The first approximation to  $\lambda_{1,0}^*$  is calculated by multiplying the previously iterated value of  $\lambda_{0,0}^*$  by a constant specified in the input data. For  $l > 1$ , the first approximation to  $\lambda_{1,0}^*$  is given by linear extrapolation of the values of  $\lambda_{1-2,0}^*$  and  $\lambda_{1-1,0}^*$ . The approximate values of the turning points,  $R_1^*$  and  $R_2^*$  corresponding to  $\lambda_{1,0}^*$  for each value of  $l$  are calculated by scanning the function  $Q^*$  (see (3.9a)), noting where it changes sign and applying the "method of similar triangles". For  $n > 0$ , the approximate value of  $\lambda_{1,n}^*$  is taken as the previously iterated value of  $\lambda_{1,n-1}^*$  and the approximate values of  $R_1^*$  and  $R_2^*$  as those corresponding to  $\lambda_{1,n-1}^*$ . For each  $l$  value, the increase of  $n$  is terminated when, for some value of  $n$ ,  $\lambda_{1,n}^*$  is greater than or equal to a quantity,  $\lambda_{\max}^*$ , input as a datum number. When this is the case, the eigenvalues and their volume derivatives corresponding to the current value of  $l$  are stored,  $n$  reset to zero,  $l$  increased by unity, and the calculations continued. The complete termination of eigenvalue calculations occurs when, for some value of  $l$ ,  $\lambda_{1,0}^* \geq \lambda_{\max}^*$ . Following this, the values of  $\lambda_{1,n}^*$ ,  $d\lambda_{1,n}^*/dV^*$  and  $d^2\lambda_{1,n}^*/dV^{*2}$  ( $l=0,1,2,\dots$ ;  $n=0,1,2,\dots$ ) are removed from store, the appropriate sums over  $l$  and  $n$  formed and checked to be accurate to a specified accuracy limit and the iteration formula (4.8) applied to give a better value of  $V^*$ .

The above procedure is repeated until  $V^*$  is iterated to an accuracy specified in the input data, the first approximation to  $\lambda_{0,0}^*$  for the  $k$ th value of reduced volume,  $V_k^*$ , being taken as the value of  $\lambda_{0,0}^*$  appropriate to the  $(k-1)$ th value,  $V_{k-1}^*$ . Using the values of  $\lambda_{1,n}^*$ ,  $d\lambda_{1,n}^*/dV^*$  and  $d^2\lambda_{1,n}^*/dV^{*2}$  ( $l=0,1,2,\dots$ ;  $n=0,1,2,3,\dots$ ) appropriate to the final value of  $V^*$ , other thermodynamic properties are evaluated by forming the appropriate sums over  $l$  and  $n$  and using expressions (3.7a) to (3.7h).

The results of the calculations for the EXP-6 and LJ 12:6 potential functions are tabulated in Appendix 4 and plotted as the full and dashed curves respectively in Figs. 8a-8g for neon, 9a-9g for argon, 10a-10g for krypton and 11a-11g for xenon. In each case, the figures labelled a-f give plots of the zero pressure values of the lattice constant,  $a_0$ , isothermal compressibility,  $\chi_T (= -(1/V)(\partial V/\partial p)_T)$ , volume expansivity,  $\beta (= (1/V)(\partial V/\partial T)_p)$ , isochoric specific heat,  $C_v$ , isobaric specific heat,  $C_p$ , and entropy,  $S$ , respectively as functions of temperature,  $T$ . Those labelled g give the variation of molar volume,  $V$ , normalised by the zero pressure value,  $V(0)$ , with pressure,  $p$ , at a specified temperature -  $4^\circ\text{K}$  for neon,  $77^\circ\text{K}$  for argon and krypton and  $150^\circ\text{K}$  for xenon. The reason a plot of  $V/V(0)$  versus  $p$  is given rather than one of  $V$  versus  $p$ , is that the removal of temperature dependence at zero pressure by normalisation with respect to  $V(0)$  gives a clearer picture of the effect of pressure.

The results were obtained by determining sufficient eigenvalues to cause the required sums over  $l$  and  $n$  to converge to an accuracy of at least  $10^{-3}\%$  and using an iteration accuracy of  $10^{-2}\%$  for the evaluation of  $V^*$ . They are consistent with the results of the characterisation calculations in that the parts in the EXP-6 static lattice terms corresponding to repulsion were calculated over sufficient shells of neighbours to give an accuracy of  $10^{-2}\%$  and the reduced eigenvalues were iterated to an accuracy of  $10^{-2}\%$  using values of the turning points iterated to  $10^{-3}\%$ . Again 10 Gauss-Mehler quadrature intervals proved sufficient for the accurate evaluation of the integrals required and the results are for three shells of neighbours included in the calculation of  $\overline{w^*(R^*)}$ , which, as mentioned before, is sufficient to lead to results insignificantly different from those given by calculations involving more distant neighbours.

Before detailed calculations of thermodynamic properties were undertaken, the accuracy of the WKB solution of the EXP-6 radial equation was verified by comparison with the results given by the "exact" finite difference technique given by Hillier, Islam and Walkley (1965) and fully described in Appendix 2. The comparison was made for solid neon at the triple point, the finite difference calculations being performed by use of the parameters given in Table 1 and the value of  $V^*$  given by WKB calculations. It was found that agreement between the WKB and finite difference eigenvalues was close for all  $l$  and  $n$  values considered ( $l=0-12$ ,  $n=0-6$ ) and that the accuracy of the WKB approximation, as expected from



its asymptotic nature (see Chapter 3), increased with increasing  $l$  and  $n$ . For  $l=0, n=0$  the difference between the two results was 1%, for  $l=0, n=6$ , 0.1% and for  $l=12, n=0$ , 0.06%. Differences of this order in the eigenvalues lead to insignificant changes in the values of thermodynamic properties which are not dependent on volume derivatives, the difference between the results of the two calculations for  $U$ ,  $S$  and  $C_v$  being only 0.5%, 0.25% and <sup>less than</sup> 0.1% respectively. Since the effect of anharmonicity is most pronounced in solid neon at its triple point and it is known that the WKB method becomes progressively more exact as the vibrations become more harmonic (see Chapter 3), we may be sure that the results from our other WKB calculations are accurate within the limits of the cell theory. As mentioned in Chapter 3, the accuracy of the WKB approximation in LJ 12:6 calculations has been established by Hillier and Walkley (1964).

The experimental data plotted in Figures 8a-11g are tabulated in Appendix 5 and are, in the author's opinion, the most reliable at present available. For the sources from which they are taken, the reader is referred either to the figures themselves or to Appendix 5. The experimental points in graphs of  $C_v$  and  $S$  versus  $T$  do not come directly from experimental measurements but are calculated through the thermodynamic relations:

$$C_p = C_v + \int_0^T TV/\chi_T^2 \quad (4.9)$$

and

$$S = \int_0^T (C_p/T) dT \quad (4.10)$$

respectively, using experimental values of  $C_p$ ,  $\beta$ ,  $V$  and  $\chi_T$ . Since it was felt that, in the case of krypton and xenon, the experimental data available are not sufficiently accurate for a reasonable estimate of  $\beta^2 TV / \chi_T$  to be made, no experimental points are given in the  $C_v$  versus  $T$  plots for these substances. Experimental error limits have been indicated where these are quoted and appreciable on the scale of the figures. For the moment, the reader is asked to ignore the dashed-dotted curves in Figs. 8a-11g.

Fig. 8a. Solid neon - lattice constant,  $a_0$ , as a function of temperature,  $T$ , at zero pressure

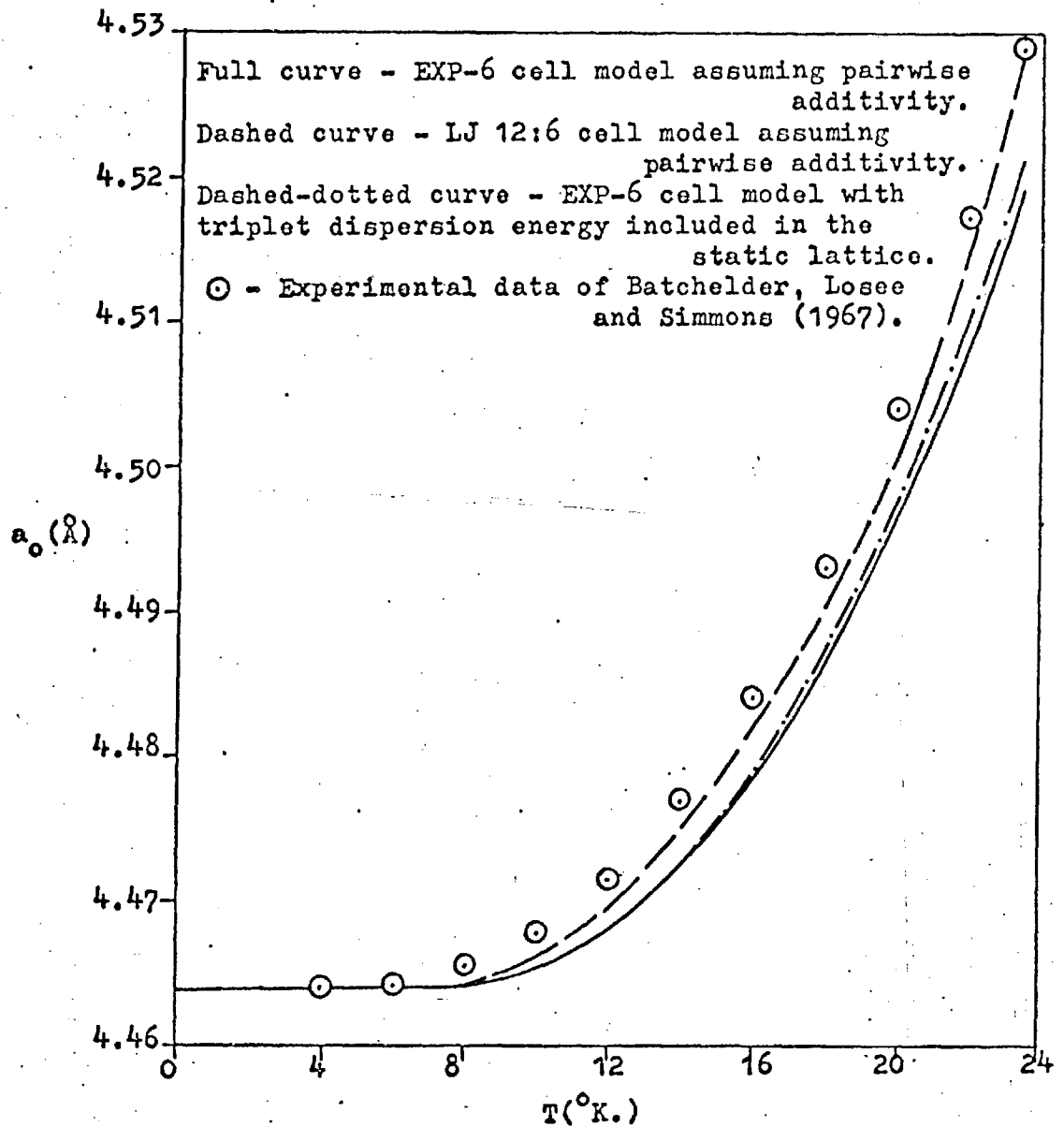


Fig.8b. Solid neon - isothermal compressibility,  $\chi_T$ , as a function of temperature,  $T$ , at zero pressure

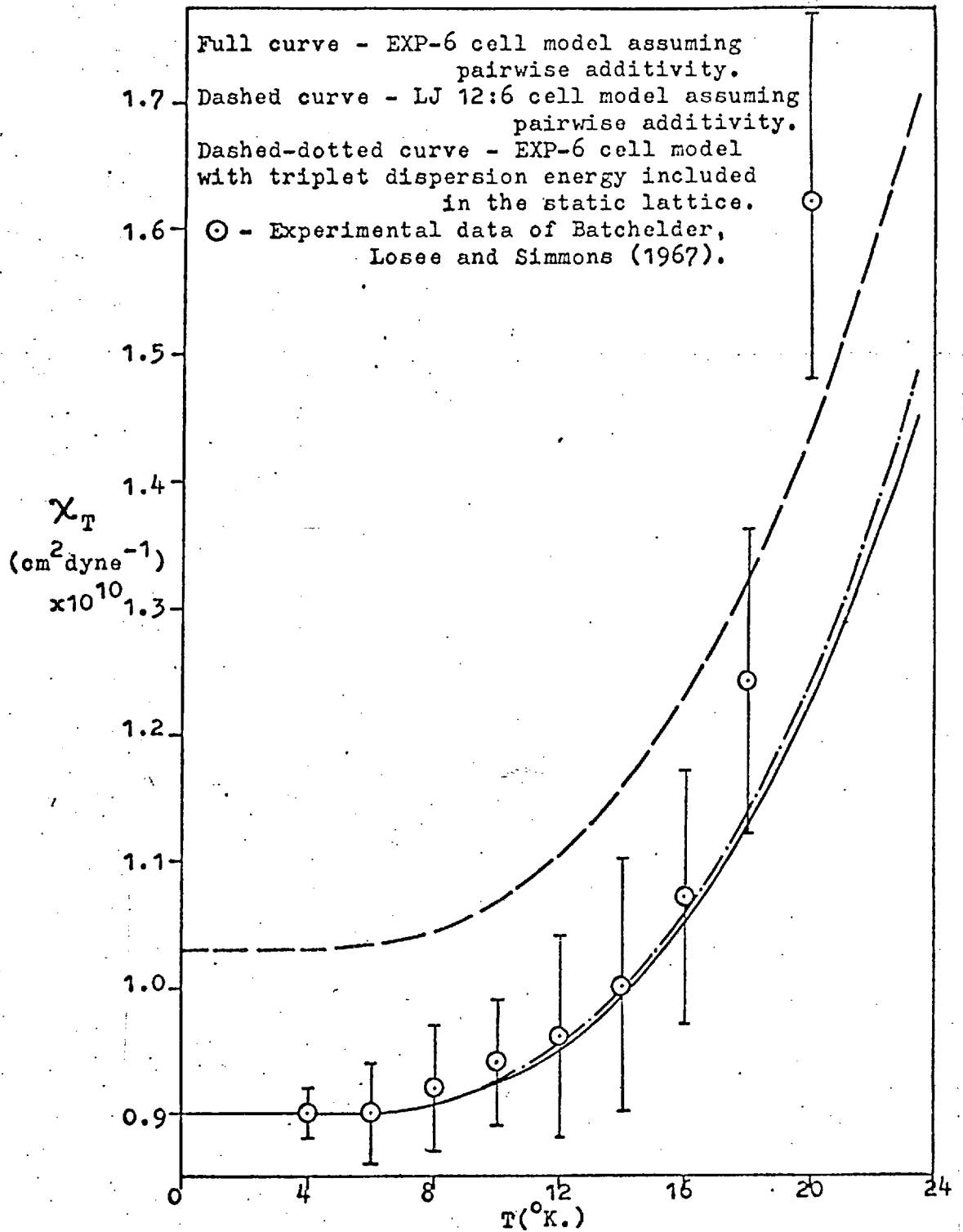


Fig. 8c. Solid neon - volume expansivity,  $\beta$ , as a function of temperature,  $T$ , at zero pressure

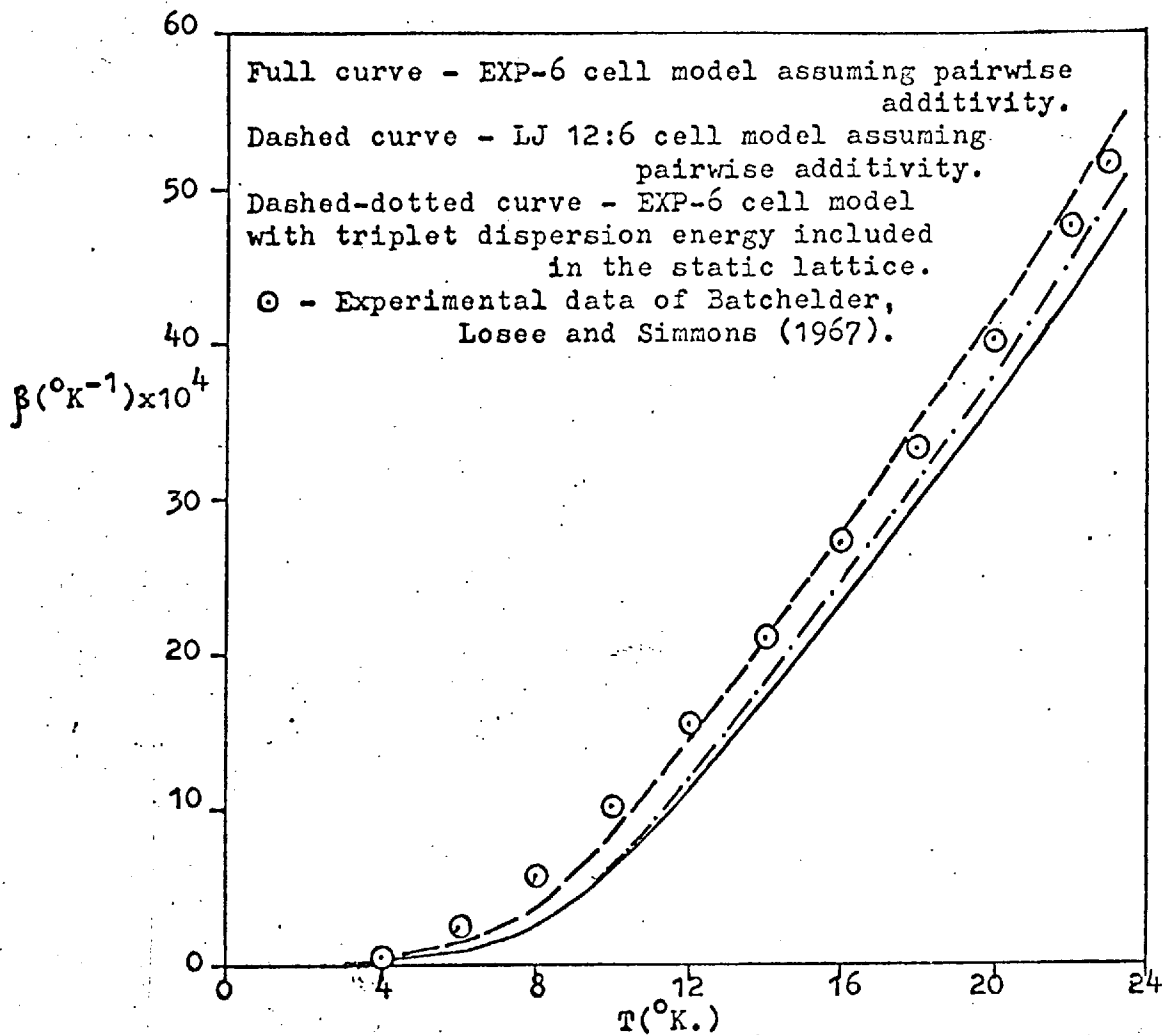


Fig. 8d. Solid neon - isochoric specific heat,  $C_v$ , as a function of temperature,  $T$ , at zero pressure

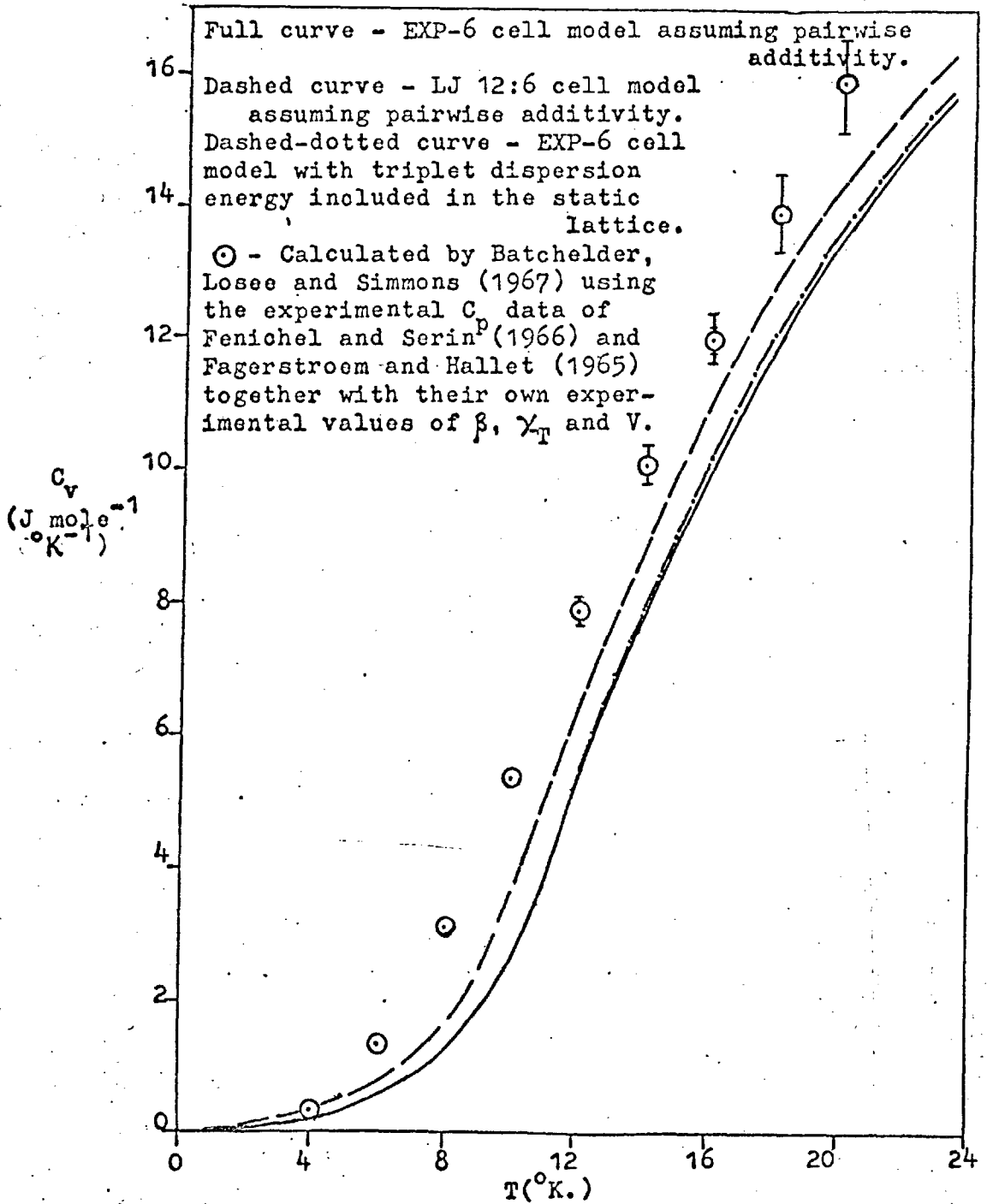


Fig. 8e. Solid neon - isobaric specific heat,  $C_p$ , as a function of temperature,  $T$ , at zero pressure

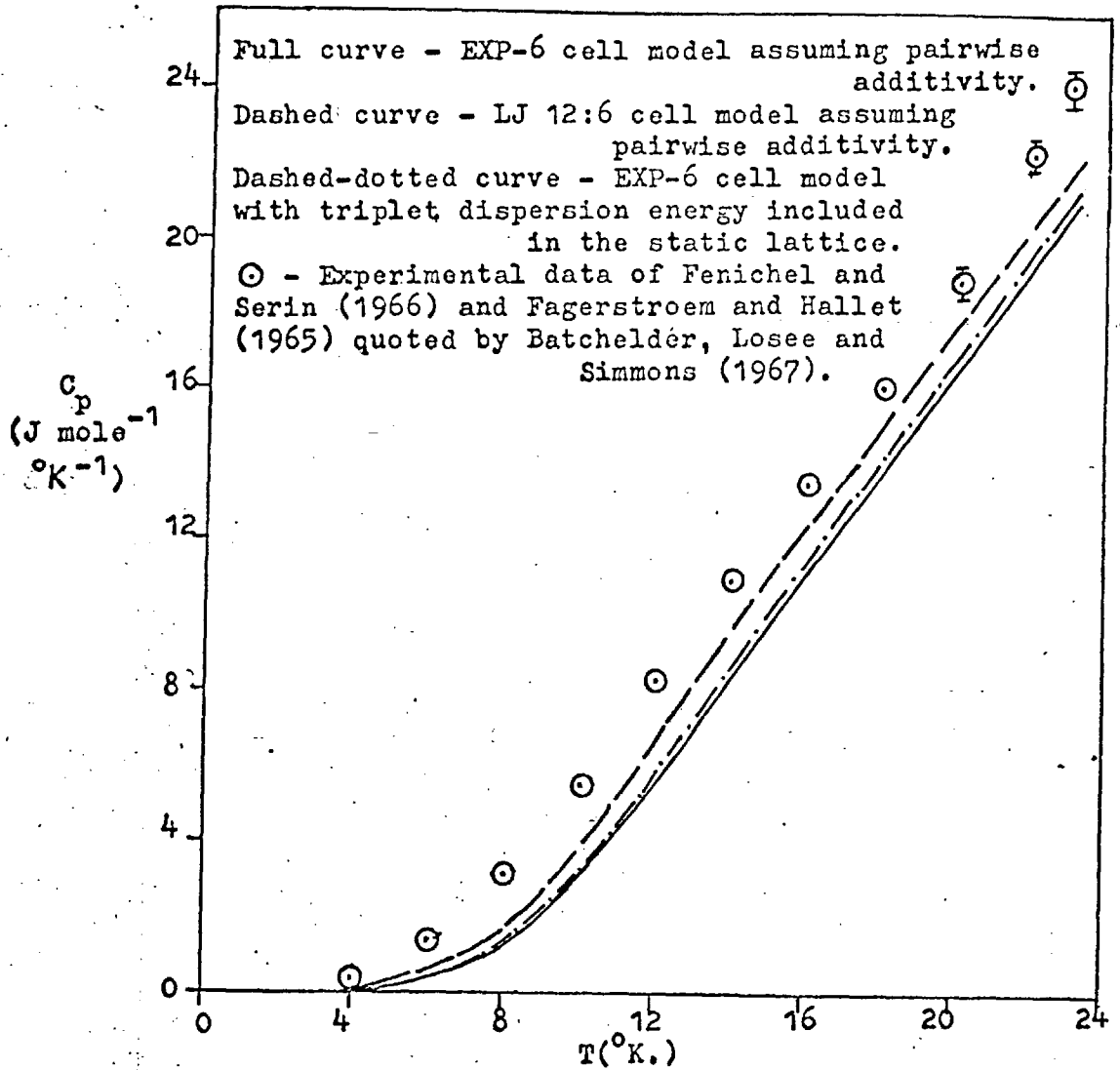


Fig. 8f. Solid neon - entropy,  $S$ , as a function of temperature,  $T$ , at zero pressure

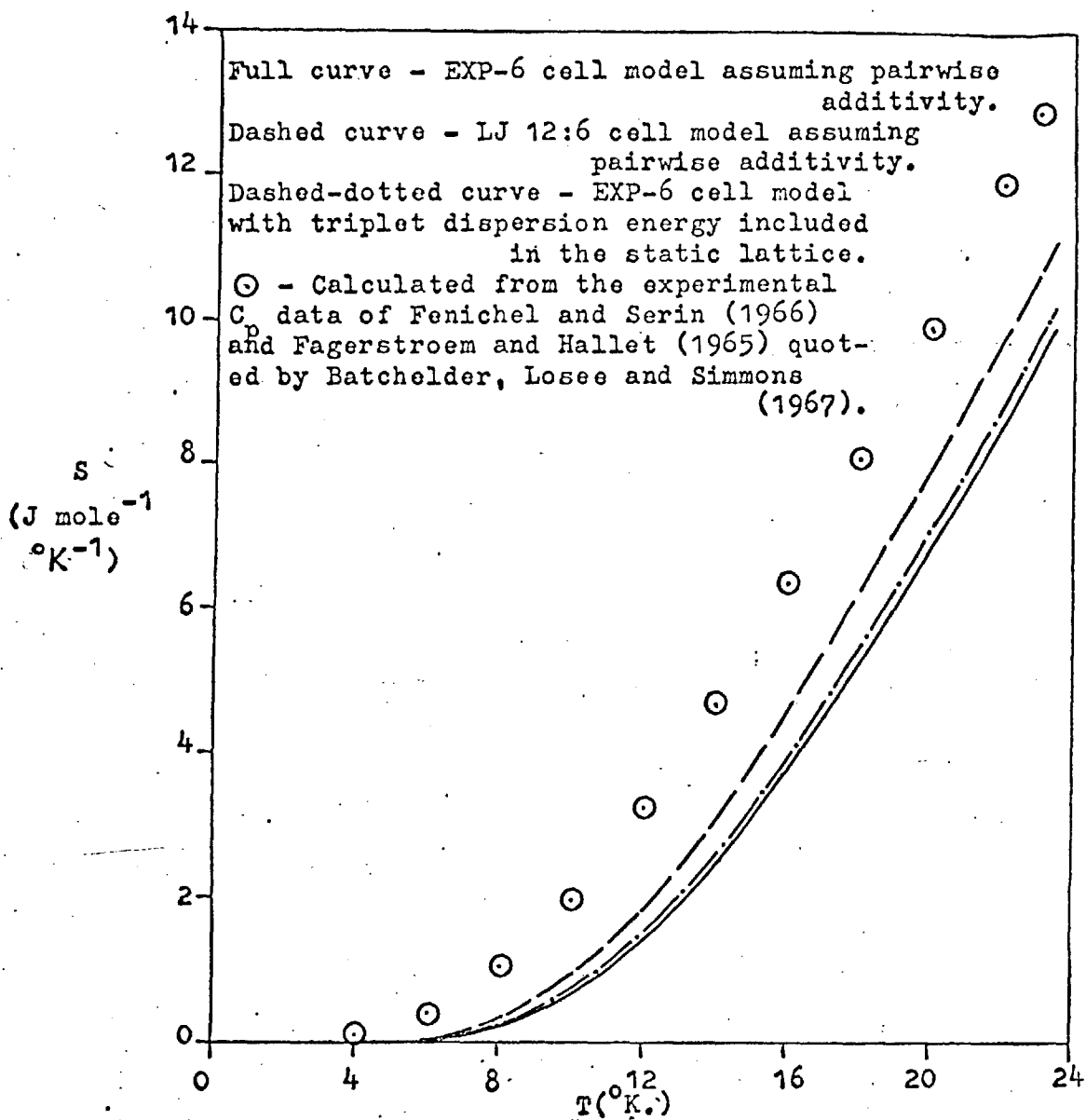




Fig. 8g Solid neon - molar volume,  $V$ , normalised by the zero pressure molar volume,  $V(0)$ , as a function of pressure,  $p$ , at  $4^\circ\text{K}$ .

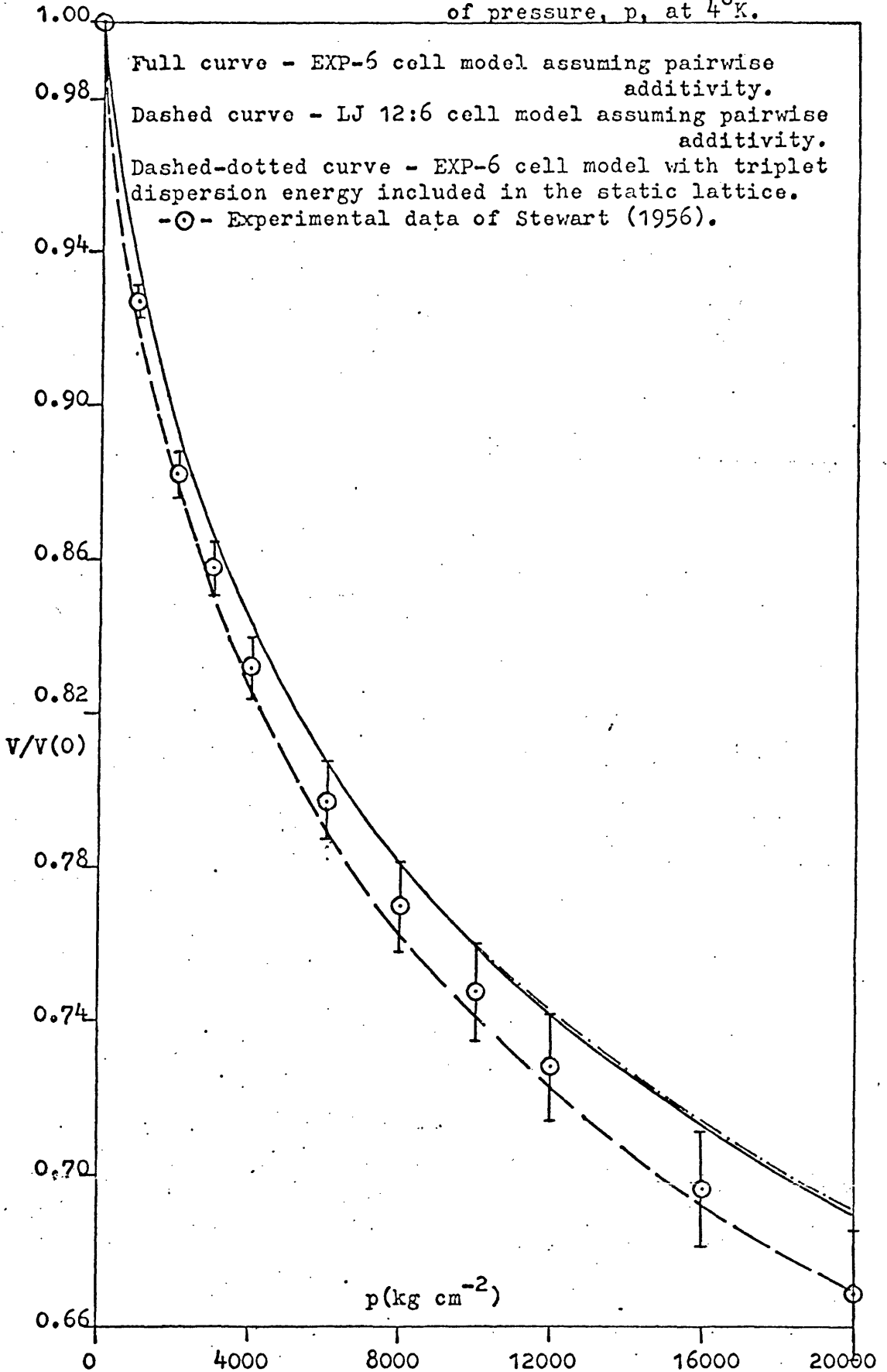


Fig. 9a. Solid argon - lattice constant,  $a_0$ , as a function of temperature,  $T$ , at zero pressure

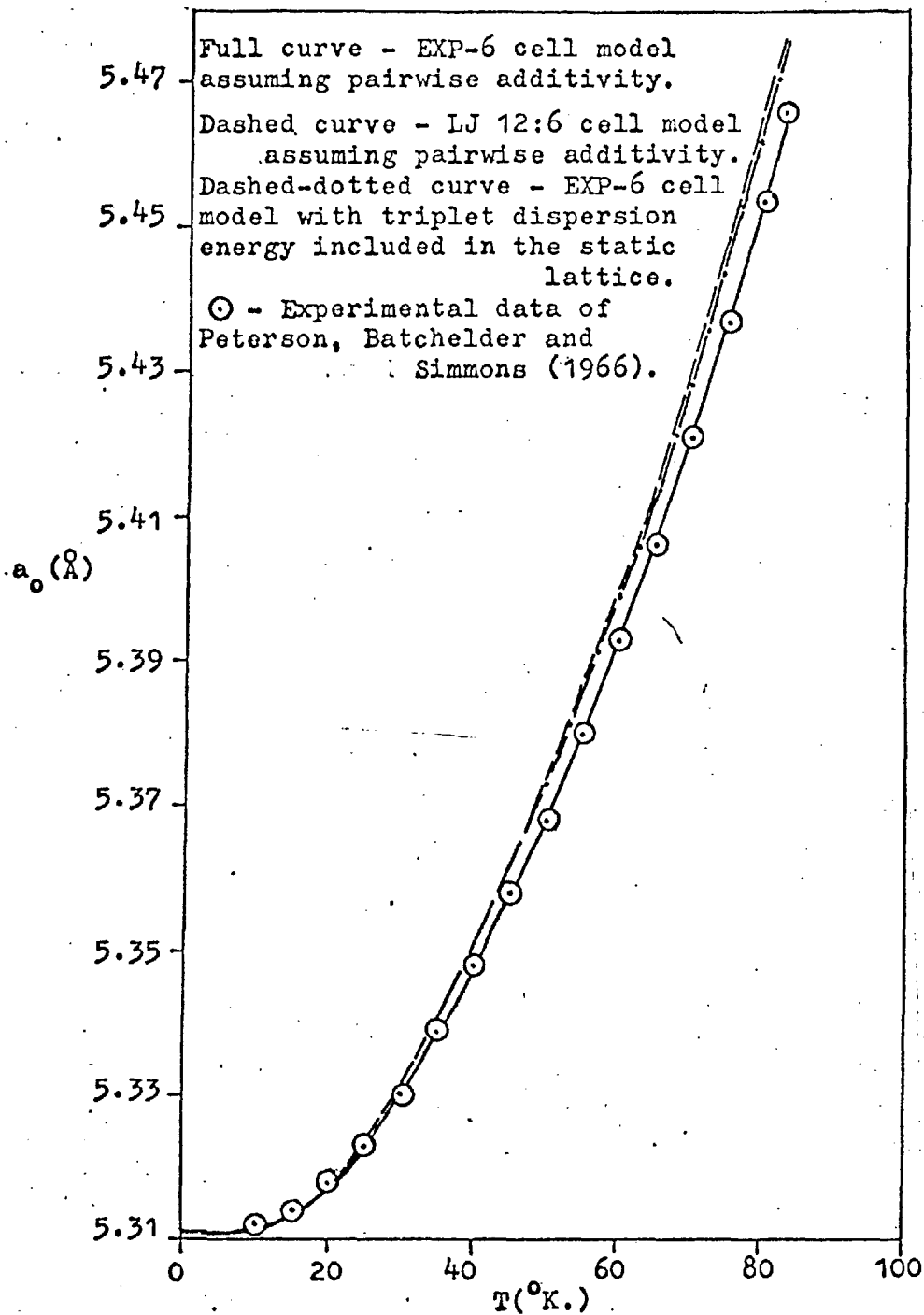


Fig. 9b. Solid argon - isothermal compressibility,  $\chi_T$ , as a function of temperature,  $T$ , at zero pressure

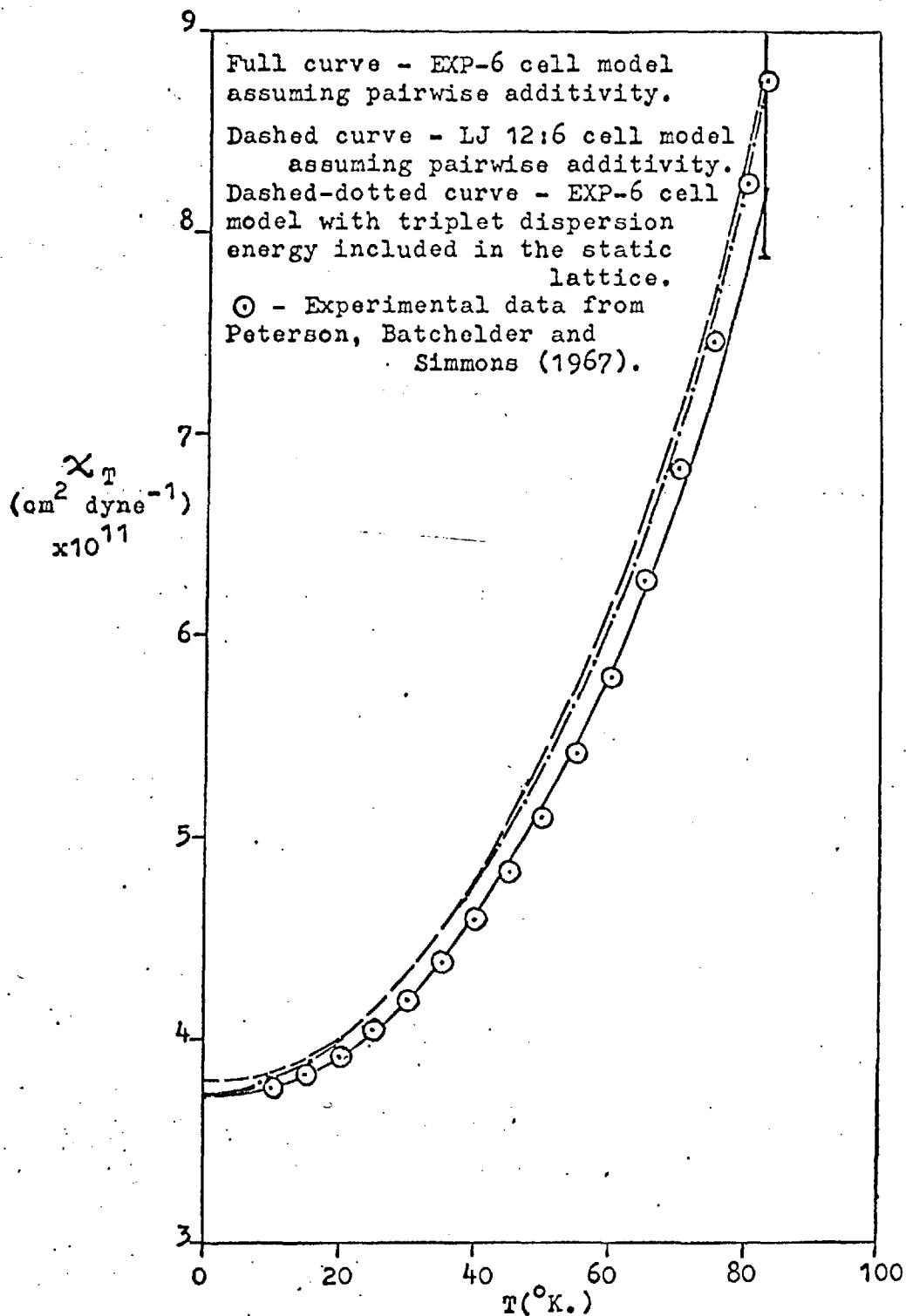


Fig.9c. Solid argon - volume expansivity,  $\beta$ , as a function of temperature, T, at zero pressure

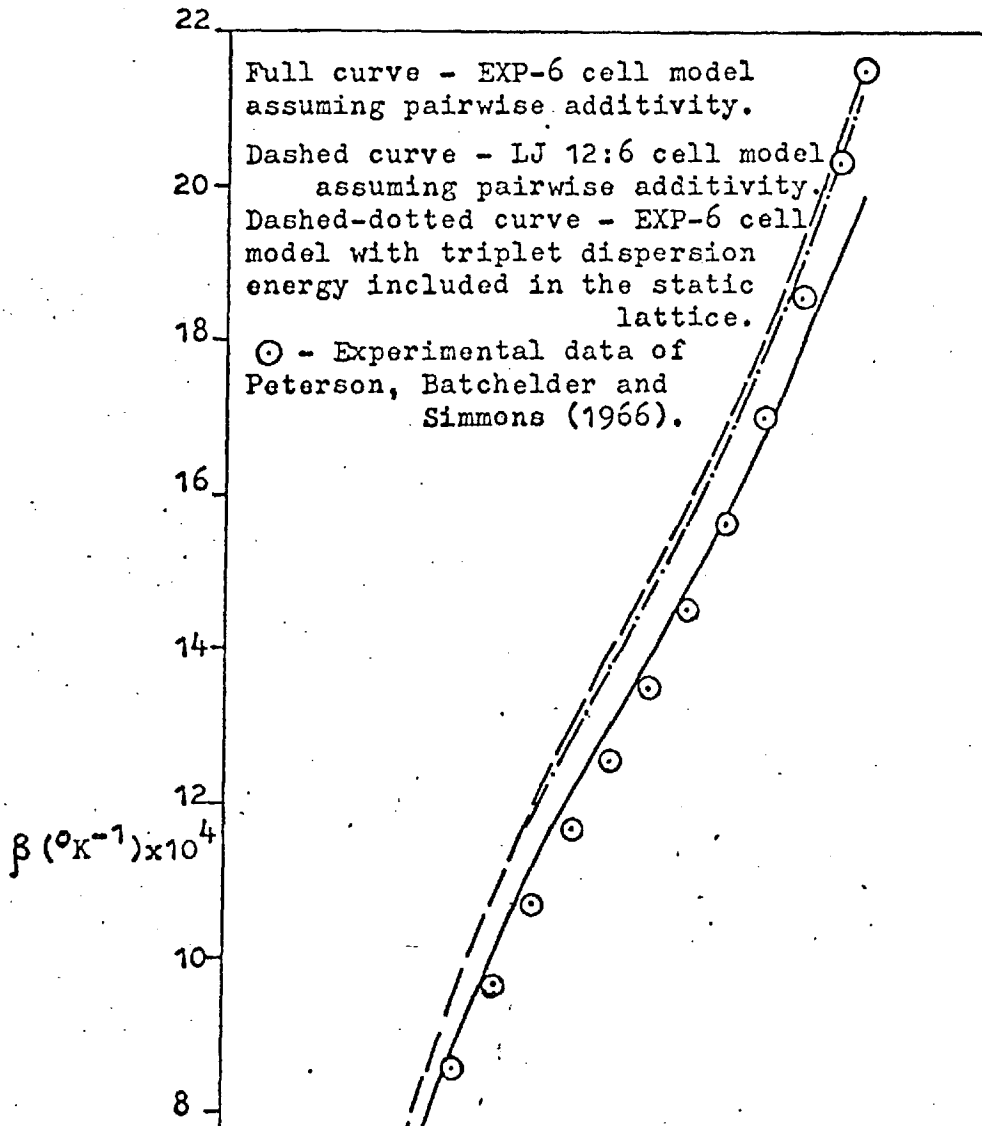


Fig. 9d. Solid argon - isochoric specific heat,  $C_v$ , as a function of temperature,  $T$ , at zero pressure.

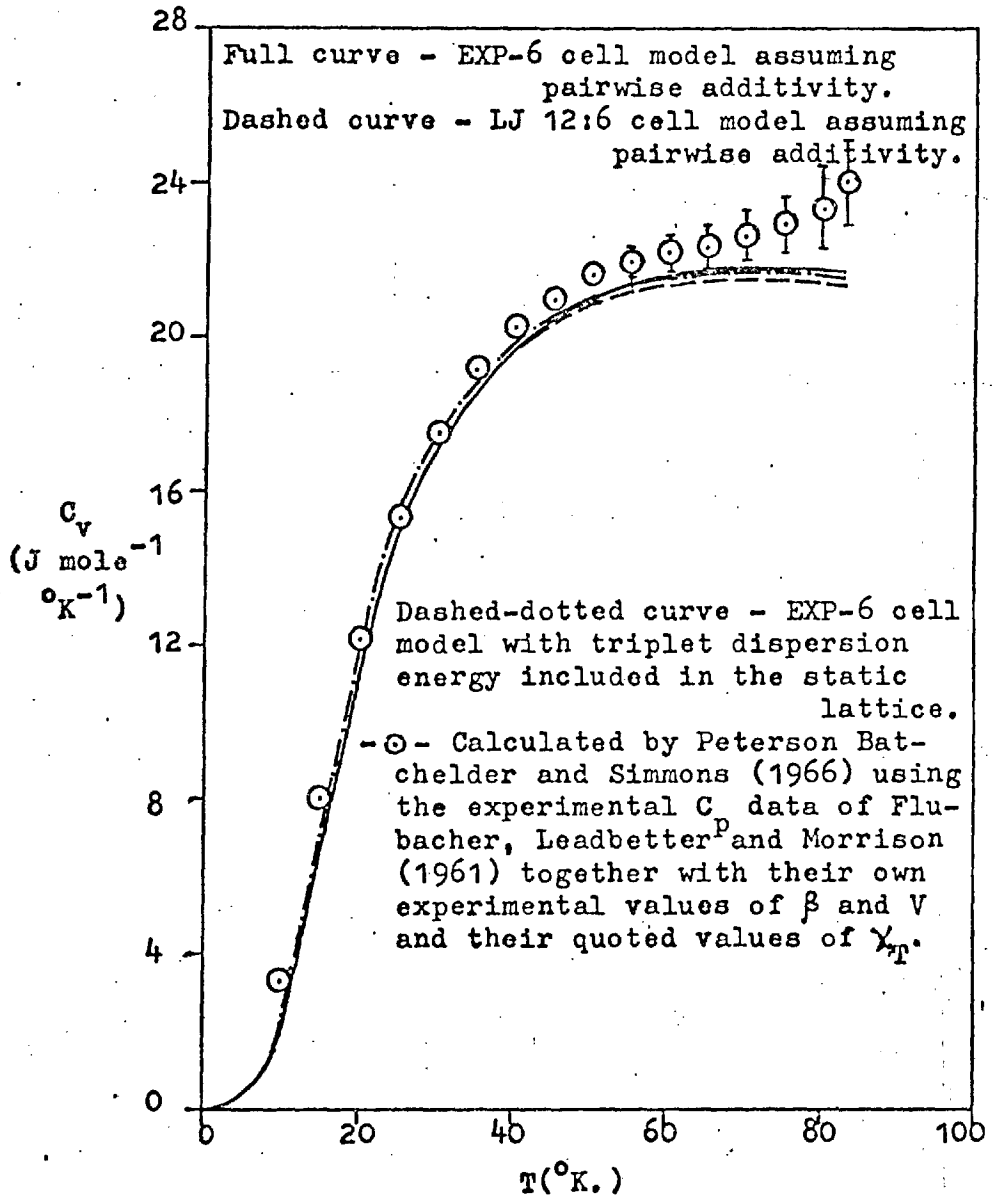


Fig. 9e. Solid argon - isobaric specific heat,  $C_p$ , as a function of temperature,  $T$ , at zero pressure .

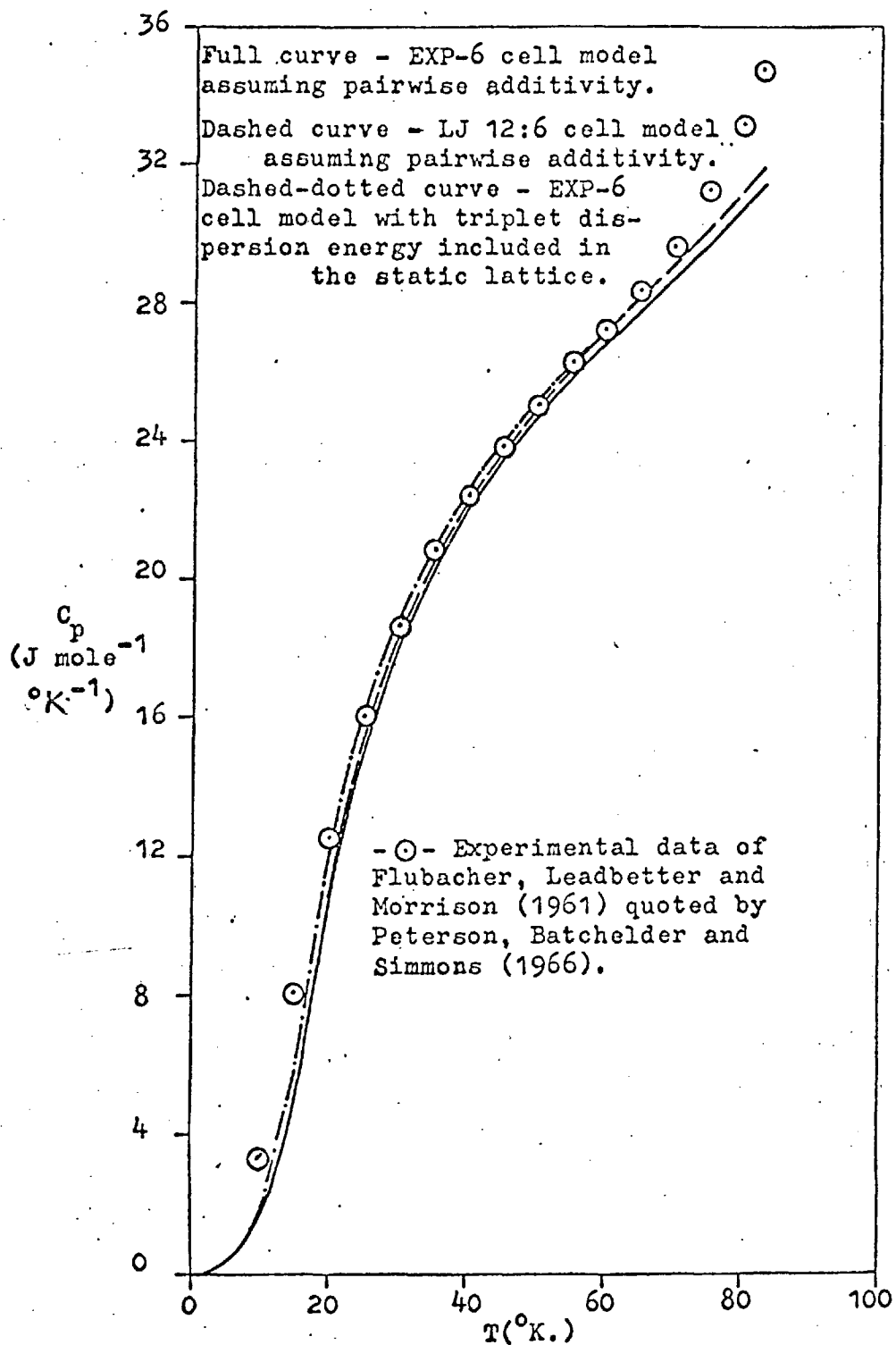


Fig. 9f. Solid argon - entropy,  $S$ , as a function of temperature,  $T$ , at zero pressure

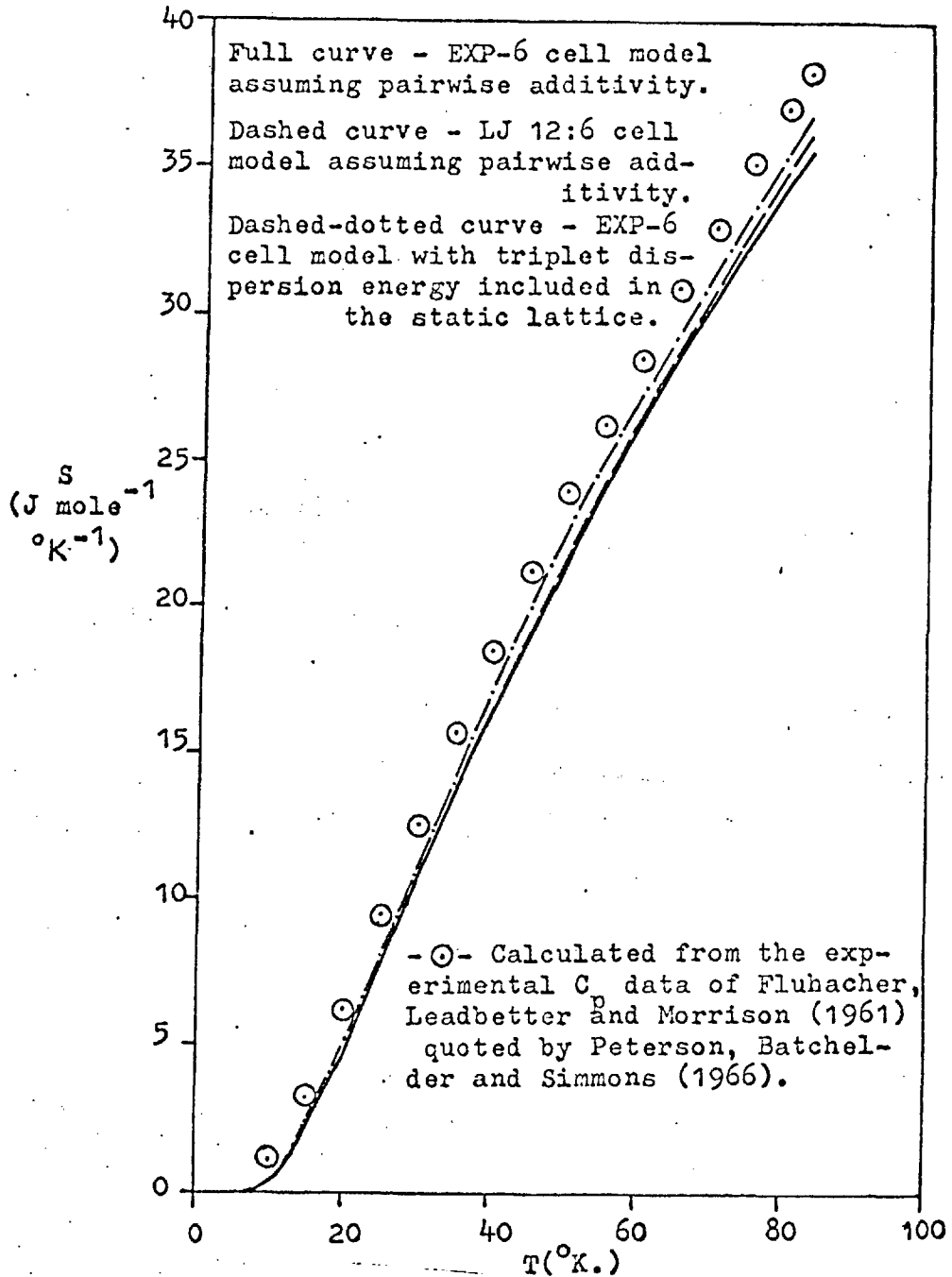


Fig. 9g. Solid argon - molar volume,  $V$ , normalised by the zero pressure molar volume,  $V(0)$ , as a function of pressure,  $p$ , at  $77^{\circ}\text{K}$ .

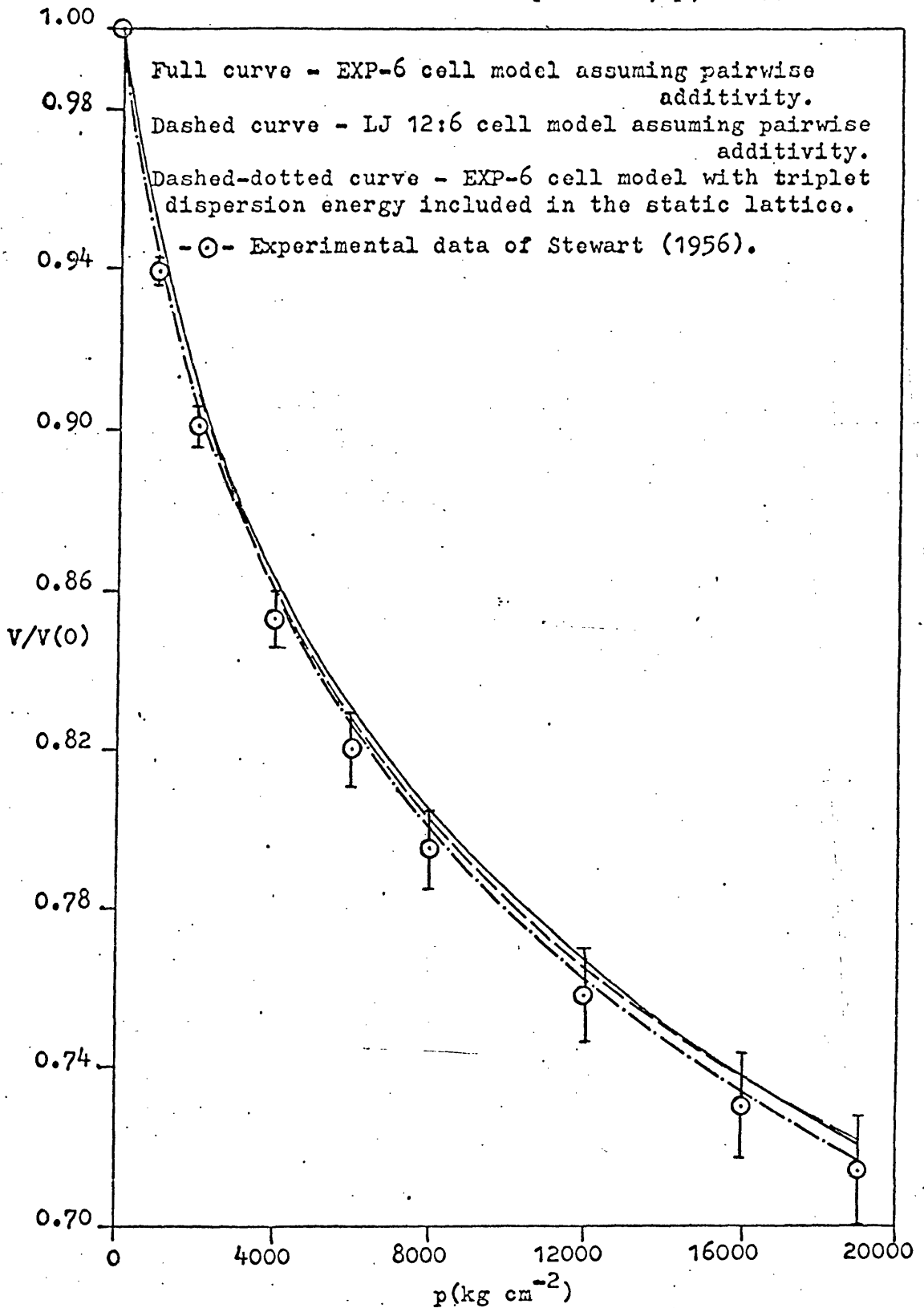




Fig.10a. Solid krypton - lattice constant,  $a_0$ , as a function of temperature,  $T$ , at zero pressure

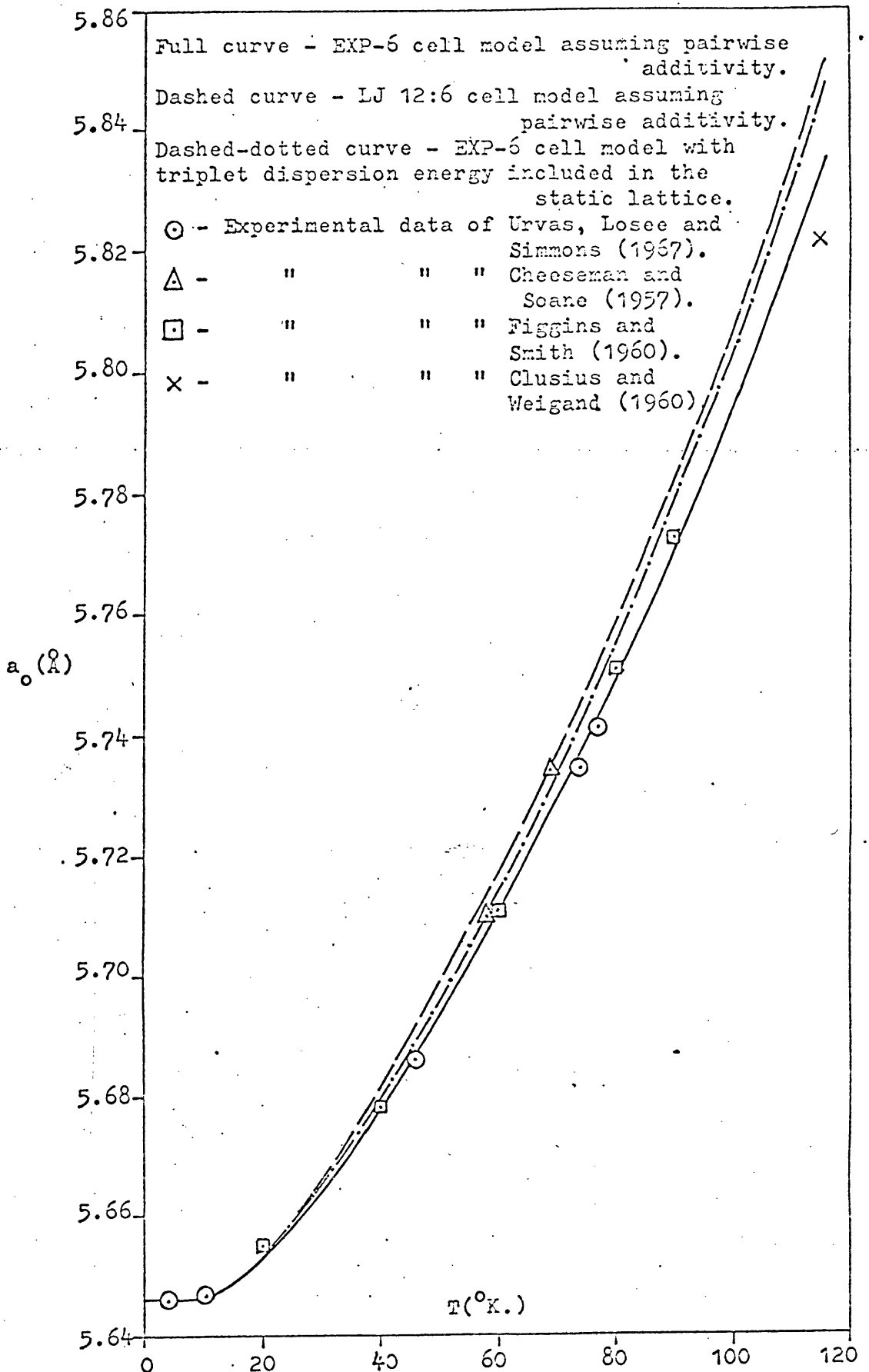


Fig.10b. Solid krypton - isothermal compressibility,  $\chi_T$ , as a function of temperature,  $T$ , at zero pressure

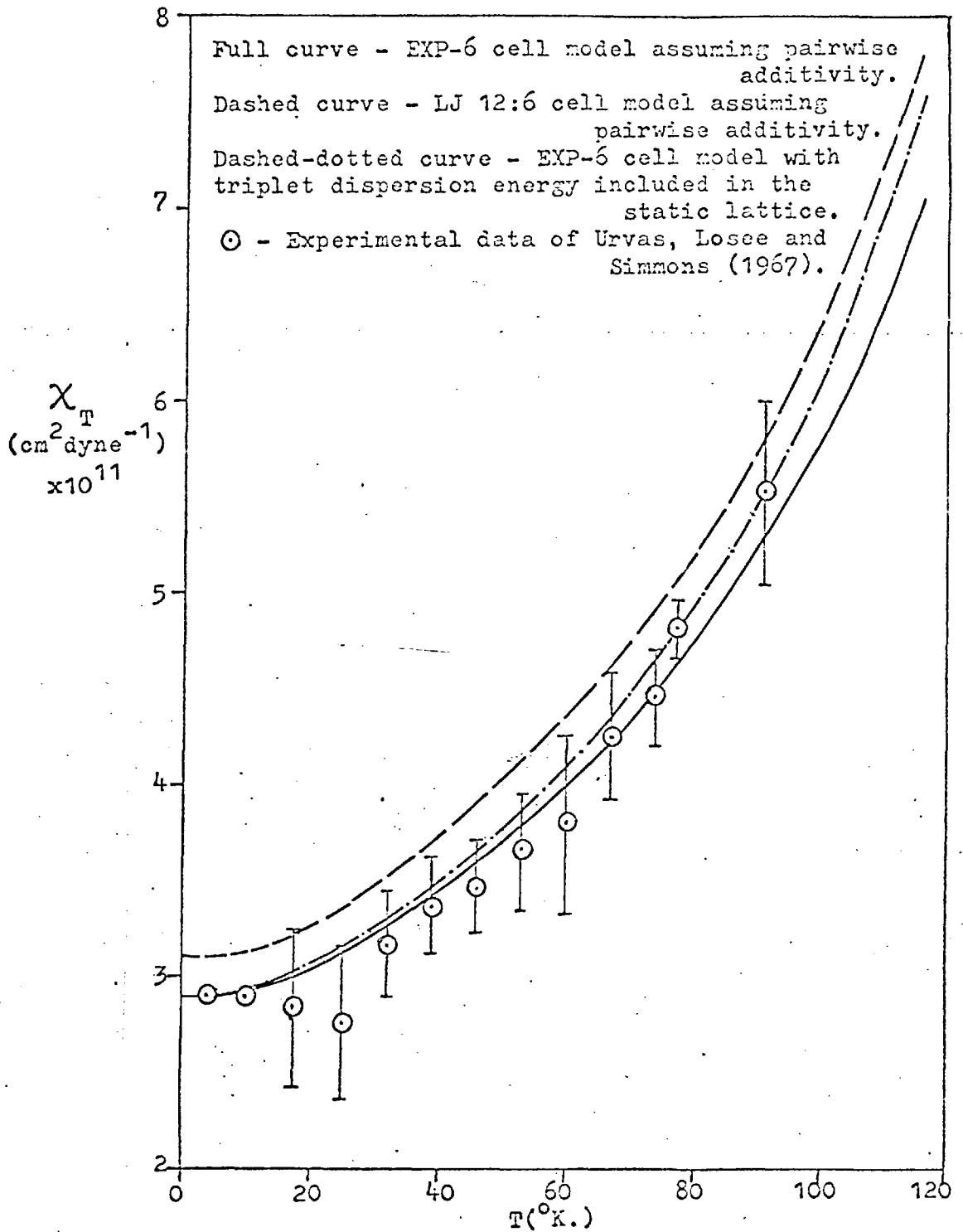


Fig. 10c. Solid krypton - volume expansivity,  $\beta$ , as a function of temperature,  $T$ , at zero pressure

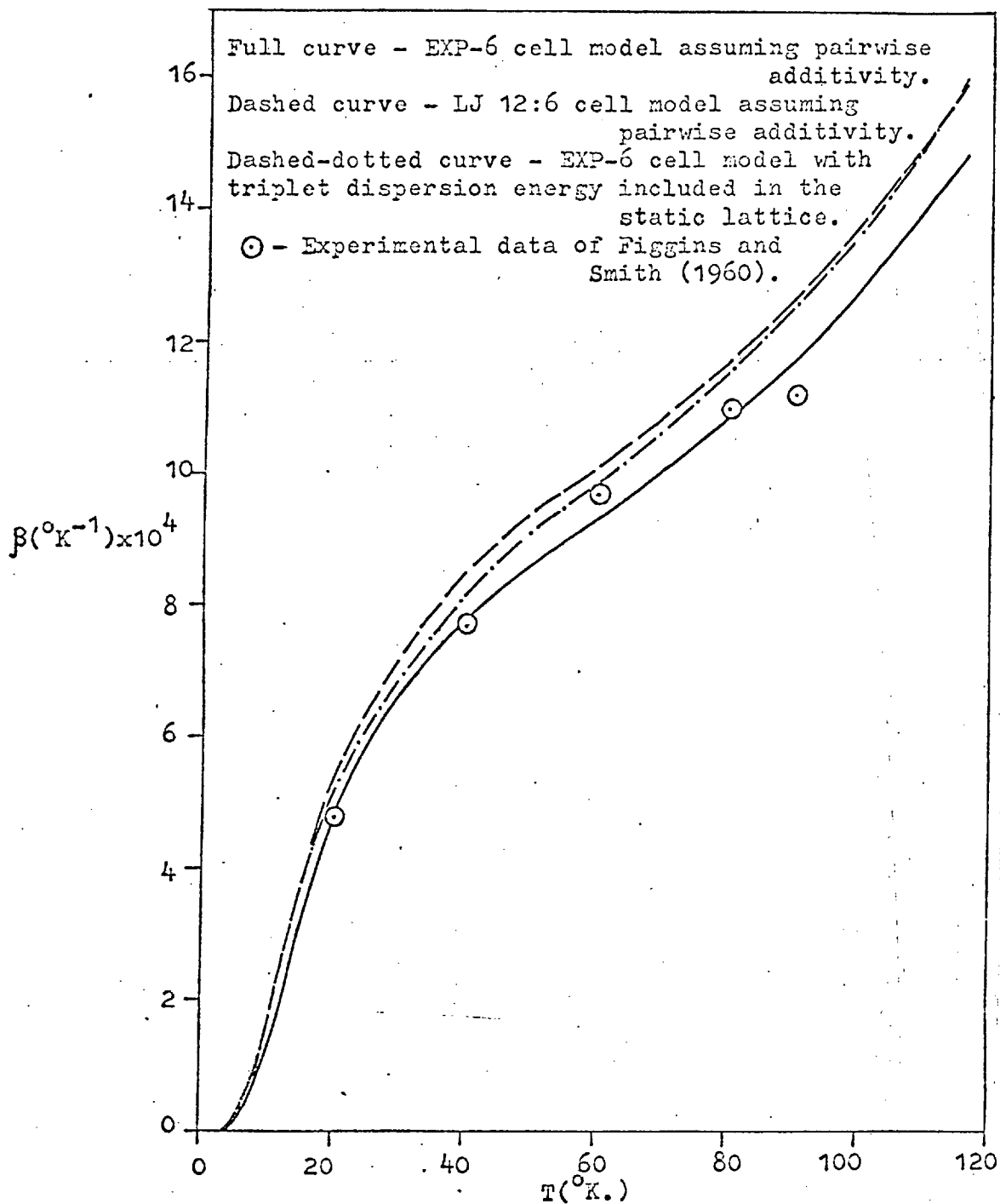


Fig.10d. Solid krypton - isochoric specific heat,  $C_V$ , as a function of temperature,  $T$ , at zero pressure

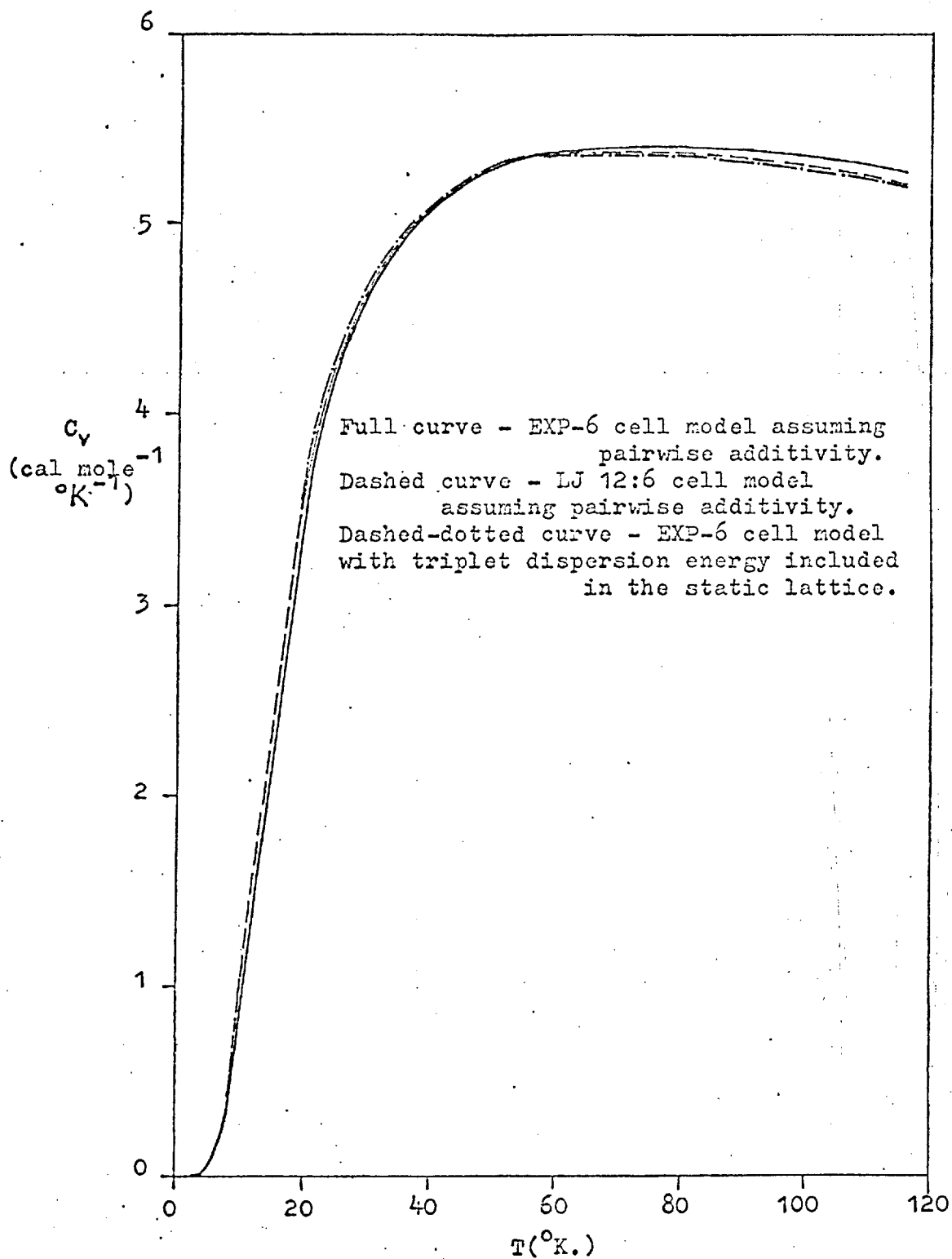


Fig. 10e. Solid krypton - isobaric specific heat,  $C_p$ , as a function of temperature,  $T$ , at zero pressure

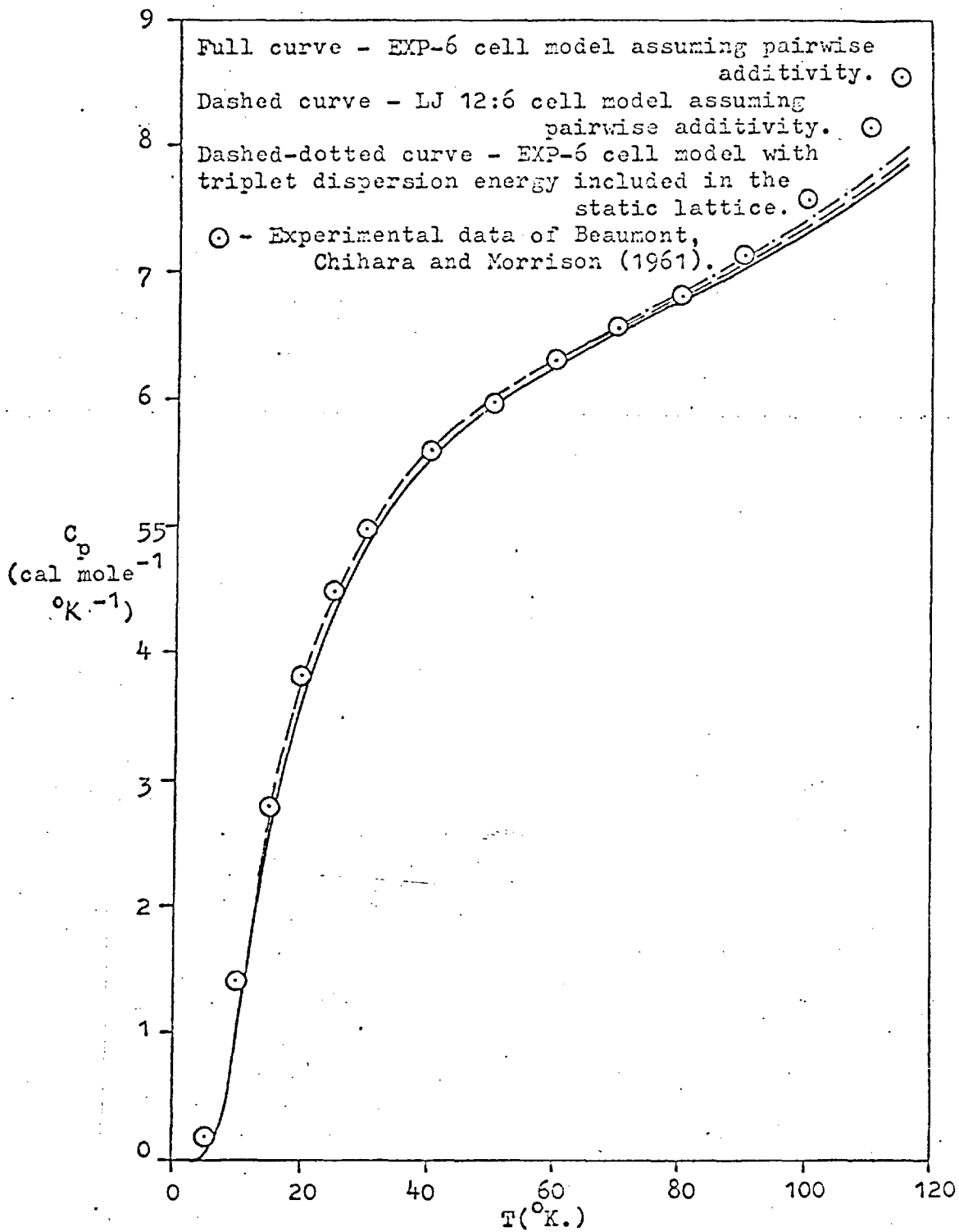


Fig. 10f. Solid krypton - entropy,  $S$ , as a function of temperature,  $T$ , at zero pressure

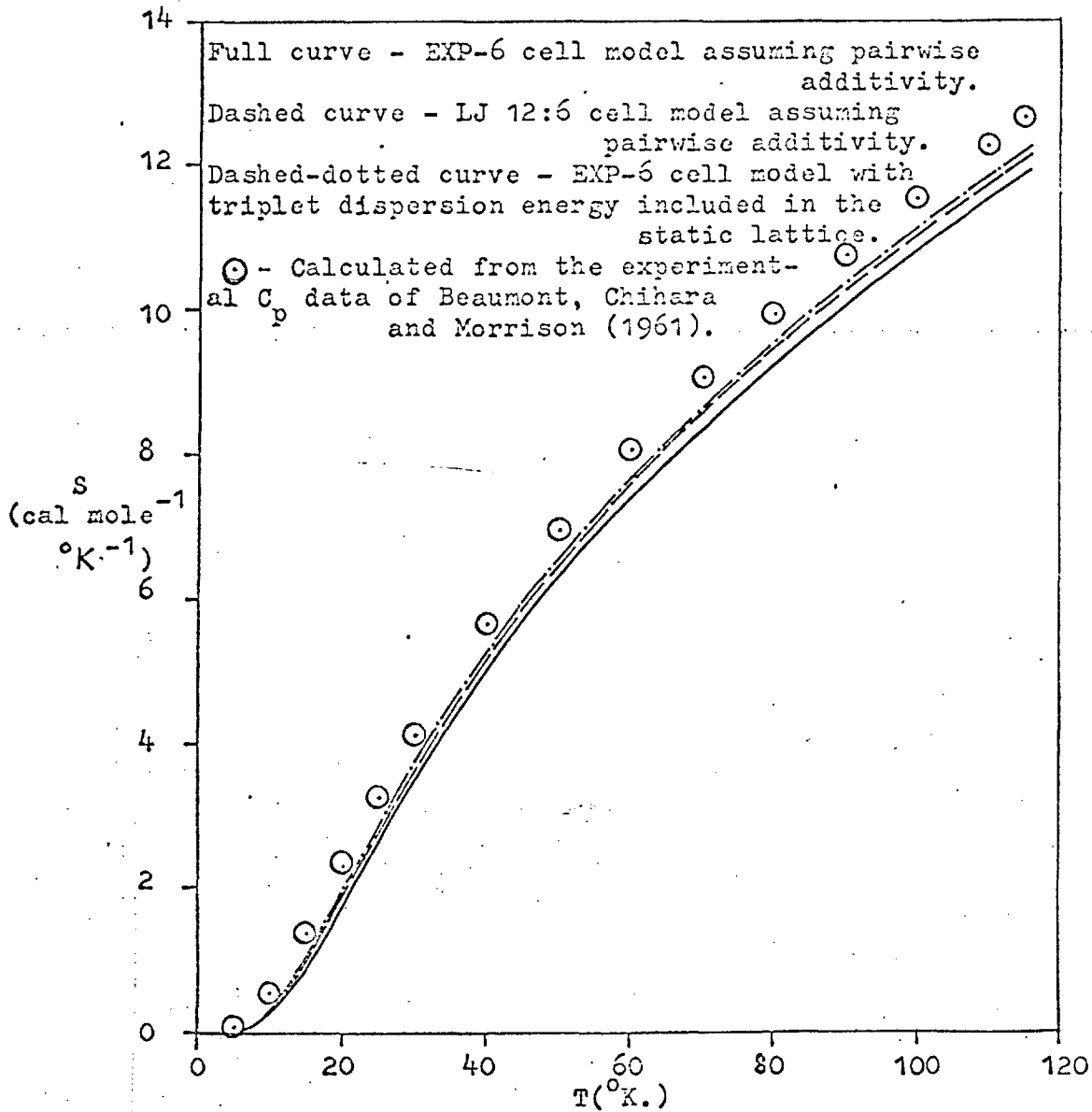


Fig. 10g. Solid krypton - molar volume,  $V$ , normalised by the zero pressure molar volume,  $V(0)$ , as a function of pressure,  $p$ , at  $77^\circ\text{K}$ .

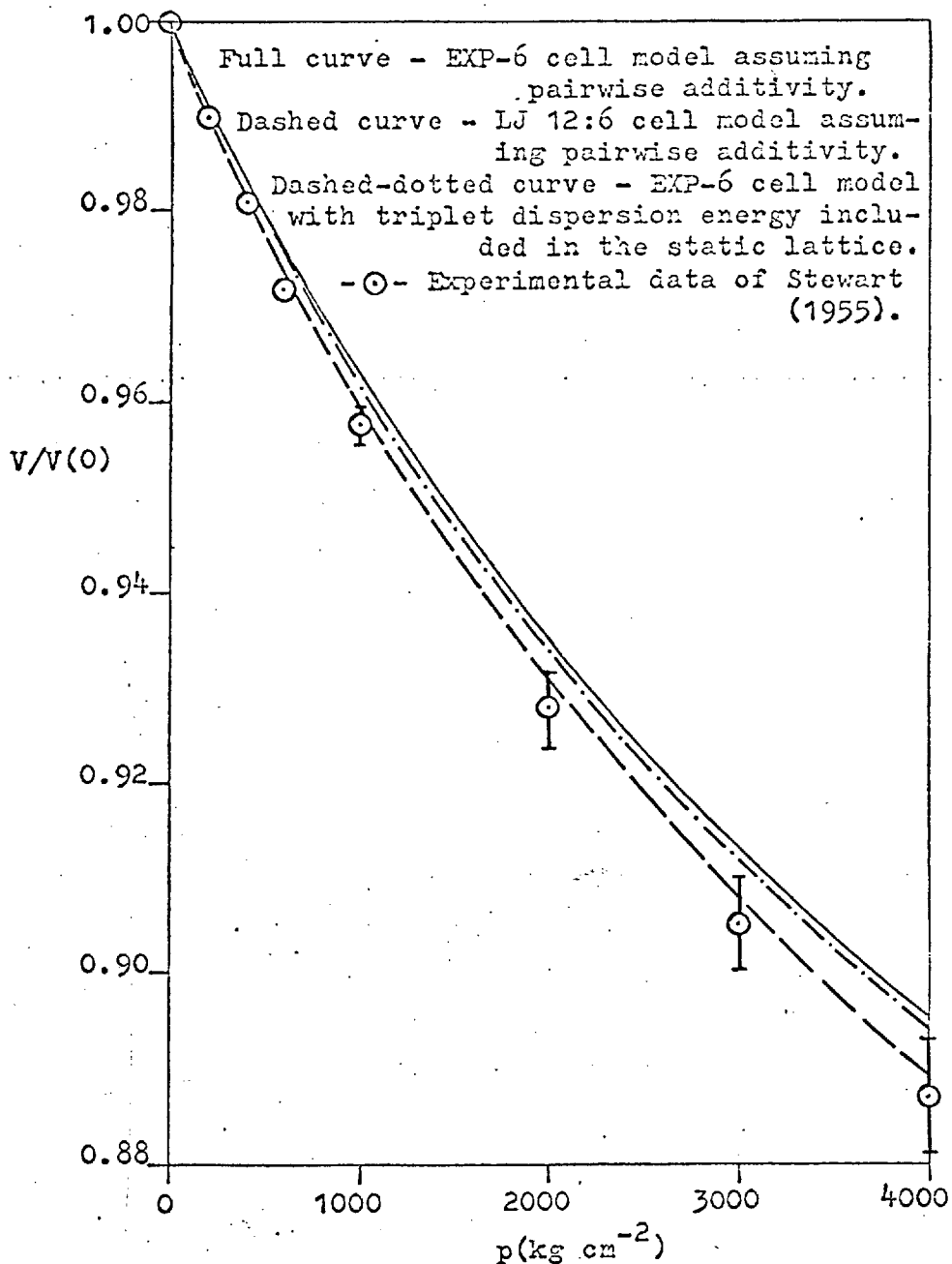


Fig. 71a. Solid xenon - lattice constant,  $a_0$ , as a function of temperature,  $T$ , at zero pressure

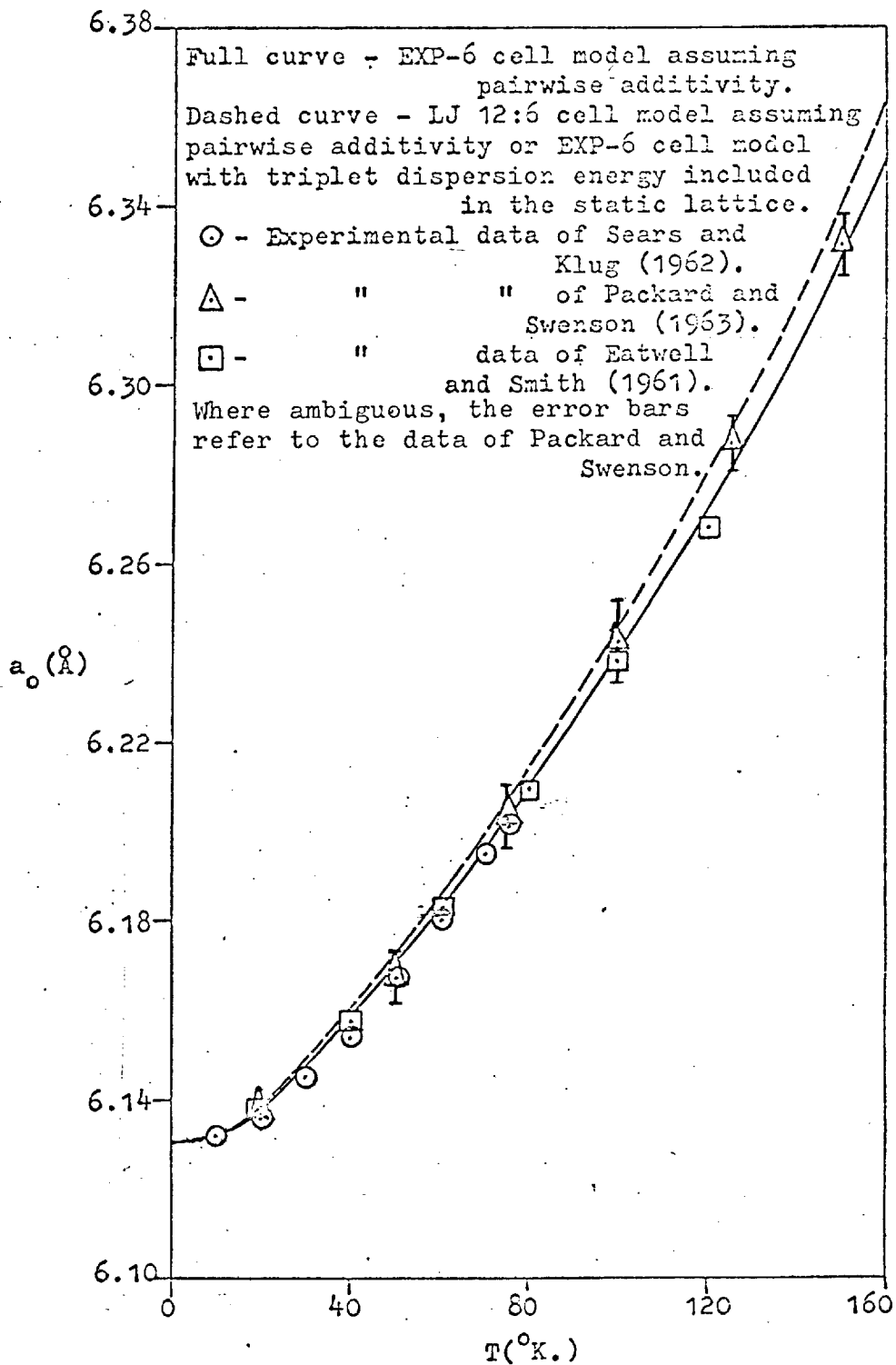




Fig. 11b. Solid xenon - isothermal compressibility,  $\chi_T$ , as a function of temperature,  $T$ , at zero pressure

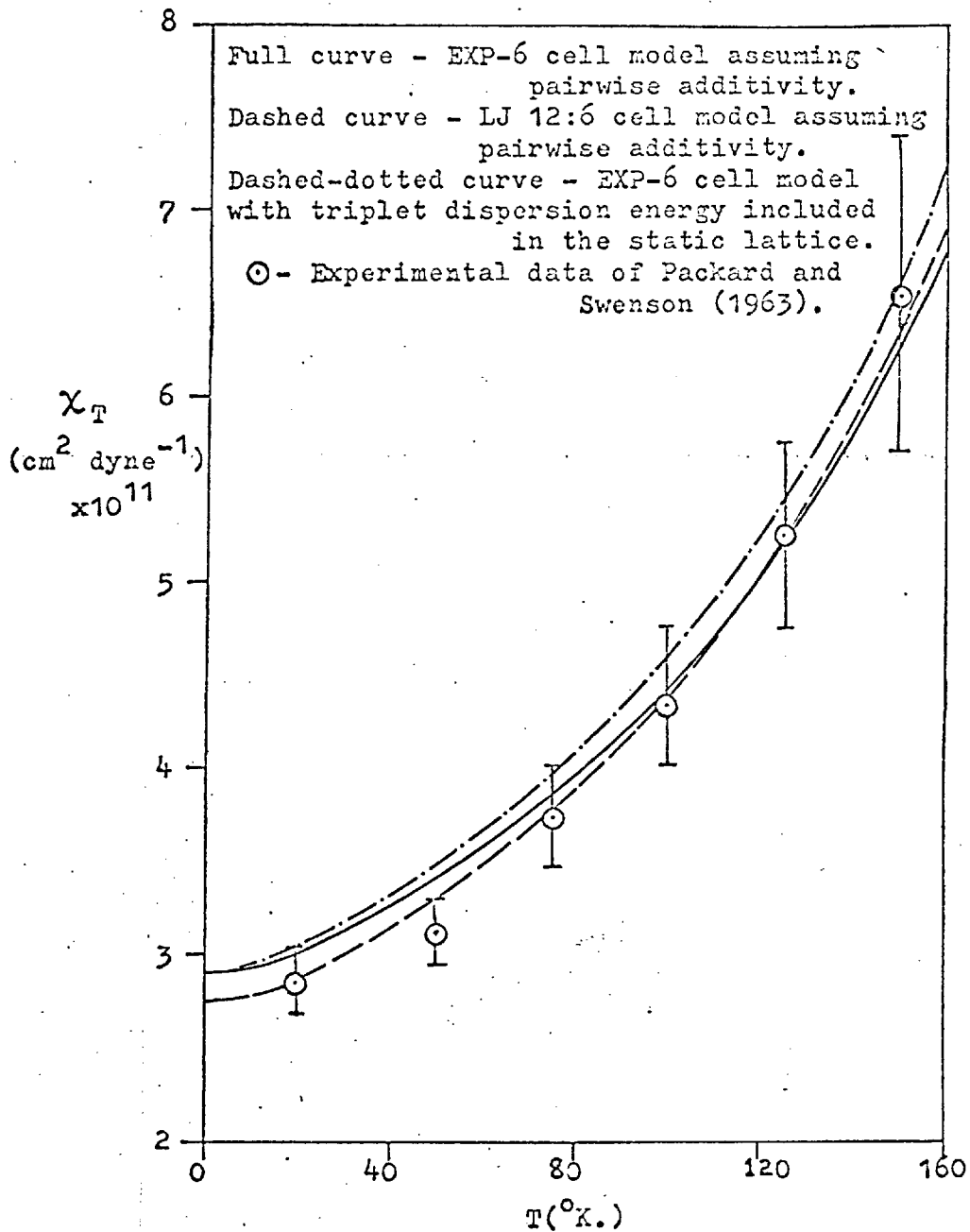


Fig. 11c Solid xenon - volume expansivity,  $\beta$ , as a function of temperature,  $T$ , at zero pressure

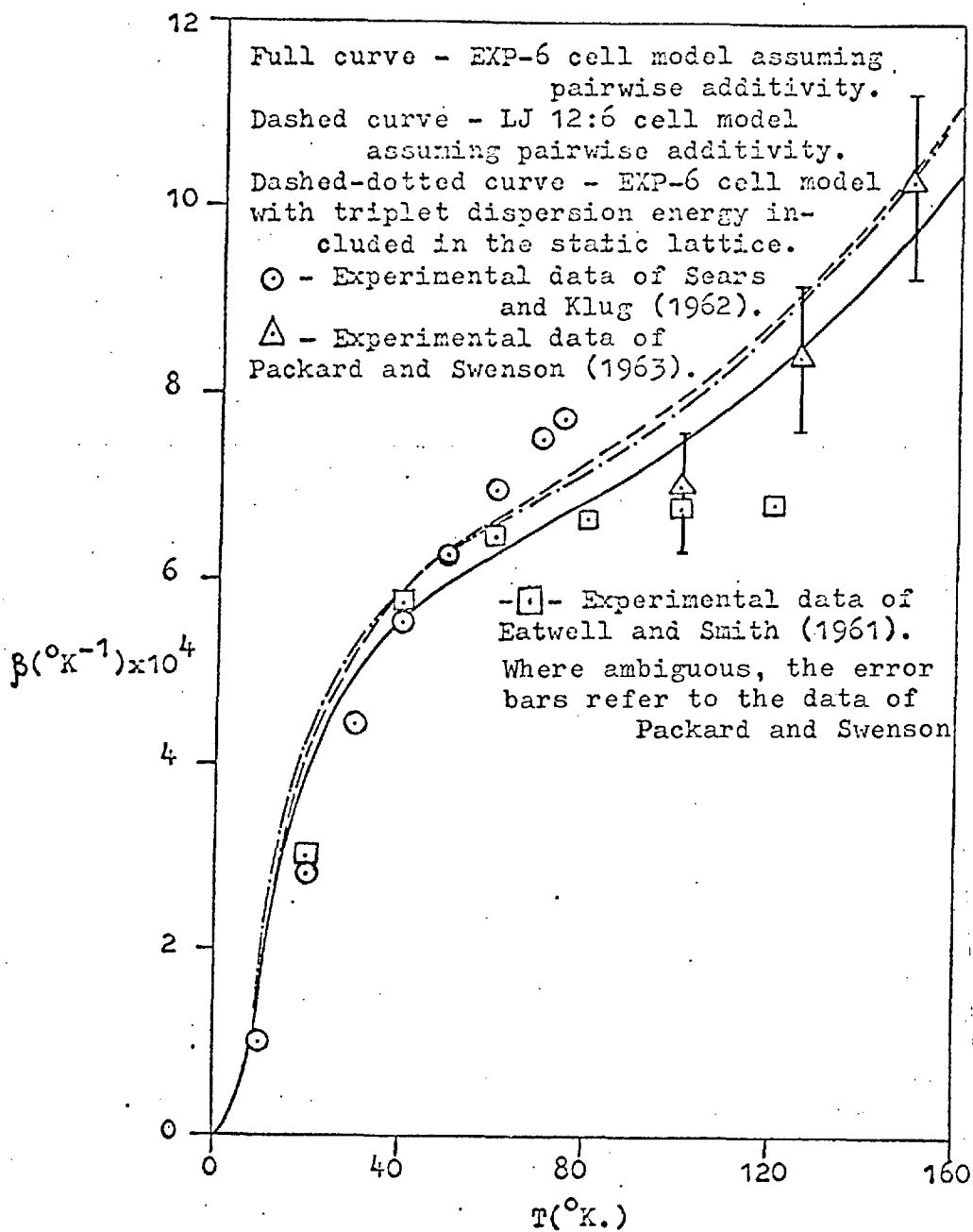


Fig. 11d. Solid xenon - isochoric specific heat,  $C_v$ , as a function of temperature,  $T$ , at zero pressure

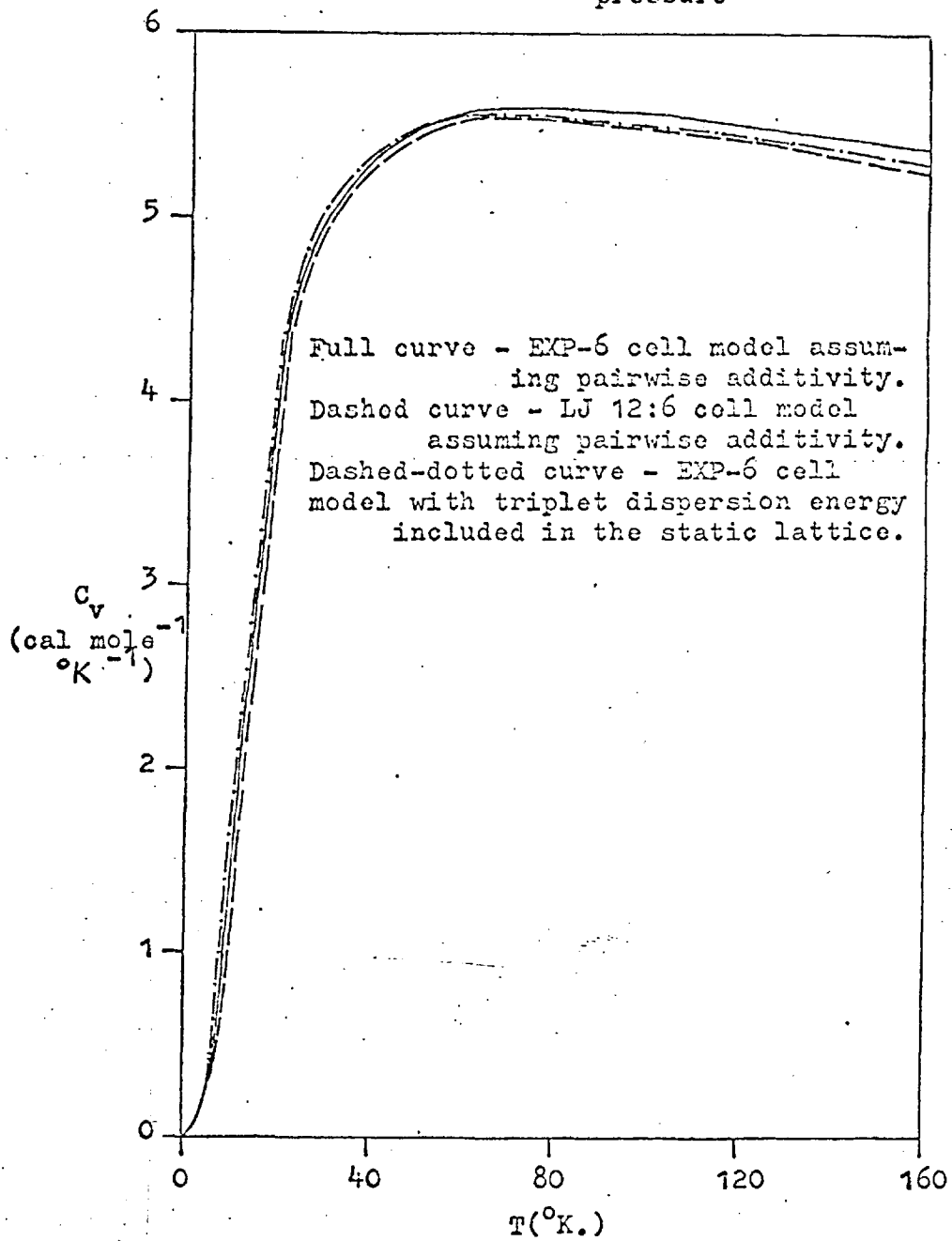


Fig. 11a Solid xenon - isobaric specific heat,  $C_p$ , as a function of temperature,  $T^p$ , at zero pressure 115.

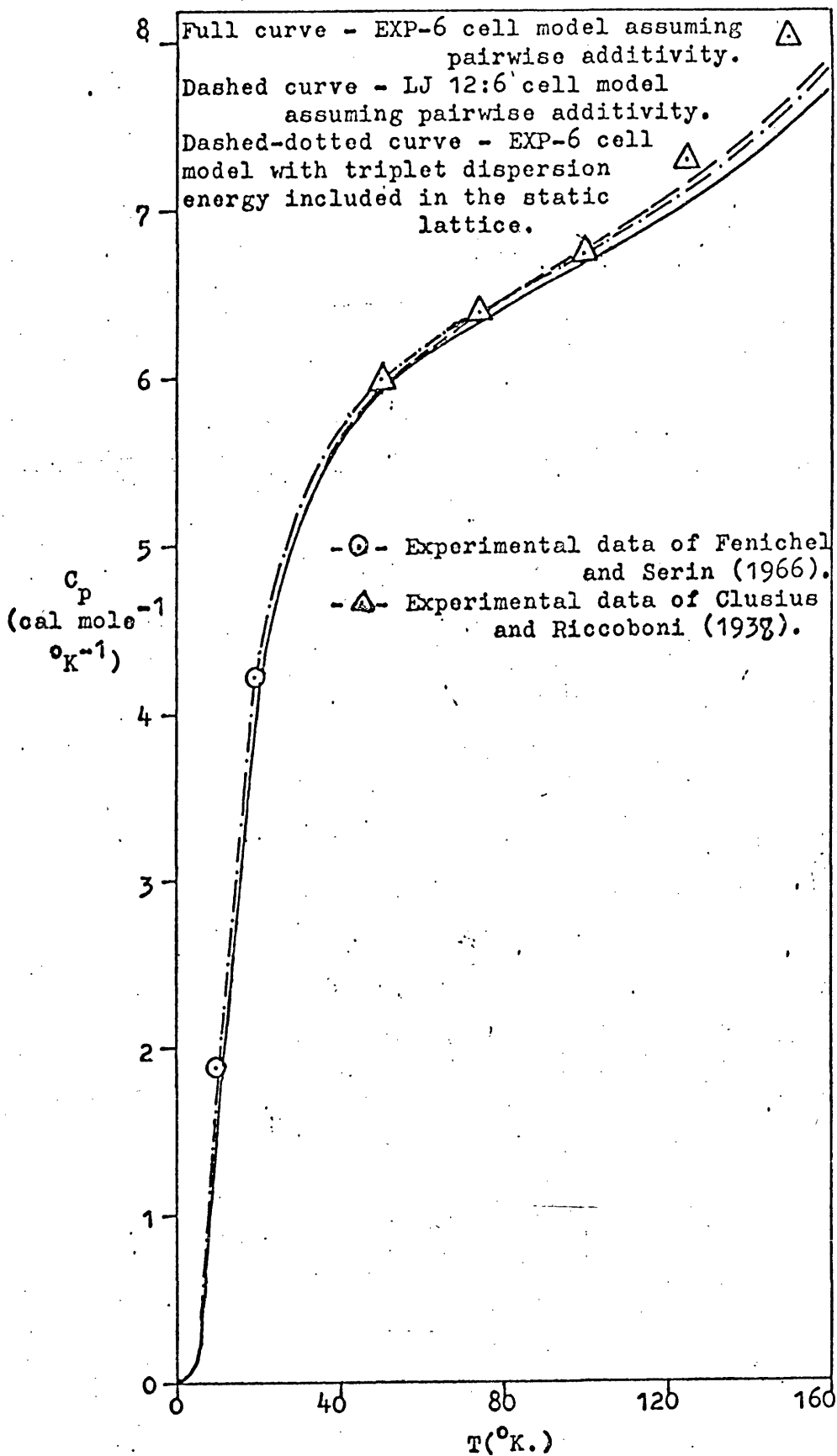


Fig.11f. Solid xenon - entropy,  $S$ , as a function of temperature,  $T$ , at zero pressure

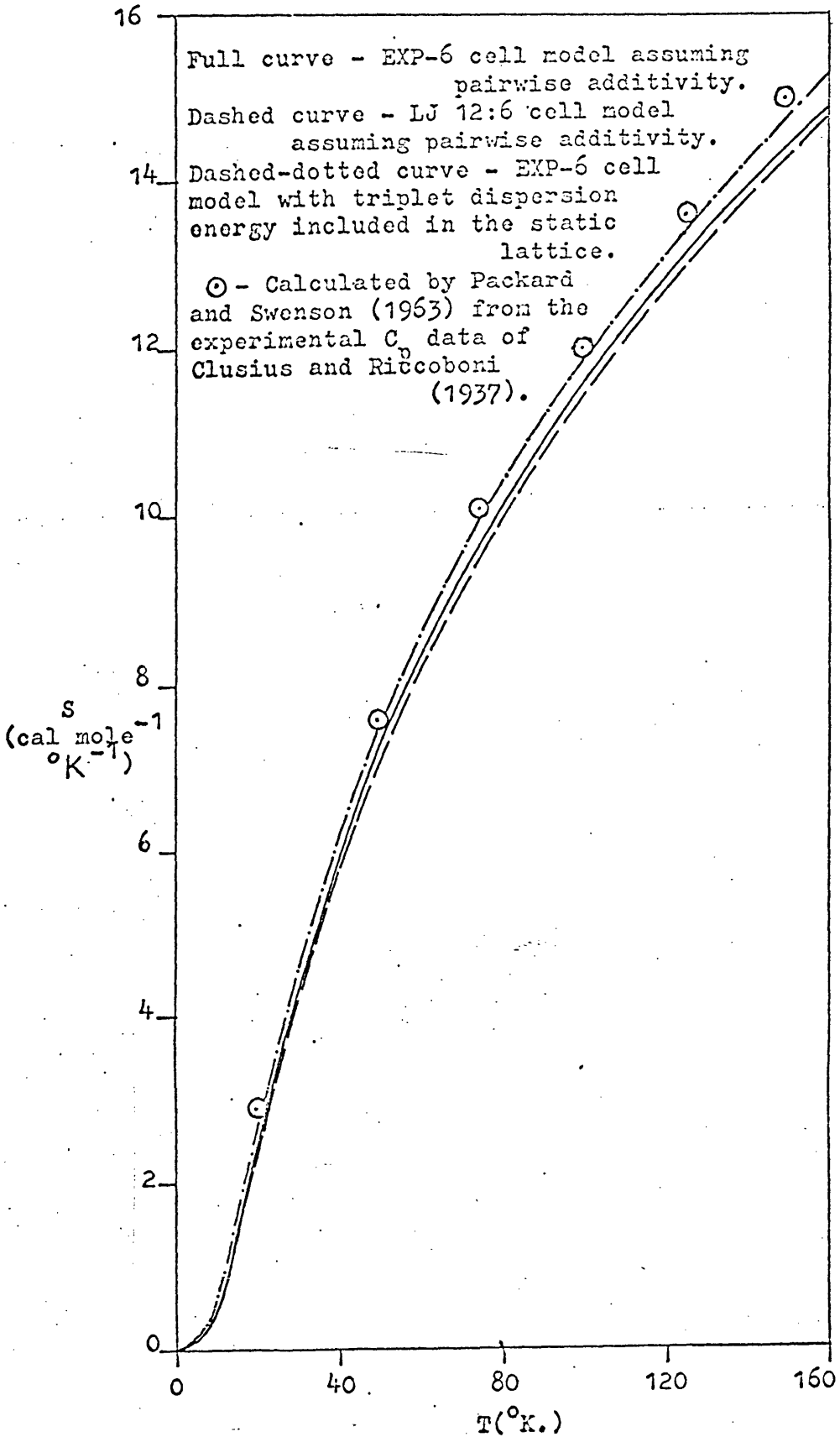
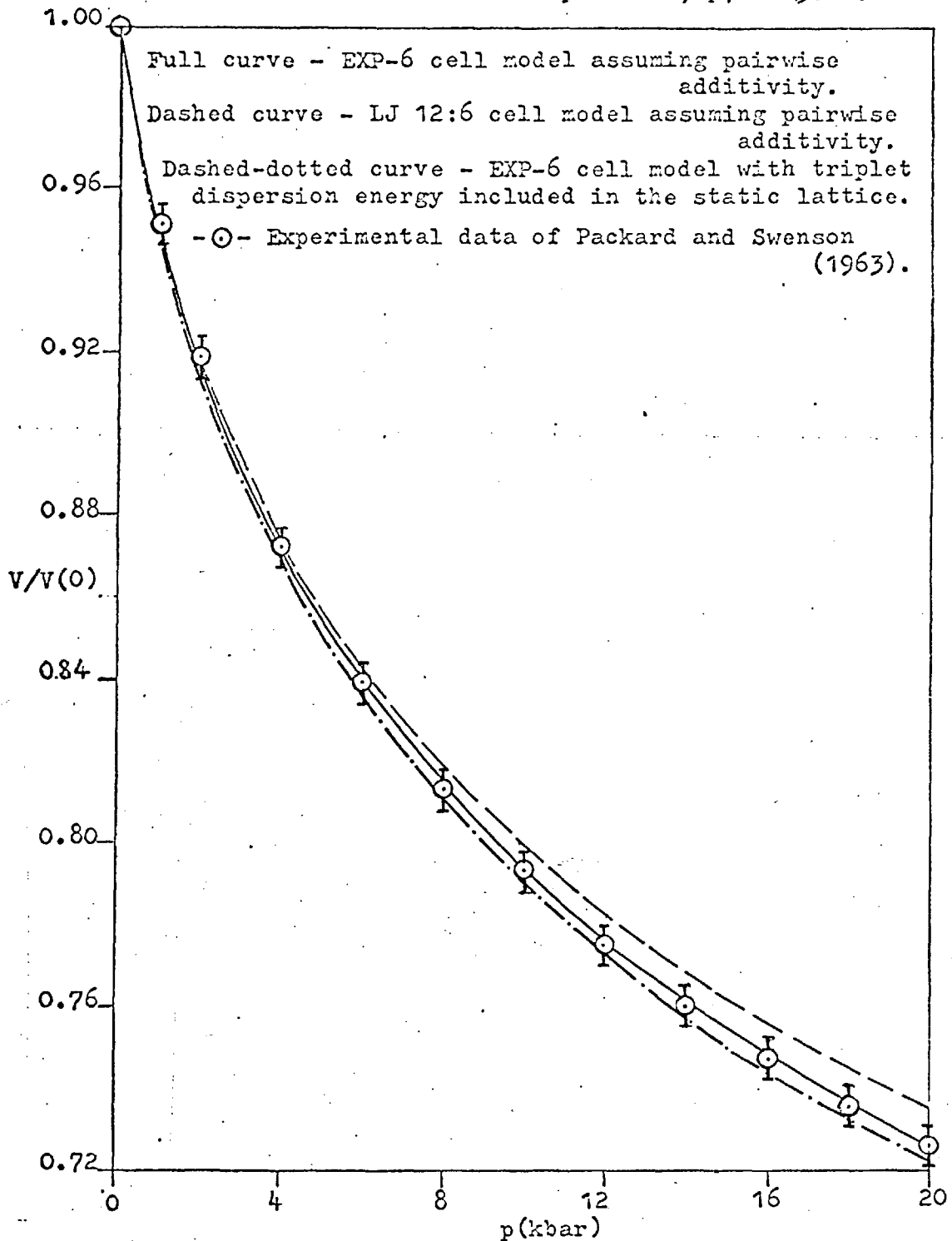


Fig.11g. Solid xenon - molar volume,  $V$ , normalised by the zero pressure molar volume,  $V(0)$ , as a function of pressure,  $p$ , at  $150^\circ\text{K}$ .



## Discussion of results

### Solid neon:

In Fig. 8a it is seen that the results given by the LJ 12:6 cell model for the variation of the lattice constant of solid neon with temperature are in good agreement with experiment. On the other hand, the EXP-6 results are appreciably too low at temperatures above 8°K. Below this temperature, the agreement between both theoretical curves and the experimental results is good, but this is not surprising since the T=0 value of the lattice constant was one of the properties used to characterise the potential functions in the first place.

Fig. 8b shows that, in the range of temperature from 0°K to 16°K, the EXP-6 model gives results for the isothermal compressibility of solid neon in agreement with experiment. The LJ 12:6 results are too large in this region. This is in direct contrast to the lattice constant results, but is not entirely unexpected when it is remembered that the T=0 value of  $\chi_T$  was used as the third property in the determination of the EXP-6 parameters, whereas characterisation of the two parameter LJ 12:6 function did not require the use of such a property. At higher temperatures than 16°K the experimental  $\chi_T$  increases more rapidly with temperature than the EXP-6 values and at 18°K the error bar associated with the experimental result spans both theoretical curves. At 20°K the experimental  $\chi_T$  is higher than both of the theoretical values but nearer to the LJ 12:6 result.

Referring to Fig. 8c, it is clear that the values of the volume expansivity of solid neon predicted by the LJ 12:6 model are in better agreement with experiment than the EXP-6 results. This is a direct consequence of the much better prediction by the LJ 12:6 model of the  $a_0$  versus  $T$  curve.

Fig. 8d shows that, although the LJ 12:6 results are in better agreement with experiment than the EXP-6 results, both models predict too small a value of  $C_v$  over the whole temperature range (excluding of course  $T=0$  where  $C_v=0$ ). Such behaviour must be attributed, at least in part, to the use of an Einstein model of the solid, the defects of which, as pointed out in earlier chapters, are expected to be most apparent in non static lattice dependent properties such as  $C_v$ . For harmonic systems, the errors given by the Einstein assumption of independent motion are such that predicted values of  $C_v$  are lower than the experimental values. It is evident that this is the case with our results. However, the harmonic Einstein values of  $C_v$  are in appreciable error only in the low temperature region and rapidly become very accurate at temperatures greater than  $\Theta_D/4$  ( $\approx 16^\circ\text{K}$  for neon, see Pollack 1964), whereas neither of the theoretical curves in Fig. 8d shows appreciably better agreement with experiment in the higher temperature range. While this discrepancy could possibly be attributed to the nature of the pair interaction, it seems likely that it can largely be put down to an inability of the Einstein approximation to take adequate account of anharmonicity, which is particularly large for solid neon, in such a property as  $C_v$ . Although a direct comparison between our results



and those of lattice dynamical calculations is not possible - our calculations take account of all anharmonic terms and are for three shells of neighbours, whereas lattice dynamical calculations performed to date consider only first order anharmonic contributions and usually only nearest neighbour interactions - Barron (1965) has pointed out that the Einstein and lattice dynamical expressions for the first order anharmonic contribution to  $C_v$  are markedly different in the limit of high temperature.

Turning to the temperature variation of  $C_p$  given in Fig.8e, it is again seen that the LJ 12:6 curve is closer to the experimental results, but that both sets of theoretical results are considerably too low. This is only to be expected from the results predicted for  $C_v$ , which is related to  $C_p$  by the thermodynamic relation (4.9).

$C_p$  is thermodynamically related to entropy by (4.10) and any discrepancy between the experimental values of  $C_p$  and the theoretical results is automatically carried over into  $S$ . In consequence, the disagreement between the theoretical and experimental entropy values for solid neon shown in Fig.8f is not surprising. Yet again the LJ 12:6 curve is closer to the experimental results but both sets of theoretical results are too low.

In fact,  $S$  is sensitive to the defects of the Einstein approximation at all temperatures, even if it may be assumed that predicted values of specific heat are in error only in the low temperature region, as is known to be the case for harmonic systems. This is because of the integral appearing in (4.10), which

means that, at any temperature,  $S$  is not only dependent on the value of  $C_p$  at that particular temperature, but also on the values at lower temperatures. Further, by virtue of the reciprocal temperature in the integrand, low temperature contributions to the integral are significant even at considerable temperatures.

Finally for solid neon, Fig. 8g shows that, with the exception of the value at  $2000 \text{ kg cm}^{-2}$ , the LJ 12:6 cell model gives a  $V/V(0)$  versus  $p$  curve which agrees with the experimental points within their quoted uncertainties. The EXP-6 results are not in such good overall agreement with experiment. In the pressure range from  $6000$  to  $12000 \text{ kg cm}^{-2}$  the EXP-6 values of  $V/V(0)$  are just within the upper experimental accuracy limit, but, for pressures outside this range, (except at  $p=0$  where agreement is automatic), they are slightly too large.

#### Solid argon:

Fig. 9a shows that, in the case of solid argon, it is the EXP-6  $a_0$  versus  $T$  curve which is in close agreement with experiment over the whole temperature range. The LJ 12:6 results, after their automatic good agreement with experiment at low temperature, become rapidly too large at temperatures above  $20^\circ\text{K}$ .

In contrast with  $\chi_T$  versus  $T$  plots relevant to the other inert gas solids, in which experimental accuracy limits are shown over the whole temperature range, it is only for the experimental  $\chi_T$  value at

83°K that an error bar has been included in Fig. 9b for argon. This is the only value of  $\chi_T$  for which an explicit experimental uncertainty is quoted, and the absence of error bars on the other  $\chi_T$  values should not be taken to imply high experimental precision. It is seen that the error limits ( $\pm 10\%$ ) on the 83°K value span both the LJ 12:6 and EXP-6 curves and it is almost certain that such behaviour would be general if experimental inaccuracies were allowed for at the low temperatures. In view of this, it appears that the existing experimental data for the isothermal compressibility of solid argon in the range from 10°K to 83°K is not sufficiently accurate to distinguish between the LJ 12:6 and EXP-6 results, even though these are significantly different over the whole temperature range.

The experimental value of  $\chi_T$  used for characterising the EXP-6 function was that at 4°K, ( $T=0$  and  $T=4$ °K may be considered as equivalent as far as  $\chi_T$  is concerned), obtained by Simmons and co-workers using a single crystal X-ray technique. This value is of much greater accuracy - the quoted error is about 1.5% - than those at higher temperatures which come from sound velocity, light scattering and torsional vibration measurements in polycrystalline samples. It is not plotted in Fig. 9b, since the corresponding EXP-6 result is automatically in agreement with it, but it is worth noting that even the use of the LJ 12:6 function, which required no  $\chi_T$  data for its characterisation, gives a value of  $\chi_T$  at this point which is only marginally outside the quoted experimental uncertainty limits.

In Fig. 9c, the experimental  $\beta$  versus T results for

solid argon are seen to be reasonably well predicted by the EXP-6 cell model for temperatures up to  $70^{\circ}\text{K}$ . Above  $70^{\circ}\text{K}$  the experimental  $\beta$  rises more rapidly with temperature than the EXP-6 value. The LJ 12:6 results are, (not suprisingly, when the  $a_0$  versus T results are considered), appreciably larger than those given by the EXP-6 calculations at all temperatures and, at temperatures approaching the triple point (i.e.  $80^{\circ}\text{K}$  to  $83^{\circ}\text{K}$ ), the LJ 12:6 curve is the one which shows better agreement with experiment.

Turning to a consideration of the temperature variation of  $C_v$  for solid argon, it is seen that the scale of Fig. 9d is not large enough to distinguish between the LJ 12:6 and EXP-6 curves in the temperature range from  $0^{\circ}\text{K}$  to  $40^{\circ}\text{K}$ , where the value of  $C_v$  is most rapidly varying. Similarly any discrepancy between theory and experiment is considerably masked in this region. Reference to Appendix 4 shows that the LJ 12:6 results are in fact slightly larger than the EXP-6 results in this range of temperature. Also, careful examination of the figure or direct numerical comparison of the tabulated data in the Appendices 4 and 5 reveals that the relevant theoretical  $C_v$  values are appreciably lower than the corresponding experimental values. Further, the discrepancy between theory and experiment is significantly larger than the difference between the theoretical results themselves.

In the temperature range from  $0^{\circ}\text{K}$  to  $35^{\circ}\text{K}$  the disagreement between the theoretical and experimental  $C_v$  is largest at very low temperatures (e.g.  $10^{\circ}\text{K}$ ) and becomes much less pronounced at higher temperatures.

Although not perfect, the agreement is undoubtedly better between 20°K and 35°K than it is at lower temperatures. Taking the value of  $\Theta_D/4$  for argon to be  $\sim 23^\circ\text{K}$  (as quoted by Pollack 1964), such behaviour is a typical result of the use of an Einstein model to represent a harmonic crystal (see the discussion for solid neon), of which solid argon and the heavier inert gas solids may be taken as fair examples at low temperature.

At 40°K the theoretical  $C_v$  results are once again substantially lower than the value given by experiment and remain so as the temperature rises to the triple point. The theoretical curves in Fig. 9d do not remain identical in the high temperature region, however. At about 40°K the EXP-6 and LJ 12:6 results cross and then diverge with increasing temperature. At temperatures near the triple point the EXP-6 curve is significantly higher than the LJ 12:6 curve and is closer to, though by no means in good agreement with, the experimental results.

Although it is not obvious in Fig. 9d, both of the theoretical curves pass through a shallow maximum value of about  $C_v = 2.6R \text{ mole}^{-1}$  at some temperature between 60°K and 83°K. Beyond this temperature the theoretical  $C_v$  falls very slowly as the triple point is approached. No such behaviour is shown by the experimental results, which, in contrast, show a marked upward trend as the triple point is approached.

This type of behaviour in the the high temperature theoretical  $C_v$  is clearly the result of anharmonicity, for it is known that the  $C_v$  versus T curve given by a

harmonic model is monotonically increasing and approaches  $C_v = 3R \text{ mole}^{-1}$  in the classical limit of high temperature. It has been pointed out in connection with solid neon that the Einstein approximation of independent molecular motion probably does not take adequate account of the effects of anharmonicity on the value of a static lattice independent property such as  $C_v$ . Nevertheless, since lattice dynamical calculations agree with ours in predicting a downward trend in the high temperature values of  $C_v$  (see for example Feldman and Horton 1967), the discrepancy between the theoretical curves and the rising experimental results at temperatures approaching the triple point cannot be entirely attributed to errors introduced by the Einstein assumption. Anomalies in the high temperature specific heats of the heavier inert gas solids are discussed later.

As mentioned earlier, any errors in the theoretical values of  $C_v$  are automatically carried over into  $C_p$  by virtue of (4.9). It is not surprising therefore that Fig. 9e shows both sets of theoretical results for the  $C_p$  versus T variation of solid argon to be lower than the corresponding experimental values at all temperatures. In the case of  $C_p$ , however, the influence of the  $\beta^2 TV / \chi_T$  term causes the LJ 12:6 values to be higher than the EXP-6 results over the whole temperature range and not just up to  $40^\circ\text{K}$  as was the case with  $C_v$ . The discrepancy between theory and experiment is again seen to be most pronounced at low temperatures ( $0-20^\circ\text{K}$ ) and at temperatures approaching the triple point ( $70-83^\circ\text{K}$ ). Between these two regions the LJ 12:6 results are in fairly good agreement with experiment and the EXP-6 results somewhat too low. However, fair agreement

between theoretical and experimental values of  $C_v$  for solid argon was apparent only in a much more restricted temperature range (20-35°K) and, further, the agreement between experiment and both sets of theoretical results was about equally good in this region. Consequently the reasonable agreement between the LJ 12:6 and experimental  $C_p$  over such a large temperature range must be due to a cancellation of errors in the theoretical values of  $\beta^2 TV/\gamma_T$  and  $C_v$  and is therefore regarded as somewhat fortuitous.

Fig. 9f shows that both models give an identical  $S$  versus  $T$  curve up to 40°K but that at higher temperatures the LJ 12:6 curve is slightly higher than the EXP-6 one. As expected from the  $C_p$  results and the large model sensitivity of calculated values of  $S$ , (see discussion for solid neon), both theoretical  $S$  versus  $T$  curves are appreciably lower than the experimental results over the whole temperature range.

From Fig. 9g it is apparent that both the EXP-6 and LJ 12:6 models give predictions of  $V/V(0)$  versus  $p$  for solid argon at 77°K within the quoted experimental uncertainty limits at pressures above 8000 kg cm<sup>-2</sup>. From 4000-8000 kg cm<sup>-2</sup> the LJ 12:6 results are still inside the experimental uncertainty, whereas the EXP-6 values of  $V/V(0)$  are somewhat too high. Even so, the EXP-6 results in this region are only marginally outside the appropriate error bars. At lower pressures the theoretical curves become identical and in slight disagreement with experiment (except of course at  $p=0$ , where agreement is automatic).

Solid krypton:

In contrast with the experimental lattice constant data of solid neon and solid argon, which came solely from the very accurate and systematic X-ray work of Simmons and co-workers on single crystals, those plotted in Fig. 10a for solid krypton are taken from a number of sources. Apart from the few values of  $a_0$  given by the Simmons group in their study of the isothermal compressibility of solid krypton, these data were obtained from X-ray measurements on polycrystalline samples or from bulk density measurements and do not approach the accuracy of the argon and neon results, which are quotable to six significant figures. Consequently the experimental points in Fig. 10a show some scatter. However, if the earliest X-ray data of Cheeseman and Soane and the bulk density value of Clusius and Weigand are ignored, it is clear that the EXP-6  $a_0$  versus T curve is in better agreement with the remaining (X-ray) data than is the LJ 12:6 curve, which is appreciably too high at temperatures above 20°K. The agreement between the EXP-6 results and the most accurate experimental values of Simmons et. al. is strikingly good. Owing to the lack of reliable experimental data no comparison can be made for temperatures above 90°K.

Fig. 10b shows that, as in the case of solid neon and solid argon, the  $\gamma_T$  versus T curve given by the EXP-6 cell model is above that derived from LJ 12:6 calculations. The EXP-6 values of  $\gamma_T$  are within the uncertainties in the experimental data over the whole temperature range of measurement (0-91°K). On the other hand, the LJ 12:6 results are within the quoted error limits only at 17°K and 91°K. As before, it



should be remembered that the good agreement between the EXP-6 and the experimental results at very low temperature is automatic by virtue of the characterisation procedure.

For the temperature variation of the volume expansivity, Fig. 10c shows the LJ 12:6 curve to be appreciably higher than the EXP-6 curve at all temperatures above  $10^{\circ}\text{K}$ . Probably the only  $a_0$  data sufficiently accurate for a reliable derivation of experimental values of  $\beta$  are those of the Simmons group and, for solid neon and argon, these workers' values of  $\beta$  have been used for comparison with the theoretical results. However, for solid krypton the only experimental  $\beta$  data readily available are those of Figgins and Smith and these show considerable scatter in Fig. 10c. Consequently, although the EXP-6 curve appears to show overall better agreement with experiment, (such would be expected from the  $a_0$  versus T results anyway), a detailed comparison of theoretical and experimental values of  $\beta$  is not possible.

Referring to Fig. 10d, it is seen that the general features of the LJ 12:6 and EXP-6  $C_v$  versus T curves for solid krypton are similar to those shown by the corresponding curves for solid argon. At  $10^{\circ}\text{K}$  the two theoretical values of  $C_v$  are identical on the scale of the figure, but between this temperature and about  $35^{\circ}\text{K}$  the LJ 12:6 results are slightly larger than the corresponding EXP-6 values. In the range from  $35^{\circ}\text{K}$  to  $60^{\circ}\text{K}$  the two curves are again identical on the scale of the figure. In this region the theoretical results cross and beyond  $60^{\circ}\text{K}$  the two curves diverge. As for solid argon, the LJ 12:6 curve is

appreciably lower than the EXP-6 curve at temperatures approaching the triple point. Also, each set of theoretical results again pass through a shallow maximum and, in this case, such behaviour is immediately apparent from the figure. The maximum value of  $C_v$  given by both curves is about  $2.7R \text{ mole}^{-1}$  and occurs at a temperature between  $60^\circ\text{K}$  and  $100^\circ\text{K}$ . As mentioned before, this type of behaviour is a direct consequence of anharmonic effects, the influence of which on  $C_v$  is probably not adequately accounted for by the cell model.

On the scale of Fig. 10e, the LJ 12:6 and EXP-6  $C_p$  versus  $T$  curves for solid krypton are identical up to  $15^\circ\text{K}$ . As expected from the Einstein nature of the cell model, the experimental  $C_p$  is higher than the theoretical results in this region, ( $\Theta_D/4 \approx 18^\circ\text{K}$  for krypton (Pollack 1964), see discussion for solid neon). From  $15^\circ\text{K}$  to the triple point the LJ 12:6 results are slightly larger than the EXP-6 values of  $C_p$  and in correspondingly closer agreement with experiment. From  $20^\circ\text{K}$  to  $80^\circ\text{K}$  the agreement between the LJ 12:6 and the experimental results is particularly good. However, in view of the indications by the theoretical  $C_v$  curves that anharmonic effects may be appreciable at temperatures as low as  $50^\circ\text{K}$  and the doubts as to the accuracy of the Einstein anharmonic contribution to the specific heat, this good agreement may be to some extent fortuitous. Also, it has been noted in connection with solid argon that cancellation of errors in the theoretical values of  $C_v$  and  $\beta^2 TV/\chi_T$  may lead to spurious good agreement between calculated and experimental values of  $C_p$ . Above  $80^\circ\text{K}$  the experimental  $C_p$  rises much more rapidly with temperature than either of the theoretical

values. Such behaviour was also apparent in the high temperature specific heat of solid argon and, as remarked previously, will be discussed later.

In Fig. 10f, both the theoretical  $S$  versus  $T$  curves for solid krypton are seen to be below the experimental values at all temperatures above  $10^\circ\text{K}$ . As expected from the  $C_p$  results, of the two, the LJ 12:6 curve is the closer to experiment. As pointed out previously, a discrepancy between theory and experiment is expected from the large model sensitivity of calculated values of entropy.

Fig. 10g shows that the LJ 12:6 model predicts the  $V/V(0)$  versus  $p$  curve of solid krypton at  $77^\circ\text{K}$  within experimental error over the whole range of pressure considered. On the other hand, the EXP-6 results for  $V/V(0)$  become progressively larger than the experimental values with increasing pressure. However, in the case of solid krypton the pressure range over which measurements of the variation of volume have been carried out is considerably smaller than that for the other inert gas solids and the scale of Fig. 10g tends to exaggerate the relative disagreement between the EXP-6 values and the experimental results. In fact, the discrepancy given by the EXP-6 cell model even at  $4000 \text{ kg cm}^{-2}$  is not much more than that for solid argon at the same pressure.

#### Solid xenon:

Similar to the corresponding data for solid krypton, the experimental lattice constant data for solid xenon plotted in Fig. 11a are drawn from a number of sources

and are of varying accuracy. None of the data approaches the accuracy of those of Simmons and co-workers for the lighter inert gas solids. However, if Packard's and Swenson's bulk density values of  $a_0$  are excluded from the comparison, the agreement between the EXP-6 curve and the remaining (X-ray) data is seen to be good, whereas the LJ 12:6 results are somewhat too large above 40°K.

Fig.11b shows that both the EXP-6 and LJ 12:6 cell models predict the experimental (in this case, bulk density) values of  $\chi_T$  within the quoted accuracy limits at all temperatures except 50°K where the experimental error bar spans only the LJ 12:6 curve. In contrast with those for the other inert gases, the theoretical  $\chi_T$  versus T curves for solid xenon cross at about 120°K. Below this temperature the EXP-6 results are larger than the LJ 12:6 values and above it the reverse is true. It is remembered that, in the case of xenon,  $\chi_T$  data was not used in the characterisation of the EXP-6 function.

As expected from the  $a_0$  versus T results, it is seen in Fig.11c that the EXP-6; versus T curve is higher than the LJ 12:6 results at all temperatures above about 10°K. The large scatter of the experimental data available does not allow a detailed comparison between theory and experiment.

In Fig.10d, the EXP-6  $C_v$  versus T curve for solid xenon is seen to be higher than that given by the LJ 12:6 cell model over the whole temperature range. In the low temperature region the difference between the curves is small but at temperatures approaching the triple point it

is appreciable. Both curves again pass through a shallow maximum in the high temperature region and then fall with temperature as the triple point is approached. In this case the maximum value of  $C_v$  given by both curves is about  $2.8R \text{ mole}^{-1}$  and occurs at a temperature between  $80^\circ\text{K}$  and  $115^\circ\text{K}$ . The position of the maximum is quite clearly shown up by the figure and the fall of specific heat beyond it appears to be linear. Anharmonic lattice dynamical calculations also give a linear fall in  $C_v$  at high temperature (see Feldman and Horton 1967). As remarked previously, however, the Einstein approximation probably does not give quantitatively correct values of  $C_v$  at high temperatures when anharmonic effects are of importance.

The scale of Fig. 11e is insufficiently large to distinguish between the LJ 12:6 and EXP-6  $C_p$  versus  $T$  curves for solid xenon at temperatures below  $40^\circ\text{K}$ . Reference to Appendix 4 shows that the EXP-6 results are in fact slightly larger in this region. The theoretical values of  $C_p$  are appreciably lower than the corresponding experimental results at  $10^\circ\text{K}$ , but at  $20^\circ\text{K}$  the agreement is better, as would be expected from the Einstein nature of the cell model ( $\Theta_D/4 \approx 14^\circ\text{K}$  for xenon (Pollack 1964), see discussion for solid neon). At  $40^\circ\text{K}$  the theoretical results cross and at temperatures above this the LJ 12:6 results become significantly larger than the EXP-6 values and in correspondingly better agreement with experiment. Between  $50^\circ\text{K}$  and  $100^\circ\text{K}$  this agreement is good, but, in view of earlier remarks, it is probably to some extent fortuitous. Once again, at temperatures approaching the triple point the experimental  $C_p$  rises much more rapidly than

both theoretical curves.

As expected from the use of the cell model, both theoretical  $S$  versus  $T$  curves for solid xenon are lower than the corresponding experimental results plotted in Fig.11f. In contrast with the other inert gas solids, however, the EXP-6 results are above the LJ 12:6 values in this case at all temperatures above  $0^{\circ}\text{K}$ . This demonstrates the already noted sensitivity of  $S$  at high temperature to the values of  $C_p$  in the low temperature region, for we have seen that, for solid xenon, the EXP-6 value of  $C_p$  is higher than the LJ 12:6 value only at temperatures up to  $40^{\circ}\text{K}$ .

In Fig.11g it is clear that the EXP-6  $V/V(0)$  versus  $p$  curve for solid xenon at  $150^{\circ}\text{K}$  is in good agreement with the experimental results over the whole pressure range. On the other hand the LJ 12:6 values of  $V/V(0)$  are appreciably larger than the experimental ones for pressures above 6kbar.

\*\*\*\*\*

It is clearly difficult to draw from the above discussion any hard and fast conclusion as to whether the EXP-6 function gives a better general representation of the inert gas pair interaction than the more commonly used LJ 12:6 function. Not only does the relative predictive ability of the two potential functions vary from substance to substance, but also, to some extent, from property to property.

However, predicted values of such properties as specific heat and entropy are probably too sensitive to the defects of the model to yield anything but spurious information as to the nature of the pair interaction and it seems sensible to make use of only predicted values of the remaining strongly lattice dependent properties for this purpose. When only such properties are considered it is possible to draw some tentative conclusions, although inevitable inconsistencies still exist. It should be pointed out, however, that, even if the static lattice dependent properties are not too sensitive to the Einstein nature of the model, any conclusions that we make must be viewed in the framework of the assumption of pairwise additivity on which the theory is based. Some investigations of the validity of this assumption are reported in the following chapter.

For solid neon, the overall agreement between experiment and the EXP-6 predictions of the static lattice dependent properties is not good. The use of the LJ 12:6 cell model leads to considerably better agreement in the case of all static lattice dependent properties except isothermal compressibility, for which the EXP-6 calculations give the better results. However, a comparison between the LJ 12:6 and EXP-6 values of  $\chi_T$  is not strictly consistent, since the better agreement between theory and experiment in the EXP-6 case is almost certainly due to the use of the  $T=0^\circ\text{K}$  value of  $\chi_T$  in the original characterisation of the potential. Where  $\chi_T$  data has been used for characterisation purposes, it seems sensible to consider better prediction of  $\chi_T$  as evidence in favour

of the EXP-6 function only if it is supported by other results. With this in mind, our calculations would appear to indicate that the EXP-6 function is not as good a representation of the neon-neon interaction as the more commonly used and mathematically simpler LJ 12:6 function.

In the case of solid argon, the EXP-6 calculations do lead to results in reasonable agreement with experimental values of the static lattice dependent properties. The good prediction of the  $a_0$  versus T variation up to the triple point and the related  $\beta$  versus T dependence up to 70°K argues especially strongly in favour of the use of the EXP-6 function to represent the argon-argon interaction. This is supported by the good agreement by the EXP-6  $\chi_T$  versus T curve with experiment, but it is remembered that the LJ 12:6 model also determines this property within experimental error, even though the characterisation of the LJ 12:6 function required the use of no  $\chi_T$  data. The EXP-6 model also predicts the  $v/V(0)$  versus p curve for solid argon at 77°K reasonably well, although not quite as well as the LJ 12:6 model.

Where the available experimental data are accurate enough for a comparison to be made, the use of the EXP-6 function is in better accord with the experimental results for solid krypton as far as the temperature dependent properties are concerned. In the case of the solid krypton  $v/V(0)$  versus p variation at 77°K the EXP-6 predictions are not as good as those given by the LJ 12:6 model, but even so, are still in fair agreement with experiment.



Where a comparison can be made, our results for the static lattice dependent properties of solid xenon unquestionably favour the EXP-6 representation of the pair interaction.

#### Thermal vacancies in the heavier inert gas solids

It has been noted that, for solid argon, krypton and xenon, the experimental  $C_p$  shows a marked upward trend at temperatures approaching the triple point and, in this region, the discrepancy between the experimental points and the cell model curves is much more marked than at lower temperatures, (see Figs. 9d, 10d, 11d).

Such behaviour in the experimental high temperature specific heat has been taken by several workers (e.g. Lidiard 1957, Beaumont, Chihara and Morrison 1961, Foreman and Lidiard 1963, Hillier and Walkley 1965, Kuebler and Tosi 1965) to be the result of the formation of thermal vacancies in the solid lattice and, by considering the temperature dependence of the difference,  $\Delta C_p$ , between the experimental specific heat and that of an assumed "no vacancy" system, various estimates of  $h_s$ , the enthalpy of vacancy formation, have been derived.

Now, while the vacancy theory cannot be dismissed out of hand, some of the methods used to calculate  $h_s$  are decidedly open to question. In particular, Hillier and Walkley, in their calculations for solid argon, took the "no vacancy" values of  $C_p$  to be the LJ 12:6 cell model ones, the accuracy of which, even if we

assume the LJ 12:6 function to be a good representation of the inert gas pair interaction, must be open to question (see previous section). Further, any errors in the no vacancy values of  $C_p$  are greatly magnified in  $\Delta C_p$ , which is a small difference between two relatively large quantities. It is true that Beaumont and co-workers (see below) have pointed out that  $h_s$  is not too sensitive to  $\Delta C_p$ , but there is clearly something dubious about Hillier's and Walkley's approach, in that further calculations using their results lead to the anomaly of an entropy of vacancy formation,  $S_s$ , of opposite sign to  $h_s$ .

More consistent results are obtained from the earlier approach of Beaumont, Chihara and Morrison, who derived "no vacancy" values of  $C_p$  for solid argon and krypton by extrapolating low temperature experimental data. Having calculated  $h_s$  these workers then derived a value of  $s_s$  of the same sign as  $h_s$  and finally an expression for  $n_s$ , the concentration of vacancies as a function of temperature. For argon, the value of  $n_s$  at the triple point given by these results is of the order of 1% mole fraction. Later analyses of the specific heat by Foreman and Lidiard and Kuebler and Tosi lead to a similar result. However, as well as being inconsistent with theoretical estimates of vacancy free energy (Nardelli and Chiarotti 1960), such a vacancy content in solid argon requires a large relaxation around the vacancy - Beaumont and co-workers estimate that a vacancy of 23% of the atomic volume is necessary - to be consistent with the observed thermal expansion of solid argon. On the other hand, calculations by Hall (1957),

Kanzaki (1957) and Gallina and Omini (1964) indicate only small relaxation effects.

Recently other objections have been lodged against the appreciable formation of lattice vacancies in solid argon. McGlashan (1965) using the Guggenheim-McGlashan piecewise potential (Guggenheim and McGlashan 1960, see Chapter 1 of this thesis) has shown that it is possible to reproduce the experimental values of  $C_p$  for solid argon without invoking vacancy phenomena. However, these results must be viewed with suspicion since McGlashan relied heavily upon specific heat data together with an Einstein model of the crystal to characterise his potential function. This forces correct values of specific heat on a model which cannot really cope with them ( see the previous section of this thesis).

A much more convincing objection to the vacancy theory for argon is that of Batchelder, Peterson and Simmons (1965) who, by comparing the results of their experimental X-ray measurements of the interatomic distances in a rather perfect single crystal with those given by bulk density measurements, conclude that, if vacancies are present at all in solid argon, their concentration even at the triple point is less than 0.2% of a mole fraction. This concentration is much less than that given by specific heat analysis.

More recently, Losee and Simmons (1967) have crystallographically measured the concentration of vacancies in solid krypton. While their results lead to a value of  $h_s$  in good agreement with that

obtained by Beaumont and co-workers from a consideration of the specific heat, they again give a much smaller value of  $n_s$  (0.3% compared with 1.5% of a mole fraction at the triple point) than that given by a specific heat analysis.

The purely experimental evidence of Simmons and co-workers cannot be disregarded and casts considerable doubt on the wisdom of estimating vacancy effects from the high temperature specific heat of the inert gas solids. In view of this and the fundamental inconsistency given by the assumption of Hillier and Walkley that a cell model system can be taken as a "no vacancy" system, it was felt that our specific heat calculations can throw no real light on the importance of vacancy effects and no such investigations were attempted in the present work.

Chapter 5

Triplet Interactions in the Inert Gas Solids and Some  
Considerations of the Second Virial Coefficient

Triplet interactions in the solid state of the inert gases

All the calculations described to date were performed under the commonly made assumption of pairwise additivity in the solid state. We now describe EXP-6 solid state calculations which make some attempt to allow for non-central many-body interactions - in particular triplet interactions.

The first calculation of many-body interactions was by Axilrod and Teller (1943) who, by means of third order perturbation theory, considered the interaction of three instantaneous dipoles. Their approach was analogous with London's use of second order perturbation theory to give the  $r^{-6}$  attraction between two instantaneous dipoles (see Chapter 1) and, in addition to the three pair interactions, led to an expression for the triplet energy of the three particles. This was:

$$\phi^{ABC} = \frac{C^{ABC} (3 \cos \theta_A \cos \theta_B \cos \theta_C + 1)}{r_{AB}^3 r_{BC}^3 r_{CA}^3} \quad (5.1)$$

where  $\theta_A$ ,  $\theta_B$ ,  $\theta_C$  are the interior angles and  $r_{AB}$ ,  $r_{BC}$ ,  $r_{CA}$  the sides of the triangle formed by the three particles A, B and C. Axilrod (1949) later estimated the proportionality constant  $C^{ABC}$  in terms of the

ionisation energies and polarisabilities of A, B and C. For three identical atoms, A, the appropriate expression is:

$$C^{AAA} = (9/16)I_A \alpha_A^3 \quad (5.2)$$

where  $I_A$  is the ionisation energy and  $\alpha_A$  the polarisability of A.  $C^{ABC}$  may also be evaluated from quantum mechanical first principles and such calculations have been performed for the inert gases by Kihara (1958) and, more recently, by Bell and Kingston (1966). The values of  $C^{ABC}$  given by Bell and Kingston are quoted to an accuracy of 10% and agree with those given by Axilrod's expression, but are in disagreement with those of Kihara.

Similar to London's dipole-dipole pair interaction energy, the energy given by (5.1) is in fact the first of a series of terms constituting the triplet dispersion energy of the three particles. Higher terms in the series, such as the dipole-dipole-quadrupole interaction, have been derived by Ayres and Tredgold (1956). However, such terms are small and, in the present work, the use of the expression "triplet dispersion energy" refers only to the triple dipole interaction given by (5.1).

The triplet dispersion energy takes no account of electron overlap and represents only the long range interaction. Jansen and co-workers (see Jansen and Lombardi 1965 and the references quoted therein) have made several investigations of the short range exchange triplet interaction, using a Gaussian effective electron model. However, such an approach does not lead to

explicit expressions and, moreover, Swenberg (1967) has recently cast doubt on the validity of one of the approximations made in Jansen's calculations. Consequently, the detailed nature of short range triplet effects must, as yet, be considered uncertain. As was pointed out in Chapter 1, such is also the case with the short range pair interaction.

Recent investigations of triplet interactions in the solid state of the inert gases have been concerned with their effect on such properties as stacking fault energy (Pliskin and Greenberg 1965, Bullough, Glyde and Venables 1966), elastic constant (Götze and Schmidt 1966), vacancy formation energy (Jansen 1965) and lattice relaxation around a vacancy (Foreman 1963). However, such interactions have been of interest mainly because of the possibility of their explaining why neon, argon, krypton and xenon crystallise with a face centred cubic (f.c.c.) rather than a hexagonal close packed (h.c.p.) structure.

Kihara and Koba (1952) and Kihara (1953) showed that pairwise additive LJ m:6 and EXP-6 calculations of the static energies of f.c.c. and h.c.p. lattices invariably favour the h.c.p. structure. The relative difference in pair energy is only small - of the order of 0.01% - but is nevertheless constant for different pair potentials. This conclusion is unaltered by the consideration of zero point energy (Barron and Domb 1955, Jansen and Dawson 1955, Wallace 1964). Axilrod (1951) had previously calculated the static triplet dispersion energy in the f.c.c. and h.c.p. structures by summing over a large (but finite) cylindrical lattice.

In both cases he found the energy to be repulsive (i.e. of positive sign) and such that the f.c.c. structure is favoured. The difference, however, is not enough to overcome the stability of the h.c.p. lattice predicted by pairwise additive calculations. The work of Jansen and co-workers on the short range interaction predicts the correct f.c.c. structure, but, as mentioned previously, this work has been questioned.

Although many-body interactions have been generally recognised as probably decisive in determining the stable structure of the inert gas solids, the very small difference between the energies of the two possible lattices has been taken by some (e.g. Pollack 1964) to show that many-body effects may be neglected in the calculation of thermodynamic properties. Such a conclusion, however, ignores an important result of Axilrod's work. Taking the f.c.c. structure as read, the expression derived by Axilrod for the contribution of triplets to the static energy of a lattice of N atoms of type A may be written:

$$W(0)^{\text{triplets}} = (N/3)56.7C^{\text{AAA}}/a_1^9 \quad (5.3)$$

and, using (5.2) to evaluate  $C^{\text{AAA}}$ , Axilrod showed that this energy is by no means negligible, at least in the case of the heavier inert gas solids. For solid xenon, he found the magnitude of  $W(0)^{\text{triplets}}$  given by (5.3) to be of the order of 10% of the total energy of the crystal at 0°K. Bell and Kingston's values of  $C^{\text{AAA}}$  lead to similar results.



The values of  $W(O)^{\text{triplets}}$  for solid neon, argon, krypton and xenon at  $0^{\circ}\text{K}$  and zero pressure, calculated from (5.3) using the values of Bell and Kingston for  $C^{\text{AAA}}$  and the values of  $a_1$  corresponding to those of  $a_{00}(0)$  given in Table 1 (p.70), are given in Table 4. They are compared with the corresponding  $0^{\circ}\text{K}$ , zero pressure values of the sublimation energy,  $L_0(0)$  (which is the negative of the free energy of the crystal at  $0^{\circ}\text{K}$  and zero pressure), given in Table 1.

Table 4

The static lattice triplet dispersion energy of the inert gas solids at  $0^{\circ}\text{K}$  and zero pressure

Substance (A)	$C^{\text{AAA}}$ (erg $\text{\AA}^9$ ) $\times 10^{12}$	$W(O)^{\text{triplets}}$ (cal mole $^{-1}$ )	$L_0(0)$ (cal mole $^{-1}$ )
Neon	1.68	15	448
Argon	74.5	136	1846
Krypton	224	236	2666
Xenon	750	377	3828

(5.3) may be written in a reduced form analogous to that corresponding to the pair static lattice energy, thus:

$$W^*(O)^{\text{triplets}} = \frac{1}{3} w^*(O)^{\text{triplets}} = \frac{1}{3} (56.7 C^{\text{AAA}} / a_1^{*9}) \quad (5.4)$$

$$\begin{aligned} \text{where } W^*(O)^{\text{triplets}} &= W(O)^{\text{triplets}} / (N_L) \\ w^*(O)^{\text{triplets}} &= w(O)^{\text{triplets}} / \epsilon \\ C^{\text{AAA}} &= C^{\text{AAA}} / (\epsilon d^9) \\ a_1^* &= a_1 / d \end{aligned}$$

$\epsilon$  and  $d$  being the characteristic energy and length parameters in the pair potential function and  $w(o)$  the potential energy experienced by a representative particle in the lattice due to all pairs of other particles in the lattice.

The direct experimental measurement of many-body contributions to the potential energy of a crystal is very difficult, since it is difficult to isolate many-body from two-body effects. From their measurements of vacancy concentrations, Losee and Simmons (1967) have obtained a rather imprecise value of  $650 \pm 300$  cal mole<sup>-1</sup> for the many-body interactions in solid krypton, but, to the author's knowledge, this is the only experimental result as yet available. The result of Losee and Simmons does not distinguish between triplet and higher order interactions, but it does lend support to the importance of many-body effects in the inert gas solids and it is reasonable to assume that triplet effects are by far the largest of these.

In view of the above, it seemed worthwhile to investigate how the results of our solid state calculations would be affected by allowing for triplet interactions. The approach taken was that of Zucker (1968 - but communicated to the author prior to publication), who made use of (5.3), together with Bell and Kingston's values of  $C^{AAA}$ , to evaluate the contribution of triplets to the total energy of the crystal.

This approach involves two major approximations. The first is that triplet effects in the vibrational energy of the crystal are ignored. At the time that

that the work described here was undertaken there was little information as to the nature of such effects. More recently, however, Chell and Zucker (1968) have explicitly evaluated the harmonic contribution of triplet dispersion interactions to the zero point energy of the inert gas solids using an Einstein model of the crystal. They found that triplet interactions lowered the zero point energy by amounts ranging from less than 1% in the case of neon to about 2% in the case of xenon. Such changes in the zero point energy lead to changes in the total crystal free energy which are minimal in comparison with the effect of the triplet dispersion energy in the static lattice.

The second approximation is that short range triplet effects are completely neglected and this is undoubtedly more serious. However, until more detailed information as to the nature of such effects is available, there seems no alternative but to ignore them and trust that their inclusion would not drastically alter any conclusions which we might draw. In any case the use of (5.3) should serve as a first approximation for the evaluation of triplet effects.

Zucker investigated the effect of the triplet dispersion interactions in the static lattice on LJ pair potentials, characterised from 0°K solid state data, which gave the best fit with experimental solid state isotherms, and also the effect on the predicted isotherms themselves. The appropriate LJ functions were the 12:6 for neon, argon and krypton and the 11:6 for xenon. He found that the pair parameters for

neon were only slightly affected by the inclusion of  $W(O)$  triplets but that those of the heavier gases were substantially changed. On the other hand, none of the predicted isotherms was appreciably affected.

In our work we investigated the influence of  $W(O)$  triplets given by (5.3) on the EXP-6 pair potential parameters determined from solid state data at  $0^\circ K$  and the subsequent EXP-6 prediction of all the solid state properties calculated in the previous chapter. The experimental data used for the characterisation were those used in the pairwise additive calculations (see Table 1). The numerical procedure employed in the characterisation and the subsequent calculation of the thermodynamic properties was also the same as before except that  $\frac{1}{2}w^*(o) + \frac{1}{3}w^*(o)$  triplets was used in place of  $\frac{1}{2}w^*(o)$ .

The parameters obtained are given in Table 5 below and the corresponding potential functions are plotted as the dashed-dotted curves in Figs. 4, 5, 6 and 7 (pp. 75-78) for neon, argon, krypton and xenon respectively. The results of the calculations of the thermodynamic properties are tabulated in Appendix 6 and plotted as the dashed-dotted curves in Figs. 8a-11g (pp. 90-117). (The reader is asked to note that, on the scale of Fig. 11a, the  $a_0$  versus  $T$  curve for xenon derived by including triplet dispersion interactions in the static lattice is identical to the corresponding "pairwise additive" LJ 12:6 curve over the whole temperature range.)

Table 5

EXP-6 parameters derived from solid state data at 0°K with triplet dispersion energy included in the static lattice

Substance	$\epsilon(\text{erg}) \times 10^{15}$	$r_m(\text{\AA})$	$\alpha$	$\Lambda^* = h / [ (m\epsilon)^{1/2} r_m ]$
Neon	5.642	3.077	16.27	0.4952
Argon	18.37	3.774	14.13	0.1590
Krypton	26.07	4.020	14.87	0.08654
Xenon	36.10	4.387	13.47	0.05384

Comparison of the values of the parameters in Table 5 with those in Table 2 (p. 74), or of the full curves with the dashed-dotted ones in Figs. 4, 5, 6 and 7, shows that the inclusion of triplet dispersion interactions in the static lattice lowers the depth of the EXP-6 well (i.e. increases  $\epsilon$ ) and moves it to a slightly smaller intermolecular separation (i.e. decreases  $r_m$ ). Such is in agreement with Zucker's results for the best fit LJ potentials. Similarly the effect on  $\epsilon$  and  $r_m$  is only small for neon, but is appreciable for argon, krypton and xenon. In all cases the value of  $\alpha$  is not significantly altered.

From comparison of the full and dashed-dotted curves in Figs. 8a-c, 9a-c, 10a-c and 11a-c, it is clear that the effect of the inclusion of  $W(0)$  triplets, evaluated from (5.3), on the EXP-6 prediction of the temperature variation of lattice constant, isothermal compressibility and volume expansivity of the inert

gas solids, is to increase the values of these properties at temperatures above 0°K.

In the case of solid neon this has the effect of bringing the predicted values of  $a_0$  and  $\beta$  (see Figs. 8a, 8c) marginally closer to the corresponding experimental values, but by no means into good agreement with them. The EXP-6 values of  $\chi_T$  for solid neon (see Fig. 8b) predicted by the inclusion of  $W(0)$  triplets in the static lattice energy are, like the corresponding pairwise additive values, in agreement with experiment within the quoted error limits over the whole temperature range.

For the heavier inert gas solids the inclusion of  $W(0)$  triplets given by (5.3) removes the good agreement between the EXP-6 and experimental  $a_0$  versus T curves (see Figs. 9a, 10a, 11a). In these cases the discrepancy between the EXP-6+ $W(0)$  triplets curves and the experimental results is approximately the same as that between the pairwise additive LJ 12:6 curves and experiment. A similar discrepancy is also shown by the  $\beta$  versus T plot for solid argon up to 70°K (see Fig. 9c). As mentioned in Chapter 4, the volume expansivity data for solid krypton and xenon is not accurate enough for a detailed comparison between theoretical and experimental values of this property to be carried out, but for these substances too the EXP-6+ $W(0)$  triplets  $\beta$  versus T curves are similar to the corresponding pairwise additive LJ 12:6 curves (see Figs. 10c, 11c). Both the EXP-6 pairwise additive and EXP-6+ $W(0)$  triplets models predict the available  $\chi_T$  versus T data for solid argon, krypton and xenon within the experimental uncertainties

quoted (see Figs. 9b, 10b, 11b).

Owing to the independence of  $C_v$  of the static lattice energy, the new EXP-6  $C_v$  versus T curves differ from the old only by virtue of the difference between the two sets of parameters in Tables 2 and 5. The small difference between these sets of parameters in the case of neon leads to a small increase in the predicted  $C_v$  at the higher temperatures, but does not significantly improve agreement with experiment (see Fig. 8d). The new  $C_v$  versus T curves for the heavier inert gas solids show the same general features as those derived from the "pairwise additive" parameters, but are considerably different from a quantitative point of view (see Figs. 9d, 10d, 11d). It appears that the use of the new parameters leads to an increase in  $C_v$  in the low temperature region and a decrease at temperatures approaching the triple point. Also the fall of the  $C_v$  versus T curves in the high temperature region appears to be slightly more rapid. In the case of solid argon, which is the only one of the heavier inert gas solids for which experimental  $C_v$  data are given, Fig. 9d shows that the new EXP-6  $C_v$  versus T curve is in better agreement with experiment at the lower temperatures and in worse agreement at the higher temperatures than is the corresponding "pairwise additive" curve. However, for reasons given in Chapter 4, a detailed comparison between experimental and cell model values of  $C_v$  is probably not meaningful.

In analogy with the corresponding  $C_v$  versus T results, the EXP-6+W(0) triplets  $C_p$  versus T curve for solid neon is slightly above that given by pairwise

additive calculations and, therefore, slightly closer to (but by no means in agreement with) the experimental results (see Fig. 8e). The new EXP-6  $C_p$  versus  $T$  curves for the heavier inert gas solids are considerably higher than the corresponding pairwise additive ones at all appreciable temperatures (see Figs. 9e, 10e, 11e). In all cases the agreement between theory and experiment is better over the whole temperature range, and is remarkably good at the lower temperatures. However, in view of remarks made in Chapter 4, such agreement is probably to some extent fortuitous.

The increased values of  $C_p$  given by the inclusion of  $W(O)$  triplets automatically lead to increased values of the entropy and, consequently, the appropriate  $S$  versus  $T$  curves in Figs. 8f, 9f, 10f and 11f are closer to the experimental results than those derived from pairwise additive calculations. In the case of solid xenon the agreement between the new  $S$  values and experiment is reasonably good, but, once again, owing to the previously mentioned (see Chapter 4) model sensitivity of the entropy, this is almost certainly fortuitous.

The effect of the static lattice triplet dispersion energy on the predicted  $V/V(O)$  versus  $p$  curves is once again small in the case of solid neon (see Fig. 8g), but more marked in the case of argon, krypton and xenon (see Figs. 9g, 10g, 11g). For solid neon the effect of  $W(O)$  triplets is to slightly increase the values of  $V/V(O)$  at high pressure. On the other hand, the values of  $V/V(O)$  predicted for the heavier inert gas solids are lowered. The agreement with experiment is somewhat improved in the case of solid argon and solid



krypton. For solid xenon both EXP-6 models predict the experimental  $V/V(0)$  versus  $p$  data within the appropriate experimental uncertainties.

It is clear then that the inclusion of  $W(O)$  triplets given by (5.3) does lead to changes both in the pair potentials and in the predicted values of the thermodynamic properties of the inert gas solids.

For solid neon these changes are not large enough either to seriously question the assumption of pairwise additivity or to alter the conclusion arrived at in Chapter 4 that the EXP-6 function does not give a good representation of the pair interaction, which appears to be better described by the LJ 12:6 function.

In the case of solid argon, krypton and xenon, however, the effect of  $W(O)$  triplets is significant and, for these substances, the speculation in Chapter 4, that solid state, "pairwise additive" parameters can be regarded as defining an "effective" pair interaction, which, in turn, may be used in the pairwise additive calculation of the thermodynamic properties, appears to be contradicted.

Once again we draw no conclusions from a consideration of  $C_v$ ,  $C_p$  and  $S$  versus  $T$  plots, since, as pointed out in Chapter 4, the calculated values of these properties are probably too sensitive to the Einstein nature of the cell model for a meaningful comparison with experiment to be made. Leaving such properties aside then, we have seen that the inclusion of  $W(O)$  triplets in the EXP-6 cell model does lead to somewhat better

predictions of the  $V/V(0)$  versus  $p$  data of solid argon and krypton. However, taking account of experimental error, this improvement is not substantial. For solid xenon the two EXP-6 models predict the  $V/V(0)$  versus  $p$  data equally well within the quoted experimental error limits. The rather imprecise  $\chi_T$  data for all the heavier inert gas solids is also predicted within experimental error by both models. On the other hand, the good agreement between the EXP-6  $a_0$  versus  $T$  curves and experiment, which was taken to argue so strongly for the use of the EXP-6 function for argon, krypton and xenon in the pairwise additive case, is destroyed by the inclusion of  $W(0)$  triplets. This, in turn, is also the case for the  $\beta$  versus  $T$  curve of solid argon, which is the only one of the heavier inert gas solids for which the volume expansivity data is accurate enough for a reliable comparison between theory and experiment to be made. Such  $a_0$  versus  $T$  and  $\beta$  versus  $T$  results, however, do not alter the conclusion drawn in Chapter 4 that the EXP-6 function gives a better description of these properties of the heavier inert gases than does the LJ 12:6 function, for the inclusion of the value of  $W(0)$  triplets given by (5.3) in the LJ 12:6 calculations would lead to results even further removed from experiment. Nevertheless, if the use of (5.3) is a valid way of allowing for the effect of triplet interactions, these results would appear to indicate that the EXP-6 function is not such a good representation of the argon-argon, krypton-krypton and xenon-xenon interactions as would be supposed from pairwise additive calculations.

Some considerations of the second virial coefficient

It is well known that the equation of state of a non-ideal gas may be written as the virial expansion:

$$\frac{pV}{NkT} = 1 + \frac{B(T)}{V} + \frac{C(T)}{V^2} + \frac{D(T)}{V^3} \dots \quad (5.4)$$

where  $p$ ,  $V$ ,  $N$ ,  $k$  and  $T$  have their usual significance and  $B(T)$ ,  $C(T)$ ,  $D(T)$  ... are called the second, third, fourth ... virial coefficients of the gas. The term  $B(T)/V$  represents the contribution of interacting pairs of molecules, outside the perturbing field of others in the system, to the compressibility factor of the gas. Higher terms represent contributions from groups of three, four ... molecules and involve triplet, quadruplet ... interactions as well as the pair interaction. The study of  $B(T)$ , therefore, provides a means of obtaining information as to the nature of the pair interaction itself, without having to consider many-body effects. In consequence, it is of interest to compare pair potentials derived from a consideration of  $B(T)$  with those given by a consideration of a multiparticle system such as the solid state.

The second virial coefficient,  $B(T)$ , in quantum statistical mechanics may be written as:

$$B(T) = \frac{-N}{2V} \iint [W_2(\underline{r}_1, \underline{r}_2) - 1] d\underline{r}_1 d\underline{r}_2 \quad (5.4)$$

where  $W_2(\underline{r}_1, \underline{r}_2)$  is the Slater sum for two molecules with position vectors  $\underline{r}_1$  and  $\underline{r}_2$  and is given by:

$$W_2(r_1, r_2) = 2! \left( \frac{h^2}{2\pi mkT} \right)^3 \sum_i \psi_i^*(r_1, r_2) \exp \left( \frac{-H}{kT} \right) \psi_i(r_1, r_2) \quad (5.4a)$$

In (5.4a)  $\psi_i$  ( $i=1, 2, 3, \dots$ ) is a complete set of orthonormal wave functions,  $\psi_i^*$  ( $i=1, 2, 3, \dots$ ) is the corresponding complex conjugate set and  $H$  is the quantum mechanical Hamiltonian operator for the two particles. On choosing  $\psi_i$  ( $i=1, 2, 3, \dots$ ) to be the momentum wave functions, (5.4) may be expanded in even powers of  $(h^2/m)$  to give:

$$B(T) = B_{Cl}(T) + \left( \frac{h^2}{m} \right) B_I(T) + \left( \frac{h^2}{m} \right)^2 B_{II}(T) + \dots \quad (5.5)$$

where  $B_{Cl}(T)$  is the classical value of the second virial coefficient and is given in terms of the pair interaction,  $\phi(r)$ , by:

$$B_{Cl}(T) = -2\pi N \int_0^\infty \left[ \exp \left( \frac{-\phi(r)}{kT} \right) - 1 \right] r^2 dr \quad (5.5a)$$

Higher terms in the series represent quantum corrections,  $B_I(T)$  and  $B_{II}(T)$  being given by:

$$B_I(T) = \frac{2\pi N}{48\pi^2 k^3 T^3} \int_0^\infty \left[ \exp \left( \frac{-\phi(r)}{kT} \right) \right] \left[ \frac{d\phi(r)}{dr} \right]^2 r^2 dr \quad (5.5b)$$

and

$$B_{II}(T) = \frac{-2\pi N}{1920\pi^4 k^4 T^4} \int_0^\infty \exp \left( \frac{-\phi(r)}{kT} \right) \left\{ \left[ \frac{d^2\phi(r)}{dr^2} \right]^2 + \frac{2}{r^2} \left[ \frac{d\phi(r)}{dr} \right]^2 \right. \\ \left. + \frac{10}{9kTr} \left[ \frac{d\phi(r)}{dr} \right]^3 - \frac{5}{36k^2 T^2} \left[ \frac{d\phi(r)}{dr} \right]^4 \right\} r^2 dr \quad (5.5c)$$

(see Hirschfelder, Curtiss and Bird 1954, p.420).

A further term  $(h^2/m)^{3/2} B_0(T)$  ( $B_0(T) = -5/2 (2\pi kT)^{-3/2}$ ) must be included in this series to account for Bose-Einstein (B.E.) or Fermi-Dirac (F.D.) statistics (de Boer and Michels 1938). The sign of this term is negative for B.E. statistics (i.e. for systems of molecules consisting of an even number of nucleons and electrons) and positive for F.D. statistics (i.e. for systems of molecules consisting of an odd number of nucleons and electrons). The final expression may be written in reduced form as an expansion in powers of the quantum parameter,  $\Lambda^*$  (see (2.28) in Chapter 2), thus (Hirschfelder, Curtiss and Bird 1954, p.420):

$$B^*(T^*) = \left[ B_{Cl}^*(T^*) + \Lambda^{*2} B_I^*(T^*) + \Lambda^{*4} B_{II}^*(T^*) + \dots \right] + \Lambda^{*3} B_0^*(T^*) \quad (5.6)$$

where  $B^*(T^*) = B(T) / (2\pi Nd^3)$ ,  $d$  being the characteristic length parameter of the pair potential.  $B_{Cl}^*(T^*)$ ,  $B_I^*(T^*)$ ,  $B_{II}^*(T^*)$ ,  $B_0^*(T^*)$  are given by:

$$B_{Cl}^*(T^*) = -3 \int_0^{\infty} \left[ \exp\left(\frac{-\phi^*(r^*)}{T^*}\right) - 1 \right] r^{*2} dr^* \quad (5.6a)$$

$$B_I^*(T^*) = \frac{1}{16\pi^2 T^{*3}} \int_0^{\infty} \exp\left(\frac{-\phi^*(r^*)}{T^*}\right) \left[ \frac{d\phi^*(r^*)}{dr^*} \right]^2 r^{*2} dr^* \quad (5.6b)$$

$$B_{II}^*(T^*) = -\frac{1}{640\pi^4 T^{*4}} \int_0^{\infty} \exp\left(\frac{-\phi^*(r^*)}{T^*}\right) \left\{ \left[ \frac{d^2\phi^*(r^*)}{dr^{*2}} \right]^2 + \frac{2}{r^{*2}} \left[ \frac{d\phi^*(r^*)}{dr^*} \right]^2 + \frac{10}{9T^* r^*} \left[ \frac{d\phi^*(r^*)}{dr^*} \right]^3 - \frac{5}{36T^{*2}} \left[ \frac{d\phi^*(r^*)}{dr^*} \right]^4 \right\} r^{*2} dr^* \quad (5.6c)$$

$$B_o^*(T^*) = \left( \frac{3}{32\Lambda^{5/2}} \right) T^{*-3/2} \quad (5.6d)$$

For fuller details of the formulation and the range of its validity the reader is referred to Hirschfelder, Curtiss and Bird (1954, p.419 et.seq.) and de Boer and Michels (1938). For the calculation of high temperature values of the second virial coefficient, terms beyond the classical one may be neglected, but at low temperatures higher terms may become significant, especially for light substances. In our work we took account of terms up to and including that in  $\Lambda^{*4}$ , using the expressions given below.

Experimental measurements of the second virial coefficient have been widely used in the characterisation of empirical pair potential functions. Typical of such work is that of Nicholson and Schneider (1955), Sherwood and Prausnitz (1964), Dymond, Rigby and Smith (1965) and Weir, Wynne Jones, Rowlinson and Saville (1967). Nicholson and Schneider characterised the LJ 12:6 and EXP-6 potentials for neon by calculating the parameters which gave the best fit with their own and earlier B(T) data. They found that each function predicted the B(T) data equally well, but that the EXP-6 function gave a slightly deeper potential well. Sherwood and Prausnitz made use of all the relevant B(T) data available at the time to determine the best fit parameters of, among others, the LJ12:6, EXP-6 and Kihara 12:6 potential functions for argon, krypton and xenon. They found that, in each case, the EXP-6 and Kihara 12:6 potentials gave a better overall fit with experiment, a deeper well and smaller equilibrium

separation than the LJ 12:6 function. The use of the five term empirical function proposed by Dymond, Rigby and Smith leads to results similar to those given by the EXP-6 and Kihara 12:6 functions. The results of Weir, Wynne Jones, Rowlinson and Saville, who used their own recent measurements of  $B(T)$  and those of others to characterise the LJ 12:6 and Kihara 12:6 functions for argon and krypton, are in agreement with those given by the corresponding calculations of Sherwood and Prausnitz, but give a deeper well for the Kihara potential.

In our work we decided to recharacterise the EXP-6 function for neon, argon, krypton and xenon using the most modern  $B(T)$  data available and to compare the pair interactions obtained with those given by solid state data with and without  $W(0)$  triplets included. In contrast to the second virial coefficients corresponding to the LJ 12:6 and Kihara 12:6 potentials, which may be evaluated analytically in terms of gamma functions, the calculation of those corresponding to the EXP-6 potential requires the use of numerical integration. In view of this it seemed sensible to study the nature of the integrals in (5.6a), (5.6b) and (5.6c) as a preliminary to more detailed calculations.

First it should be remembered that the spurious maximum in the EXP-6 pair potential requires the imposition of an infinite cutoff at a reduced intermolecular separation of  $r^*$ . For distances between  $r^*=0$  and  $r^*=r^*_{\max}$ , therefore, the value of  $\exp(-\phi^*(r^*)/T^*)$

is zero and the contribution to  $B_{C1}^*(T^*)$  in this region is:

$$-3 \int_0^{r_{\max}^*} (-r^{*2}) dr^* = r_{\max}^{*3} \quad (5.7)$$

The corresponding contributions to  $B_I^*(T^*)$  and  $B_{II}^*(T^*)$  are zero. The value of  $r_{\max}^*$  is easily obtained for any value of  $\alpha$  by the numerical solution of the transcendental equation (4.5) in Chapter 4.

It is relevant to note the  $r^*$  dependence of the integrands,  $I_{C1}^*$ ,  $I_I^*$  and  $I_{II}^*$  appearing in the expressions (5.6a), (5.6b) and (5.6c). The  $r^*$  dependence of  $I_{C1}^*$  is such that this quantity passes through a negative minimum followed by a positive maximum in the region of  $r^*=1$ . The behaviour of  $I_I^*$  with  $r^*$  is such that  $I_I^*$  is always positive and passes through two positive maxima on either side of a minimum value of zero at  $r^*=1$ . The  $r^*$  dependence of  $I_{II}^*$  is of a similar form to that of  $I_{C1}^*$ . All three functions approach zero at small and large values of  $r^*$ . The values of  $r^*$  at which the various maxima and minima appear are virtually independent of the values of  $\alpha$  and  $T^*$ , both of which affect only the values of  $I_{C1}^*$ ,  $I_I^*$  and  $I_{II}^*$  at these points. The values of  $r^*$  corresponding to the minimum and maximum in  $I_{C1}^*$  are about 0.8 and 1 respectively, those corresponding to the two maxima in  $I_I^*$  are about 0.9 and 1.1 and those corresponding to the minimum and maximum values of  $I_{II}^*$  are about 0.85 and 0.9 respectively.

The major contributions to the various integrals clearly come from the restricted regions around the



various maxima and minima in  $I_{C1}^*$ ,  $I_I^*$  and  $I_{II}^*$ , and it is wise to consider these regions separately from those where the integrands are approaching zero. This is especially the case in the evaluation of  $B_I^*(T^*)$  and  $B_{II}^*(T^*)$  for which the relevant maxima and minima are so sharp that, if the range of integration is divided without regard to the behaviour of the integrands, the major contributions may be missed altogether. With this in mind, we divided the range of integration for  $r^* \geq r_{\max}^*$  into five separate sub-ranges for each integral. In each case the first four of these sub-ranges covered intermolecular distances from  $r^* = r_{\max}^*$  to  $r^* = 3$ . For  $B_{C1}^*(T^*)$  they were  $r_{\max}^* \leq r^* \leq 0.6$ ;  $0.6 \leq r^* \leq 0.9$ ;  $0.9 \leq r^* \leq 1.2$ ;  $1.2 \leq r^* \leq 3$ ; for  $B_I^*(T^*)$ ,  $r_{\max}^* \leq r^* \leq 0.7$ ;  $0.7 \leq r^* \leq 1$ ;  $1 \leq r^* \leq 1.3$ ;  $1.3 \leq r^* \leq 3$ ; and for  $B_{II}^*(T^*)$ ,  $r_{\max}^* \leq r^* \leq 0.6$ ;  $0.6 \leq r^* \leq 0.9$ ;  $0.9 \leq r^* \leq 1.1$ ;  $1.1 \leq r^* \leq 3$ .

In each case the integration in the four sub-ranges was by 8, 12, 12 and 8 point Gaussian quadrature formulae, (see Kopal 1955 p.367 et seq.), respectively. For all three integrals the fifth sub-range of integration was from  $r^* = 3$  to  $r^* = \infty$ . For  $r^* \geq 3$ , the repulsive energy in the pair interaction was found to be negligible and, retaining only the  $r^{*-6}$  attractive term, the contributions of this region to the three integrals were simply evaluated by expanding the integrands as series in inverse powers of  $r^*$  and integrating term by term.

The EXP-6 potential parameters for neon, argon, krypton and xenon giving the optimum fit with the experimental  $B(T)$  data were calculated using the least squares refinement technique described in

Appendix 7. The relevant experimental data are given in Appendix 8, together with sources. All experimental data were given equal weight in the calculations, but the very accurate results of Michels and co-workers and of Weir, Wynne Jones, Rowlinson and Saville were taken in preference to those measured by other workers in corresponding temperature ranges.

The parameters obtained are shown in Table 6, together with the root mean square deviation of the experimental  $B(T)$  values from the calculated values. The experimental and calculated values of  $B(T)$  are compared in Appendix 8.

Table 6

EXP-6 parameters derived from a consideration of the second virial coefficient

Substance	$\epsilon(\text{erg}) \times 10^{15}$	$r_m(\text{\AA})$	$\alpha$	rms devn. ( $\text{cm}^3 \text{mole}^{-1}$ )
Neon	5.800	2.980	17.00	0.13
Argon	23.29	3.539	20.68	1.23
Krypton	32.42	3.787	20.49	1.95
Xenon	43.70	4.203	20.87	0.93

The potential curves corresponding to the parameters in Table 6 are plotted as the dashed-double dotted curves in Figs. 4, 5, 6 and 7 (pp. 75-78).

From Tables 2 (p. 74), 5 (p. 148) and 6 and Figs. 4, 5, 6 and 7 it is seen that the use of second virial data leads to EXP-6 potential functions for neon,

argon, krypton and xenon which have deeper wells (i.e. larger  $\epsilon$  values) and smaller equilibrium separations (i.e. smaller  $r_m$  values) than those given by solid state calculations either with or without  $W(O)^{\text{triplets}}$  included. The values of  $\alpha$  given by second virial calculations are larger than those given by the solid state calculations and this leads to narrower potential wells. The differences between the solid state and second virial potential functions is small in the case of neon but considerable in the case of argon, krypton and xenon. Of the two sets of potential functions derived from solid state data, the well depths and equilibrium separations of those calculated by including  $W(O)^{\text{triplets}}$  are, in all cases, more in line with the results of the second virial calculations. As pointed out earlier, both sets of  $\alpha$  values given by solid state calculations are virtually the same and, therefore, neither set is nearer the second virial values.

We have pointed out earlier that the LJ 12:6 potential leads to worse predictions of the second virial coefficients of argon, krypton and xenon than the EXP-6 function. There is also another point worth noting in connection with the application of the LJ 12:6 function to these substances. This is that, in contrast to the EXP-6 case, the LJ 12:6 parameters derived from pairwise additive solid state calculations are similar to those given by second virial data (compare the LJ 12:6 values of  $\epsilon$  and  $\sigma$  obtained by Sherwood and Prausnitz with those in Table 3, p. 74). In the absence of many-

body effects in the solid state this could be taken to indicate the LJ 12:6 function to be a good representation of the pair interaction of these substances. However, if triplet effects are adequately evaluated by (5.3), this is not so, because the inclusion of  $W(0)^{\text{triplets}}$ , by increasing  $\xi$  and decreasing  $\sigma$ , pushes the solid state parameters away from the second virial ones. The contrasting behaviour of the EXP-6 solid state parameters of argon, krypton and xenon is another indication that the EXP-6 function is a better representation of the pair interactions of the heavier inert gases.

Since the use of second virial coefficient data does not always determine a unique pair interaction (Keller and Zumino 1959), we also tested how well the two sets of EXP-6 solid state parameters themselves (see Table 2, p.74, and Table 5, p.148) predicted the experimental values of  $B(T)$  for neon, argon, krypton and xenon. The evaluation of  $B(T)$  was carried out in precisely the same way as in the characterisation procedure. For neon, argon and krypton it was found that the parameters obtained by the inclusion of  $W(0)^{\text{triplets}}$  lead to values of  $B(T)$  in better overall agreement with experiment than do those given by pairwise additive solid state calculations. For xenon, on the other hand, it is the pairwise additive solid state parameters which lead to the better predictions of  $B(T)$ . The rms deviations from experiment given by the pairwise additive solid state parameters for neon, argon, krypton and xenon are 0.94, 10.31, 25.5 and 2.52  $\text{cm}^3 \text{mole}^{-1}$  respectively, whereas those given by the

"W(0) triplets" parameters are 0.76, 3.42, 8.19, 2.52 cm<sup>3</sup> mole<sup>-1</sup> respectively. The values of B(T) calculated using both sets of solid state parameters are compared with the corresponding experimental values in Appendix 8. In no case, does either set of solid state parameters predict the experimental B(T) data with an accuracy even approaching that given by the second virial parameters themselves.

## Chapter 6

### Conclusion

The solid state calculations described in this thesis are rather crude and any conclusion drawn from their results must be viewed in this light.

The approximation common to them all is the Einstein assumption of independent motion and we have taken some regard of this by not putting any weight at all on how well calculated values of specific heat and entropy agree with experiment. Instead, we have drawn definite conclusions only from predictions of solid state properties, such as lattice constant, which, in contrast to the specific heat and entropy, are strongly dependent on the static lattice energy and, therefore, should be less sensitive to the vibrational motion of the crystal. It is possible that even these properties are not adequately predicted by an Einstein model of the solid, but, in view of the fact that we used potential parameters calculated from solid state data using the same assumption as that used in the subsequent calculation of the thermodynamic properties, we felt that such an approach is justified.

However, to be sure of the results of solid state calculations it is necessary to make use of lattice dynamical techniques, in spite of the considerable computational difficulties involved. We have mentioned that, to date, only first order anharmonic effects have

been taken into account in lattice dynamical calculations and, usually, only nearest neighbour interactions are considered. Nevertheless, this is in spite of the widely held opinion of only a few years ago, that the difficulties in taking account of even low order anharmonic effects by lattice dynamical methods were formidable. With the continual development of the theory and the advent of ever larger and faster electronic computers it is well within the bounds of possibility that many of the remaining problems will be overcome in the not too far distant future. In view of the rigour of lattice dynamics it would seem more sensible to concentrate on this approach to the solid state rather than persevering with models based on the Einstein assumption. On the other hand, the mastery of lattice dynamical techniques requires considerable mathematical facility on the part of the researcher, whereas use of an Einstein approach involves comparatively easy and rapid calculations. In view of this, such an approach has much to recommend it in situations where the absolute accuracy of the results is not critical.

Another approximation that is commonly made in solid state calculations is that of assuming pairwise additivity of the potential. We have attempted to overcome this in our later EXP-6 solid state calculations by making some allowance for triplet effects. This does not substantially alter the indications of the pairwise additive calculations as to the relative ability of the EXP-6 and LJ 12:6 functions to describe the solid state of neon, argon, krypton and xenon, but it does lead to appreciably different quantitative

results in the case of the heavier inert gases. It is interesting that the values of the EXP-6 pair parameters obtained by allowing for triplet effects in the solid state are more in line with those given by a consideration of the second virial coefficient than are the corresponding values derived from pairwise additive solid state calculations. However, the method by which we allowed for triplet effects was, of necessity, approximate and took account of only dispersion interactions in the static lattice energy. To be sure of the precise effect of triplets in the solid state, more information is required as to the nature of the short range triplet interaction.

Finally we come to the pair potential itself. We have pointed out in Chapter 1 that the  $r^{-6}$  dependence of the long range part of the pair interaction of the inert gases is well established, but that the nature of the short range interaction is still subject to considerable uncertainty. Our reason for investigating the EXP-6 potential was that the use of an exponential repulsion of some sort seemed more in accord with the results of fundamental quantum mechanical considerations of simple systems, than did the use of the inverse power repulsions typical of Lennard-Jones functions. The calculations in this thesis do in fact indicate, to some extent, a superiority of the EXP-6 function over the LJ 12:6 function in the overall description of the solid state of at least the heavier inert gases. It should be remembered, however, that the EXP-6 function is still empirical in nature and the use of the LJ 12:6 potential can lead to better predictions of some properties even of systems for which the



EXP-6 gives an overall better description. To obtain a truly rigorous picture of the nature of the inert gas pair interaction it is necessary to undertake a fundamental study of a pair of isolated molecules, but, as we have pointed out, the mathematical obstacles to such an approach are formidable except for the simplest systems. Nevertheless, with the large electronic computers at present available, some progress could probably be made in this direction.

### References

- Alder, B.J., 1962, Phys.Rev., 127, 359.
- Amdur, I., & Mason, E.A., 1958, Phys.Fluids, 1, 370.
- Axilrod, B.M., 1949, J.Chem.Phys., 17, 1349.
- Axilrod, B.M., 1951, J.Chem.Phys. 19, 724.
- Axilrod, B.M., & Teller, E., 1943, J.Chem.Phys., 11, 299.
- Ayres, R.U., & Tredgold, R.H., 1956, Proc.Phys.Soc.,  
69B, 840
- Barker, J.A., 1955, Proc.Roy.Soc.A, 230, 390.
- Barker, J.A., 1956, Proc.Roy.Soc.A, 237, 63.
- Barker, J.A., 1963, "Lattice Theories of the Liquid State"  
(Pergamon Press; Oxford, London, New York,  
Paris).
- Barron, T.H.K., 1965, Disc.Faraday Soc., 40, 119.
- Barron, T.H.K., & Domb, C., 1955, Proc.Roy.Soc A, 227, 447
- Batchelder, D.N., Losee, D.L., & Simmons, R.O., 1967  
Phys.Rev., 162, 767.
- Batchelder, D.N., Peterson, O.G., & Simmons, R.O., 1965  
Phil.Mag., 12, 1193.
- Beattie, J.A., Barriault, R.J., & Brierly, J.S., 1951,  
J.Chem.Phys., 19, 1219, 1222.
- Beattie, J.A., Barriault, R.J., & Brierly, J.S., 1952,  
J.Chem.Phys., 10, 1615.
- Beaumont, R.H., Chihara, H., Morrison, J.A., 1961  
Proc.Phys.Soc., 78, 1462.
- Bell, R.J., & Kingston, A.E., 1966, Proc.Phys.Soc., 88, 901.
- Bernardes, N., 1960, Phys.Rev., 120, 807.
- Born, M., & von Karman, T., 1912, Z.Phys., 13, 297.
- Born, M., & von Karman, T., 1913, Z.Phys., 14, 15.
- Brown, W.B., & Rowlinson, J.S., 1960, Mol.Phys., 3, 35.
- Buckingham, R.A., & Corner, J., 1947, Proc.Roy.Soc.A,  
189, 118.
- Bullough, R., Glyde, H.R., & Venables, J.A., 1966,  
Phys.Rev.Letters, 17, 249.

References (Cont.)

- Casimir, H.B.G., & Polder, D., 1948, Phys.Rev., 73, 360.
- Cheeseman, G.H., & Soane, C.M., 1957, Proc.Phys.Soc.,  
70B, 700.
- Chell, G.G., & Zucker, I.J., 1968, Proc.Phys.Soc.C,  
(Solid State Physics), 1, 35.
- Clusius, K., Flubacher, P., Piesbergen, U., Schleich, K.,  
& Sperandio, A., 1960, Z.Naturforsch.,  
15, 1.
- Clusius, K., & Riccoboni, L., 1938, Z.Phys.Chem., B38, 81
- Clusius, K., & Weigand, K., 1960, Z.Phys.Chem., B46, 1.
- Cohen, E.G.D., de Boer, J., & Salsburg, Z.W., 1955,  
Physica, 21, 137.
- Cohen, E.G.D., de Boer, J., & Salsburg, Z.W., 1957,  
Physica, 23, 389.
- Cohen, E.G.D. & Reithmeyer, B.C., 1958, Physica, 24, 959.
- Corner, J., 1948, Trans.Faraday Soc., 44, 914.
- Corner, J., & Lennard-Jones, J.E., 1941, Proc.Roy.Soc.,  
178, 401.
- Cowley, R.A., 1963, Adv.Phys., 12, 421.
- Dalgarno, A., & Kingston, A.E., 1961, Proc.Phys.Soc.,  
78, 607.
- Danon, F., & Pitzer, K., 1962, J.Chem.Phys., 36, 425.
- de Boer, J., 1948, Physica, 14, 139.
- de Boer, J., 1954, Physica, 20, 655.
- de Boer, J., & Blaisse, B.S., 1948, Physica, 14, 149.
- de Boer, J.L & Michels, A., 1938, Physica, 5, 945.
- Debye, P., 1912, Ann.Phys., 39, 789.
- Devonshire, A.F., 1940, Proc.Roy.Soc.A, 174, 102.
- Dugdale, J.S., & MacDonald, D.K.C., 1954, Phil.Mag., 45, 811.
- Dymond, J.H., Rigby, M., & Smith, E.B., 1965, J.Chem.Phys.  
42, 2801.

References (Cont.)

- Eatwell, A.J., & Smith, B.L., 1961, *Phil. Mag.*, 6, 461.
- Einstein, A., 1907, *Ann. Phys.*, 22, 180.
- Einstein, A., 1911a, *Ann. Phys.*, 34, 170.
- Einstein, A., 1911b, *Ann. Phys.*, 35, 679.
- Eyring, H., 1936, *J. Chem. Phys.*, 4, 283.
- Fagerstroem, C.H., & Hallet, A.C.H., 1964, "Low Temperature Physics - LT9", (Plenum Press, New York) p.1092.
- Feldman, J.L., & Horton, G.K., 1967, *Proc. Phys. Soc.*, 92, 227.
- Fenichel, H., & Serin, B., 1966, *Phys. Rev.*, 142, 490.
- Figgins, B.F., & Smith, B.L., 1960, *Phil. Mag.*, 5, 186.
- Flubacher, P., Leadbetter, A.J., & Morrison, J.A., 1961, *Proc. Phys. Soc.*, 78, 1449.
- Foreman, A.J.E., 1963, *Phil. Mag.*, 8, 1211.
- Foreman, A.J.E., & Lidiard, A.B., 1963, *Phil. Mag.*, 8, 97.
- Fröman, N., & Fröman, P.O., 1965, "JWKB Approximation, Contributions to the Theory", (North Holland Publishing Company, Amsterdam).
- Gallina, V., & Omini, M., 1964, *Phys. Stat. Sol.*, 6, 391, 627.
- Götze, W., & Schmidt, H., 1966, *Z. Phys.*, 192, 409.
- Griffing, V., & Wehner, J.F., 1955, *J. Chem. Phys.*, 23, 1024.
- Guggenheim, E.A., & McGlashan, M.L., 1960, *Proc. Roy. Soc. A*, 255, 456.
- Hall, G.L., 1957, *J. Phys. Chem. Solids*, 3, 210.
- Henderson, D., & Reed, R.D., 1964, *J. Chem. Phys.*, 40, 975.
- Henkel, J.H., 1955, *J. Chem. Phys.*, 23, 681.
- Hillier, I.H., Islam, M.S., & Walkley, J., 1965, *J. Chem. Phys.*, 43, 3705.
- Hillier, I.H., & Walkley, J., 1964, *J. Chem. Phys.*, 41, 2168.
- Hillier, I.H., & Walkley, J., 1965, *J. Chem. Phys.*, 43, 3713.
- Hirschfelder, J.O., Curtiss, C.F., & Bird, R.B., 1954, "Molecular Theory of Gases and Liquids" (John Wiley & Sons, Inc., New York; Chapman & Hall Limited, London.)
- Holborn, L., & Otto, J., 1925, *Z. Phys.*, 33, 1.
- Horton, G.K., & Leech, J.W., 1963, *Proc. Phys. Soc.*, 82, 816.
- Hurst, R.P., & Levelt, J.M.H., 1961, *J. Chem. Phys.*, 34, 54.

References (Cont.)

- Jansen, J., & Dawson, L.M., 1955, J.Chem.Phys., 23, 482.
- Jansen, L., 1965, Phil.Mag. 8, 1305.
- Jansen, L., & Lombardi, E., 1965, Disc.Faraday Soc., 40, 78.
- Janssens, P., & Prigogine, I., 1950, Physica, 16, 895.
- Jenkins, W.I., 1966, Ph.D Thesis, University of London.
- Jenkins, W.I., & Walkley, J., 1965, Chem.Phys., 43, 3721.
- Kamerlingh Onnes, H., & Crommelin, C.A., 1915, Leiden Comm. 147d.
- Kamerling Onnes, H., Crommelin, C.A., & Martinez, 1919, Leiden Comm., 154a.
- Kanzaki, H., 1957, J.Phys.Chem.Solids, 2, 24.
- Keller, J.B., & Zumino, B., 1959, J.Chem.Phys. 30, 1351.
- Kestner, W.R. & Sinanoglu, O., 1966, J.Chem.Phys. 45, 194.
- Kihara, T., 1951, Proc.Phys.Soc.Japan, 6, 289.
- Kihara, T., 1953, Rev.Mod.Phys., 25, 831.
- Kihara, T., 1955, Rev.Mod.Phys., 27, 412.
- Kihara, T., 1958, Adv.Chem.Phys., 1, 267.
- Kihara, T., & Koba, S., 1952, J.Phys.Soc.Japan, 7, 348.
- Kopal, Z., 1955, "Numerical Analysis", (Chapman & Hall Ltd., London.)
- Kuebler, J., & Tosi, M.P., 1965, Phys.Rev., 137, A1617.
- Langer, R.E., 1937, Phys.Rev., 51, 669.
- Lecocq, A., 1960, J. de Recherche CNRS, 11, 55.
- Loibfried, G., & Ludwig, W., 1961, Solid St.Phys., 12, 275. (Academic Press, New York.)
- Lennard-Jones, J.E., 1924, Proc.Roy.Soc.A, 106, 463.
- Lennard-Jones, J.E., & Devonshire, A.F., 1937, Proc.Roy. Soc.A, 163, 53.
- Lennard-Jones, J.E., & Devonshire, A.F., 1938, Proc.Roy. Soc.A, 165, 1.
- Lennard-Jones, J.E., & Devonshire, A.F., 1939a, Proc.Roy. Soc.A, 169, 317.
- Lennard-Jones, J.E., & Devonshire, A.F., 1939b, Proc.Roy. Soc.A, 170, 469.
- Lennard-Jones, J.E., & Ingham, A.E., 1925, Proc.Roy.Soc.A, 107, 636.

References (Cont.)

- Levelt, J.M.H., & Hurst, R.P., 1960, J.Chem.Phys., 32, 96.
- Lidiard, A.B., 1957, Handbook of Physics, 20, 246,  
(Springer-Verlag, Berlin).
- London, F., 1930, Z.Physik Chem. B11, 222.
- Losee, D.L., & Simmons, R.O., 1967, Phys.Rev.Letters,  
18, 451.
- McGlashan, M.L., 1965, Disc.Faraday Soc., 40, 59.
- McWeeny, R., 1959, Proc.Roy.Soc.A, 253, 242.
- McWeeny, R., 1960, Rev.Mod.Phys., 32, 335.
- Margenau, H., 1939a, Rev.Mod.Phys., 11, 1.
- Margenau, H., 1939b, Phys.Rev., 56, 1000.
- Mason, E.A., & Rice, W.E., 1954, J.Chem.Phys., 22, 843.
- Michels, A., Levelt, J.M., & de Graaf, W., 1958, Physica,  
24, 659.
- Michels, A., Wassenaar, T., & Louwerse, P., 1954, Physica,  
20, 99.
- Michels, A., Wassenaar, T., & Louwerse, P., 1960, Physica,  
26, 539.
- Michels, A., Wijker, H., & Wijker, H., 1949, Physica, 15, 627.
- Mie, G., 1903, Ann.Phys.(Leipzig), 11, 657.
- Montroll, E.W., 1942, J.Chem.Phys., 10, 218.
- Montroll, E.W., 1943, J.Chem.Phys., 11, 481.
- Montroll, E.W., & Peaslee, D.C., 1944, J.Chem.Phys., 12, 98.
- Murrell, J.N., Randic, M., & Williams, D.R., 1965, Proc.  
Roy.Soc.A, 284, 566.
- Nardelli, G.F., & Chiarotti, A., 1960, Nuovo Cim, 18, 1053.
- Nicholson, G.A., & Schneider, W.G., 1955, Can.J.Chem, 33, 589.
- Peterson, O.G., Batchelder, D.N., & Simmons, R.O., 1966,  
Phys.Rev., 150, 703.
- Packard, J.R. & Swenson, C.A., 1963, J.Phys.Chem.Solids,  
24, 1405.
- Phillipson, P.E., 1962, Phys.Rev., 125, 1981.
- Pliskin, Yu.M., & Greenberg, B.A., 1965, Phys.Letters,  
19, 375.
- Pollack, G.L., 1964, Rev.Mod.Phys., 36, 748.
- Pople, J.A., 1951, Phil.Mag., 42, 459.

- Reissland, J.A., 1965, *Disc. Faraday Soc.*, 40, 123.
- Rosen, P., 1950, *J. Chem. Phys.*, 18, 1182.
- Rossi, J.C. & Danon, F., 1965, *Disc. Faraday Soc.*, 40, 97.
- Sakamoto, M., & Ishiguro, E., 1956, *Progr. Theoret. Phys.*  
(Japan), 15, 37.
- Salem, L., 1965, *Disc. Faraday Soc.*, 40, 140.
- Salsburg, Z.W., Cohen, E.G.D., Reithmeyer, B.C. & de Boer, J.,  
1957, *Physica*, 23, 400.
- Salter, L., 1954, *Phil. Mag.*, 45, 360.
- Schiff, L.I., 1955, "Quantum Mechanics" (McGraw-Hill Book  
Company Inc., New York, Toronto, London;  
Kogakusha Company Ltd., Tokyo).
- Sears, D.R., & Klug, H.P., 1962, *J. Chem. Phys.*, 37, 3002.
- Sherwood, A.E., & Prausnitz, J.M., 1964, *J. Chem. Phys.*,  
41, 429.
- Slater, J.C., 1928, *Phys. Rev.*, 32, 349.
- Slater, J.C. & Kirkwood, J.G., 1931, *Phys. Rev.*, 37, 682.
- Stewart, J.W., 1955, *Phys. Rev.*, 97, 578.
- Stewart, J.W., 1956, *J. Phys. Chem. Solids*, 1, 146.
- Swenberg, C.E., 1967, *Phys. Letters*, 24A, 163.
- Urvas, A.O., Losee, D.L., & Simmons, R.O., 1967,  
*J. Phys. Chem. Solids*, 28, 2269.
- Wallace, D.C., 1963, *Phys. Rev.*, 131, 2046.
- Wallace, D.C., 1964, *Phys. Rev.*, 133, 153.
- Weir, R.D., Wynne Jones, I., Rowlinson, J.S., & Saville, G.,  
1967, *Trans. Faraday Soc.*, 63, 1320.
- Whalley, E., Lupien, Y., & Schneider, W.G., 1955, *Can.*  
*J. Chem.*, 33, 633.
- Whalley, E., & Schneider, W.G., 1955, *J. Chem. Phys.*,  
23, 1644.
- Zucker, I.J., 1956, *J. Chem. Phys.*, 25, 915.
- Zucker, I.J., 1961, *Proc. Phys. Soc.*, 77, 889.
- Zucker, I.J., 1964, *Proc. Camb. Hil. Soc.*, 60, 273.
- Zucker, I.H., 1968, *Nuovo Cim.*, 54, 177.

Appendix 1The Derivation of the Spherically Symmetric Cell Potential for the EXP-6 Potential

The reduced spherically symmetric cell potential is given by:

$$\overline{w^*(R^*)} = \sum_i z_i \left\{ \frac{1}{2} \int_0^\pi \left[ \phi^*(\sqrt{a_i^{*2} + R^{*2} - 2R^*a_i^* \cos \theta}) \sin \theta \frac{d\theta}{(A.1.1.)} - \phi^*(a_i^*) \right] \right.$$

If we make the transformation,  $x = (a_i^{*2} + R^{*2} - 2R^*a_i^* \cos \theta)^{\frac{1}{2}}$ , expression (A.1.1.) becomes:

$$\overline{w^*(R^*)} = \sum_i z_i \left[ \frac{1}{2R^*a_i^*} \int_{(a_i^* - R^*)}^{(a_i^* + R^*)} x \phi^*(x) dx - \phi^*(a_i^*) \right] \quad (A.1.2)$$

For the EXP-6 pair potential, which may be written in reduced form as:

$$\phi^*(r^*) = \frac{\alpha}{\alpha - 6} \left[ \frac{6e^\alpha}{\alpha} \exp(-\alpha r^*) - r^{*-6} \right]$$

$\overline{w^*(R^*)}$  becomes:

$$\begin{aligned} \overline{w^*(R^*)} &= \frac{\alpha}{\alpha - 6} \sum_i z_i \left\{ \frac{1}{2R^*a_i^*} \left[ \frac{6e^\alpha}{\alpha} \int_{(a_i^* - R^*)}^{(a_i^* + R^*)} x \exp(-\alpha x) dx \right. \right. \\ &\quad \left. \left. - \int_{(a_i^* - R^*)}^{(a_i^* + R^*)} x^{-5} dx \right] - \frac{6e^\alpha}{\alpha} \exp(-\alpha a_i^*) + \frac{1}{a_i^{*6}} \right\} \quad (A.1.3) \end{aligned}$$



Now:

$$\int_{(a_i^* - R^*)}^{(a_i^* + R^*)} x^{-5} dx = \left[ \frac{-x^{-4}}{4} \right]_{(a_i^* - R^*)}^{(a_i^* + R^*)}$$

$$= \frac{1}{4} [(a_i^* - R^*)^{-4} - (a_i^* + R^*)^{-4}] \quad (\text{A.1.4})$$

and the integration

$$\int_{(a_i^* - R^*)}^{(a_i^* + R^*)} x \exp(-\alpha x) dx$$

may be performed by parts, thus:

$$\int_{(a_i^* - R^*)}^{(a_i^* + R^*)} x \exp(-\alpha x) dx = \left[ \frac{-x \exp(-\alpha x)}{\alpha} \right]_{(a_i^* - R^*)}^{(a_i^* + R^*)} + \frac{1}{\alpha} \int_{(a_i^* - R^*)}^{(a_i^* + R^*)} \exp(-\alpha x) dx$$

$$= \left[ \frac{-x \exp(-\alpha x)}{\alpha} \right]_{(a_i^* - R^*)}^{(a_i^* + R^*)} + \frac{1}{\alpha^2} [\exp(-\alpha x)]_{(a_i^* - R^*)}^{(a_i^* + R^*)}$$

On substitution of the limits and suitable grouping of terms, this expression becomes:

$$\int_{(a_i^* - R^*)}^{(a_i^* + R^*)} x \exp(-\alpha x) dx = \frac{2 \exp(-\alpha a_i^*)}{\alpha} \left[ \left( a_i^* + \frac{2}{\alpha} \right) \sinh(\alpha R^*) - R^* \cosh(\alpha R^*) \right]$$

$$(\text{A.1.5})$$

Substitution of (A.1.5) and (A.1.3) and again suitable grouping of terms, gives:

$$\overline{w^*(R^*)} = \frac{\alpha}{\alpha - b} \frac{b e^{\alpha} \left[ A \frac{\sinh(\alpha R^*)}{R^*} - \frac{R(-1) \cosh(\alpha R^*)}{a_1^*} \right] - \frac{T(4)_6}{8 a_1^* R^*}}{-\frac{b e^{\alpha} R(0)}{\alpha} + \frac{S(b)}{a_1^* b}}$$

where

$$R(u) = \sum_i z_i (a_i^*/a_i)^u \exp(-\alpha a_i^*)$$

$$S(u) = \sum_i z_i (a_i^*/a_i)^{-u}$$

$$T(u)_m = \sum_i z_i (a_i^*/a_i)^{(u-m+1)} [(a_i^*-R)^{-u} - (a_i^*+R)^{-u}]$$

$$A = R(0) + \frac{R(-1)}{\alpha a_1^*}$$

Appendix 2

The "Exact" Finite Difference Solution of the Radial Wave Equation, (Hillier, Islam and Walkley 1965)

The radial Schrodinger equation corresponding to the cell potential,  $w^*(R^*)$ , may be written in reduced variables as:

$$S_{l,n}^{*''} + f(\lambda_{l,n}^*, R^*) S_{l,n}^* = 0 \quad (\text{A.2.1})$$

where

$$f(\lambda_{l,n}^*, R^*) = \frac{8\pi^2}{\lambda^2} \lambda_{l,n}^* - \frac{l(l+1)}{R^{*2}} - \frac{8\pi^2}{\lambda^2} w^*(R^*)$$

and primes denote differentiation with respect to  $R^*$ .

Assuming a first approximation to  $\lambda_{1,n}$  to be  $(\lambda_{1,n}^*)_0$  and a better approximation to be  $(\lambda_{1,n}^*)_0 + \delta\lambda_{1,n}^*$ , the boundary condition at  $R^*=R_c^*$  is written:

$$S_{l,n}^* [(\lambda_{l,n}^*)_0 + \delta\lambda_{l,n}^*, R_c^*] = 0$$

which gives:

$$\delta\lambda_{l,n}^* \approx \frac{-S_{l,n}^* [(\lambda_{l,n}^*)_0, R_c^*]}{\left(\frac{\partial S_{l,n}^*}{\partial \lambda_{l,n}^*}\right)_{\lambda_{l,n}^* = (\lambda_{l,n}^*)_0, R^* = R_c^*}} \quad (\text{A.2.2})$$

Putting:

$$\begin{aligned} Y_1 &= S_{l,n}^* \\ Y_2 &= S_{l,n}^{*''} \\ Y_3 &= \delta S_{l,n}^* / \delta \lambda_{l,n}^* \end{aligned} \quad (\text{A.2.3})$$

(A.2.1) and (A.2.2) become:

$$Y_2' + f(\lambda_{l,n}^*, R^*) Y_1 = 0 \quad (\text{A.2.4})$$

$$\delta \lambda_{l,n}^* \simeq (-Y_1/Y_3) \lambda_{l,n}^* = (\lambda_{l,n}^*)_0, R^* = R_0^* \quad (\text{A.2.5})$$

Differentiation of (A.2.4) with respect to  $\lambda_{l,n}^*$  and putting:

$$Y_4 = Y_3' \quad (\text{A.2.6})$$

gives:

$$Y_4' + f(\lambda_{l,n}^*, R^*) Y_3 - Y_1 = 0 \quad (\text{A.2.7})$$

(A.2.3), (A.2.4), (A.2.5), (A.2.6) and (A.2.7) provide the basis for the determination of  $\lambda_{l,n}^*$  to any desired degree of accuracy. For any value of  $\lambda_{l,n}^*$ , (A.2.3), (A.2.4), (A.2.6) and (A.2.7) may be integrated in a stepwise manner using the Runge-Kutta technique. Due to the singularity in the radial equation at  $R^*=0$ , the integration has to be started at some value of  $R^*=R_0^*$  close to  $R^*=0$ , rather than at  $R^*=0$  itself. The initial values of  $Y_1$ ,  $Y_2$ ,  $Y_3$  and  $Y_4$  are calculated from the Levelt and Hurst (1960) series expansion:

$$S_{l,n}^* = \sum_i a_{2i+1} (\lambda_{l,n}^*) R^{*2i+L+1}$$

where  $a_1$  has an arbitrary value determined by normal-

isation;  $a_3$  is given by:

$$a_3 = \frac{8\pi^2}{\Lambda^{*2}} \left[ \frac{-\lambda_{l,n}^* a_1}{(l+3)(l+2) - l(l+1)} \right]$$

and the other coefficients by the recursion relations

$$a_{2m+1} = \frac{8\pi^2}{\Lambda^{*2}} \left[ \frac{\sum_{j=1}^{m-1} C_{2m-2j}^* a_{2j-1} - \lambda_{l,n}^* a_{2m-1}}{(l+2m+1)(l+2m) - l(l+1)} \right]$$

( $m=2,3,4,\dots$ )

where  $C_{2k}^*$  ( $k=1,2,3,\dots$ ) are the coefficients in the series expansion of  $\overline{w^*(R^*)}$ :

$$\overline{w^*(R^*)} = \sum_k C_{2k}^* R^{*2k}$$

Using the initial values of  $Y_1, Y_2, Y_3, Y_4$  calculated in this manner for  $\lambda_{1,n}^* = (\lambda_{1,n}^*)_0$  the equations (A.2.3), (A.2.4), (A.2.6) and (A.2.7) are integrable step by step from  $R^*=R_0^*$  to  $R^*=R_c^*$ . By correcting the eigenvalue by the amount  $\delta_{1,n}^*$  given by (A.2.5) and repeating the procedure,  $\lambda_{1,n}^*$  can be calculated to any desired accuracy.

Appendix 3The Numerical Characterisation of an n Parameter  
Potential Function from Zero Point Solid State Data

Let the n parameters appearing in the potential function be  $P_j$  ( $j=1,2,\dots,n$ ) and the n appropriate zero point equations be:

$$F_i(P_1, \dots, P_n) = 0 \quad (i=1, \dots, \mu) \quad (\text{A.3.1})$$

Taking a first approximation to the solution of these equations to be  $P_{j0}$  ( $j=1,\dots,n$ ) and a better solution to be  $(P_{j0} + \delta P_j)$  ( $j=1,\dots,n$ ) we write:

$$F_i(P_{10} + \delta P_{10}, \dots, P_{n0} + \delta P_{n0}) = 0 \quad (i=1, \dots, \mu) \quad (\text{A.3.2})$$

Expanding the equations (A.3.2) as Taylor series and truncating after terms linear in  $\delta P_j$  ( $j=1,\dots,n$ ), we obtain:

$$F_i(P_{10}, \dots, P_{n0}) + \sum_{j=1}^n P_j (\partial F_i / \partial P_j)_0 = 0 \quad (i=1, \dots, \mu) \quad (\text{A.3.3})$$

which rewritten in terms of difference quotients become:

$$F_i(P_{10}, \dots, P_{n0}) + \sum_{j=1}^n P_j (\Delta F_i / \Delta P_j)_0 = 0 \quad (i=1, \dots, \mu) \quad (\text{A.3.4})$$

where

$$\left( \frac{\Delta F_i}{\Delta P_j} \right)_0 = \frac{F_i(P_{10}, \dots, P_{j0} + \Delta P_{j0}, \dots, P_{n0}) - F_i(P_{10}, \dots, P_{j0}, \dots, P_{n0})}{\Delta P_{j0}}$$

and  $\Delta P_{j0}$  is chosen to be some small increment in  $P_{j0}$ , e.g.  $\Delta P_{j0} = 0.01 P_{j0}$ .

Calculation of  $F_i(P_{10}, \dots, P_{n0})$  ( $i=1, \dots, n$ ) and  $(\Delta F_i / \Delta P_j)_0$  ( $i=1, \dots, n; j=1, \dots, n$ ) allows the equations (A.3.4) to be solved for  $\delta P_j$  ( $j=1, \dots, n$ ). Addition of  $\delta P_j$  ( $j=1, \dots, n$ ) to the first approximation  $P_{j0}$  ( $j=1, \dots, n$ ) then gives a better approximation. Continued application of this procedure gives the parameters to any specified degree of accuracy.

Appendix 4Results of Pairwise Additive EXP-6 and LJ 12:6 Cell Model Calculations for Solid Neon, Argon, Krypton and Xenon.

In the following tables  $T$ ,  $a_0$ ,  $\chi_T$ ,  $C_v$ ,  $C_p$ ,  $S$ ,  $p$  and  $V/V(0)$  stand for temperature, lattice constant, isothermal compressibility, volume expansivity, isochoric specific heat, isobaric specific heat, entropy, pressure and molar volume at a specified temperature, respectively. In all cases,  $T$  is expressed in  $^{\circ}\text{K}$ ,  $a_0$  in  $\text{\AA}$ ,  $\chi_T$  in  $\text{cm}^2 \times 10^{-11} \text{ dyne}^{-1}$  and in  $^{\circ}\text{K}^{-1} \times 10^{-4}$ .  $C_v$ ,  $C_p$  and  $S$  are expressed in  $\text{J mole}^{-1} \text{ }^{\circ}\text{K}^{-1}$  for solid neon and solid argon and in  $\text{cal mole}^{-1} \text{ }^{\circ}\text{K}^{-1}$  for solid krypton and solid xenon.  $p$  is expressed in  $\text{kg cm}^{-2}$  for solid neon, solid argon and solid krypton and in  $\text{kbar}$  for solid xenon.

Solid neon

- (i) Zero pressure EXP-6 values of  $a_0$ ,  $\chi_T$ ,  $\beta$ ,  $C_v$ ,  $C_p$  and  $S$  as functions of  $T$ .

$T$	$a_0$	$\chi_T$	$\beta$	$C_v$	$C_p$	$S$
0	4.4637	9.00	0	0	0	0
8	4.4641	9.06	2.39	1.18	1.18	0.20
12	4.4679	9.51	11.42	5.37	5.60	1.43
16	4.4782	10.51	23.32	10.01	11.12	3.79
20	4.4960	12.21	36.10	13.55	16.47	6.86
23.5	4.5182	14.49	48.54	15.66	20.96	9.86

- (ii) EXP-6 values of  $V/V(0)$  as a function of  $p$  at  $4^{\circ}\text{K}$ .

$p$	2043	4000	6000	8000	10000	12000	16000	20000
$V/V(0)$	0.894	0.843	0.807	0.780	0.759	0.741	0.712	0.690



(iii) Zero pressure LJ 12:6 values of  $a_0$ ,  $\chi_T$ ,  $\beta$ ,  $C_v$ ,  $C_p$  and  $S$  as functions of  $T$ .

$T$	$a_0$	$\chi_T$	$\beta$	$C_v$	$C_p$	$S$
0	4.4637	10.32	0	0	0	0
8	4.4642	10.42	3.48	1.60	1.61	0.29
12	4.4694	11.02	14.55	6.36	6.67	1.83
16	4.4820	12.28	27.91	11.06	12.44	4.54
20	4.5029	14.34	41.64	14.42	17.75	7.89
23.5	4.5281	17.04	54.70	16.33	22.10	11.10

(iv) LJ 12:6 values of  $V/V(0)$  as a function of  $p$  at  $4^\circ\text{K}$ .

$p$	2043	4000	6000	8000	10000	12000	16000	20000
$V/V(0)$	0.882	0.828	0.790	0.762	0.740	0.722	0.693	0.670

#### Solid argon

(i) Zero pressure EXP-6 values of  $a_0$ ,  $\chi_T$ ,  $\beta$ ,  $C_v$ ,  $C_p$  and  $S$  as functions of  $T$ .

$T$	$a_0$	$\chi_T$	$\beta$	$C_v$	$C_p$	$S$
0	5.3111	3.75	0	0	0	0
10	5.3113	3.76	0.76	1.63	1.63	0.30
20	5.3167	3.92	5.41	11.13	11.47	4.39
30	5.3296	4.24	8.85	17.01	18.28	10.47
40	5.3473	4.65	11.11	19.72	22.16	16.30
50	5.3689	5.17	12.95	20.98	24.75	21.54
59.88	5.3934	5.82	14.71	21.54	26.79	26.19
70	5.4220	6.68	16.68	21.74	28.74	30.51
83	5.4650	8.22	19.86	21.69	31.48	35.64

(ii) EXP-6 values of  $V/V(0)$  as a function of  $p$  at  $77^\circ\text{K}$ .

$p$	2043	6000	8000	12000	16000	19000
$V/V(0)$	0.909	0.830	0.804	0.766	0.738	0.721

(iii) Zero pressure LJ 12:6 values of  $a_0$ ,  $\gamma_T$ ,  $\beta$ ,  $c_v$ ,  $c_p$  and  $S$  as functions of  $T$ .

$T$	$a_0$	$\gamma_T$	$\beta$	$c_v$	$c_p$	$S$
0	5.3111	3.81	0	0	0	0
10	5.3113	3.82	0.83	1.68	1.68	0.31
20	5.3171	4.00	5.83	11.23	11.62	4.47
30	5.3310	4.35	9.50	17.03	18.45	10.61
40	5.3502	4.81	11.93	19.65	22.38	16.50
50	5.3732	5.39	13.90	20.83	25.02	21.80
60	5.3998	6.12	15.81	21.33	27.15	26.55
70	5.4304	7.07	17.94	21.47	29.15	30.88
83	5.4765	8.79	21.36	21.34	32.00	36.08

(iv) LJ 12:6 values of  $V/V(0)$  as a function of  $p$  at  $77^\circ\text{K}$ .

$p$	2043	6000	8000	12000	16000	19000
$V/V(0)$	0.906	0.827	0.802	0.765	0.738	0.722

Solid krypton

(i) Zero pressure EXP-6 values of  $a_0$ ,  $\chi_T$ ,  $\beta$ ,  $C_p$ ,  $C_v$  and  $S$  as functions of  $T$ .

T	$a_0$	$\chi_T$	$\beta$	$C_v$	$C_p$	S
0	5.6459	2.91	0	0	0	0
10	5.6463	2.92	1.21	0.913	0.916	0.21
20	5.6522	3.04	4.81	3.498	3.597	1.74
40	5.6770	3.44	7.78	5.089	5.551	4.99
60	5.7096	3.99	9.32	5.381	6.255	7.39
80	5.7480	4.75	10.85	5.410	6.765	9.26
100	5.7932	5.82	12.75	5.353	7.308	10.83
11578	5.8352	7.06	14.81	5.275	7.846	11.94

(ii) EXP-6 values of  $V/V(0)$  as a function of  $p$  at  $77^\circ\text{K}$

p	200	400	600	1000	2000	3000	4000
$V/V(0)$	0.991	0.983	0.976	0.963	0.935	0.914	0.895

(iii) Zero pressure LJ 12:6 values of  $a_0$ ,  $\chi_T$ ,  $\beta$ ,  $C_p$ ,  $C_v$  and  $S$  as functions of  $T$ .

T	$a_0$	$\chi_T$	$\beta$	$C_v$	$C_p$	S
0	5.6459	3.11	0	0	0	0
10	5.6464	3.12	1.43	0.998	1.002	0.24
20	5.6531	3.26	5.34	3.592	3.705	1.85
40	5.6803	3.72	8.48	5.104	5.613	5.15
60	5.7157	4.35	10.12	5.361	6.310	7.57
80	5.7573	5.20	11.74	5.370	6.824	9.46
100	5.8063	6.42	13.76	5.296	7.375	11.04
11578	5.8518	7.81	15.93	5.208	7.918	12.16

(iv) LJ 12:6 values of  $V/V(0)$  as a function of  $p$  at  $77^\circ\text{K}$

$p$	200	400	600	1000	2000	3000	4000
$V/V(0)$	0.991	0.982	0.974	0.960	0.931	0.908	0.889

Solid xenon

(i) Zero pressure EXP-6 values of  $a_0$ ,  $\chi_T$ ,  $\beta$ ,  $c_v$ ,  $c_p$  and  $S$  as functions of  $T$ .

$T$	$a_0$	$\chi_T$	$\beta$	$c_v$	$c_p$	$S$
0	6.1310	2.89	0	0	0	0
10	6.1316	2.91	1.42	1.504	1.510	0.42
20	6.1374	3.00	3.95	4.073	4.160	2.42
40	6.1576	3.25	5.55	5.330	5.648	5.89
80	6.2091	3.95	6.85	5.589	6.408	10.08
115	6.2630	4.85	8.05	5.529	6.888	12.49
150	6.3280	6.23	9.74	5.412	7.495	14.39
160	6.3492	6.77	10.38	5.371	7.715	14.88

(ii) EXP-6 values of  $V/V(0)$  as a function of  $p$  at  $150^\circ\text{K}$

$p$	2	5	8	14	20
$V/V(0)$	0.918	0.855	0.815	0.762	0.726

(iii) Zero pressure LJ 12:6 values of  $a_0$ ,  $\chi_T$ ,  $\beta$ ,  $C_v$ ,  $C_p$  and  $S$  as functions of  $T$ .

$T$	$a_0$	$\chi_T$	$\beta$	$C_v$	$C_p$	$S$
0	6.1310	2.75	0	0	0	0
10	6.1316	2.76	1.41	1.417	1.423	0.39
20	6.1375	2.85	4.08	3.996	4.093	2.32
40	6.1585	3.13	5.82	5.282	5.647	5.77
80	6.2129	3.87	7.25	5.526	6.463	9.98
115	6.2703	4.84	8.57	5.442	6.991	12.41
150	6.3397	6.36	10.44	5.300	7.658	14.32
160	6.3625	6.96	11.15	5.252	7.901	14.81

(iv) LJ 12:6 values of  $V/V(0)$  as a function of  $p$  at  $150^\circ\text{K}$

$p$	2	5	8	14	20
$V/V(0)$	0.919	0.857	0.819	0.769	0.735

Appendix 5Experimental Data for Solid Neon, Argon, Krypton and Xenon

The symbols used in this appendix represent the same properties as they do in Appendix 4. The properties are expressed in the same units as are the corresponding ones in Appendix 4.

Solid neon

- (i) Zero pressure values of  $a_0$ ,  $\chi_T$ ,  $\beta$ ,  $C_v$ ,  $C_p$  and  $S$  as functions of  $T$ .

$T$	$a_0$ <sup>a)</sup>	$\chi_T$ <sup>a)</sup>	$\beta$ <sup>a)</sup>	$C_v$ <sup>b)</sup>	$C_p$ <sup>c)</sup>	$S$ <sup>d)</sup>
4	4.4637	9.0±0.2	0.60±0.05	0.347	0.347	0.133
6	4.4642	9.1±0.4	2.46±0.05	1.350	1.355	0.439
8	4.4654	9.2±0.6	5.73±0.06	3.10	3.14	1.05
10	4.4677	9.4±0.6	10.17±0.07	5.36	5.51	2.00
12	4.4815	9.6±0.8	15.39±0.08	7.89	8.29	3.25
14	4.4769	10.0±1.0	21.09±0.10	10.10	10.95	4.73
16	4.4841	10.7±1.1	27.00±0.10	12.0	13.5	6.36
18	4.4930	12.4±1.2	33.12±0.12	13.9	16.1	8.10
20	4.5040	16.2±1.5	40.11±0.14	15.9	18.9	9.94
23.5	4.5287	-	51.54±0.14	-	-	-

a) Data of Batchelder, Losee and Simmons (1967)

b) Calculated by Batchelder, Losee and Simmons (1967) from the relation  $C_p = C_v + \beta^2 TV / \chi_T$ . Error due to the uncertainties in  $\beta$  and  $\chi_T$  rises to ±0.7 J mole<sup>-1</sup> °K<sup>-1</sup> at 20°K.

c) Smoothed data of Fenichel and Serin (1966) and Fagerstroem and Hallet (1965) as given by Batchelder, Losee and Simmons (1967). Fenichel and Serin estimate their error in  $C_p$  to be ±2%.

d) Calculated from the relation  $S = \int_0^T (C_p / T) dT$ .

(ii) Values of  $V/V(0)$  as a function of  $p$  at  $4^\circ\text{K}$ ,  
(Stewart 1956).

$p$	$V/V(0)$	$p$	$V/V(0)$
1000	$0.927 \pm 0.004$	8000	$0.770 \pm 0.012$
2043	$0.882 \pm 0.006$	10000	$0.747 \pm 0.013$
3000	$0.858 \pm 0.007$	12000	$0.728 \pm 0.014$
4000	$0.832 \pm 0.008$	16000	$0.696 \pm 0.015$
60000	$0.797 \pm 0.010$	20000	$0.669 \pm 0.017$

### Solid argon

(i) Zero pressure values of  $a_0$ ,  $\chi_T$ ,  $\beta$ ,  $C_v$ ,  $C_p$  and  $S$  as  
functions of  $T$ .

$T$	$a_0$ <sup>a)</sup>	$\chi_T$ <sup>b)</sup>	$\beta$ <sup>a)</sup>	$C_v$ <sup>c)</sup>	$C_p$ <sup>d)</sup>	$S$ <sup>e)</sup>
10	5.3117	3.77	1.38	3.294	3.305	1.096
15	5.3138	3.83	3.48	8.01	8.12	3.320
20	5.3179	3.93	5.55	12.16	12.51	6.278
25	5.3235	4.05	7.14	15.30	16.02	9.460
30	5.3305	4.21	8.54	17.49	18.67	12.62
35	5.3386	4.38	9.69	19.13	10.85	15.67
40	5.3477	4.59	10.68	20.25	22.54	18.56
45	5.3576	4.83	11.64	20.95	23.87	21.30
50	5.3684	5.10	12.54	21.54	25.13	23.87
55	5.3801	5.42	13.49	21.94	26.27	26.31
60	5.3926	5.81	14.50	22.19	17.31	28.63
65	5.4062	6.27	15.63	22.34	28.36	30.84
70	5.4209	6.82	16.99	22.60	29.71	32.98
75	5.4369	7.46	18.55	22.94	31.33	35.05
80	5.4546	8.24	20.31	23.34	33.17	37.09
83	5.4660	8.76	21.47	24.02	34.84	38.31

- a) Data of Peterson, Batchelder and Simmons (1966).
- b) Data quoted by Peterson, Batchelder and Simmons (1966). Error rises to  $\pm 10\%$  at the higher temperatures.
- c) Calculated from the relation  $C_p = C_v + \beta^2 TV / \chi_T$  by Peterson, Batchelder and Simmons (1966). Error due to the uncertainty in  $\chi_T$  rises to  $\pm 1.1 \text{ J mole}^{-1} \text{ } ^\circ\text{K}^{-1}$  at  $83^\circ\text{K}$ .
- d) Data of Flubacher, Leadbetter and Morrison (1961) as quoted by Peterson, Batchelder and Simmons (1967). Flubacher, Leadbetter and Morrison estimate their error in  $C_p$  to be  $\pm 2\%$  at the lowest temperatures, decreasing to  $\pm 0.2\%$  for  $T > 20^\circ\text{K}$  but increasing to  $\pm 0.5\%$  at the highest temperatures.
- e) Calculated from the relation  $S = \int_0^T (C_p/T) dT$ .

(ii) Values of  $V/V(0)$  as a function of  $p$  at  $77^\circ\text{K}$  (Stewart 1956).

$p$	$V/V(0)$	$p$	$V/V(0)$
1000	$0.939 \pm 0.003$	8000	$0.795 \pm 0.010$
2043	$0.901 \pm 0.005$	12000	$0.758 \pm 0.012$
4000	$0.853 \pm 0.007$	16000	$0.730 \pm 0.013$
6000	$0.820 \pm 0.009$	20000	$0.714 \pm 0.014$



Solid krypton

(i) Zero pressure values of  $a_0$ ,  $\chi_T$ ,  $\beta$ ,  $C_p$  and  $S$  as functions of  $T$ .

$T$	$a_0$	$\chi_T$	$\beta$ <sup>b)</sup>	$C_p$ <sup>e)</sup>	$S$ <sup>f)</sup>
4.25	5.6459 <sup>a)</sup>	2.91	-	-	-
5	-	-	-	0.3721	0.07
10	-	-	-	1.418	0.54
10.3	5.6470 <sup>a)</sup>	2.90±0.15 <sup>a)</sup>	-	-	-
15	-	-	-	2.798	1.38
17.5	-	2.84±0.42 <sup>a)</sup>	-	-	-
20	5.655 <sup>b)</sup>	-	4.8	3.817	2.32
25	-	2.77±0.40 <sup>a)</sup>	-	4.516	3.25
30	-	-	-	4.990	4.11
31.7	-	3.17±0.27 <sup>a)</sup>	-	-	-
39.2	-	3.37±0.25 <sup>a)</sup>	-	-	-
40	5.678 <sup>b)</sup>	-	7.7	5.612	5.65
45.9	5.6860 <sup>a)</sup>	3.47±0.24 <sup>a)</sup>	-	-	-
50	-	-	-	5.978	6.94
53.3	-	3.66±0.31 <sup>a)</sup>	-	-	-
58	5.710 <sup>c)</sup>	-	-	-	-
60	5.7111 <sup>b)</sup>	3.79±0.46 <sup>a)</sup>	9.7	6.296	8.06
67.1	-	4.25±0.33 <sup>a)</sup>	-	-	-
68	5.734 <sup>c)</sup>	-	-	-	-
70	-	-	-	6.569	9.05
74.0	5.7345 <sup>a)</sup>	4.46±0.25 <sup>a)</sup>	-	-	-
77.3	5.7409 <sup>a)</sup>	4.82±0.15 <sup>a)</sup>	-	-	-
80	5.751 <sup>b)</sup>	-	11.0	6.824	9.95
90	5.773 <sup>b)</sup>	-	11.2	7.146	10.77
90.8	-	5.52±0.48	-	-	-
100	-	-	-	7.585	11.55
110	-	-	-	8.139	12.29
115	5.798 <sup>d)</sup>	-	-	8.552	12.66

- a) Data of Urvas, Losee and Simmons (1967).  
 b) Data of Figgins and Smith (1960).  
 c) Data of Cheeseaman and Soane (1957).  
 d) Data of Clusius and Weigand (1960).  
 e) Data of Beaumont, Chihara and Morrison (1961).  
 f) Calculated from the relation  $S = \int_0^T (C_p/T) dT$ .  
 (ii) Values of  $V/V(0)$  as a function of  $p$  at  $77^\circ\text{K}$  (Stewart 1955)
- | $p$  | $V/V(0)$          | $p$  | $V/V(0)$          |
|------|-------------------|------|-------------------|
| 200  | $0.990 \pm 0.001$ | 2000 | $0.928 \pm 0.004$ |
| 400  | $0.981 \pm 0.001$ | 3000 | $0.905 \pm 0.005$ |
| 600  | $0.972 \pm 0.001$ | 4000 | $0.887 \pm 0.006$ |
| 1000 | $0.958 \pm 0.002$ |      |                   |

### Solid xenon

- (i) Zero pressure values of  $a_0$ ,  $\chi_T$ ,  $\beta$ ,  $C_p$  and  $S$  as functions of  $T$ .

$T$	$a_0$	$\chi_T$	$\beta$	$C_p$	$S^f$
10	$6.133^a)$	-	$1.8^d)$	$1.87^d)$	-
20	$6.136^a)$ $6.137^b)$ $6.137 \pm 0.004^c)$	$2.85 \pm 0.20^c)$	$2.8^a)$ $3.0^b)$	$4.22^d)$	2.88
30	$6.145^a)$	-	$4.4^a)$	-	-
40	$6.154^a)$ $6.157^b)$	-	$5.5^a)$ $5.8^b)$	-	-
50	$6.166^a)$ $6.167 \pm 0.006^c)$	$3.10 \pm 0.20^c)$	$6.3^a)$	$6.00^e)$	7.60
60	$6.180^a)$ $6.183^b)$	-	$6.9^a)$ $6.5^b)$	-	-
70	$6.195^a)$	-	$7.5^a)$	-	-
75	$6.202^a)$ $6.203 \pm 0.007^c)$	$3.75 \pm 0.30^c)$	$7.7^a)$	$6.39^e)$	10.11

Solid xenon (Cont.)

T	$a_0$	$\chi_T$	$\beta$	$c_p$	$S^f)$
80	6.210 <sup>b)</sup>	-	6.7 <sup>b)</sup>	-	-
100	6.238 <sup>b)</sup>	-	6.8 <sup>b)</sup>	6.74 <sup>e)</sup>	12.00
	6.243±0.009 <sup>c)</sup>		7.0±0.7 <sup>c)</sup>		
120	6.268 <sup>b)</sup>	-	6.8 <sup>b)</sup>	-	-
125	6.287±0.006 <sup>c)</sup>	5.25±0.50 <sup>c)</sup>	8.4±0.8 <sup>c)</sup>	7.30 <sup>e)</sup>	13.57
150	6.331±0.007 <sup>c)</sup>	6.55±0.90 <sup>c)</sup>	10.3±1.0 <sup>c)</sup>	8.02	14.97

- a) Data of Sears and Klug (1962).  
 b) Data of Eatwell and Smith (1961).  
 c) Data of Packard and Swenson (1963).  
 d) Data of Fenichel and Serin (1966).  
 e) Smoothed data of Clusius and Riccoboni (1938) as quoted by Packard and Swenson (1963).  
 f) Calculated from the relation  $S = \int_0^T (C_p/T) dT$  by Packard and Swenson (1963) using the  $C_p$  data of Clusius and Riccoboni (1938).

(ii) Values of  $V/V(0)$  as a function of  $p$  at 150°K (Packard and Swenson 1963).

$p$	$V/V(0)$	$p$	$V/V(0)$
1	0.952	12	0.775
2	0.919	14	0.760
4	0.873	16	0.747
6	0.840	18	0.736
8	0.814	20	0.726
10	0.794		

The error in  $V/V(0)$  is ±0.005 at all pressures.

Appendix 6Results of EXP-6 Cell Model Calculations with Triplet  
Dispersion Interactions Included in the Static Lattice  
for Solid Neon, Argon, Krypton and Xenon

The symbols used in this appendix represent the same properties as they do in Appendix 4. The properties are expressed in the same units as are the corresponding ones in Appendix 4.

Solid neon

(i) Zero pressure values of  $a_0$ ,  $\chi_T$ ,  $\beta$ ,  $C_v$ ,  $C_p$  and  $S$  as functions of  $T$ .

$T$	$a_0$	$\chi_T$	$\beta$	$C_v$	$C_p$	$S$
0	4.4637	9.00	0.	0	0	0
8	4.4640	9.07	2.58	1.25	1.26	0.22
12	4.4682	9.55	12.05	5.56	5.80	1.51
16	4.4790	10.61	24.38	10.21	11.42	3.93
20	4.4975	12.41	37.62	13.70	16.83	7.08
23.5	4.5207	14.85	50.66	15.76	21.41	10.15

(ii) Values of  $V/V(0)$  as a function of  $p$  at  $4^\circ\text{K}$

$p$	2043	4000	6000	8000	10000	12000	16000	20000
$V/V(0)$	0.894	0.843	0.807	0.781	0.759	0.742	0.713	0.691

Solid argon

(i) Zero pressure values of  $a_0$ ,  $\chi_T$ ,  $\beta$ ,  $C_v$ ,  $C_p$  and  $S$  as functions of  $T$ .

$T$	$a_0$	$\chi_T$	$\beta$	$C_v$	$C_p$	$S$
0	5.3111	3.75	0	0	0	0
10	5.3113	3.80	0.93	1.93	1.93	0;36
20	5.3174	3.99	5.93	11.76	12.16	4.84
30	5.3313	4.33	9.43	17.42	18.83	11.17
40	5.3503	4.78	11.75	19.93	22.60	17.15
50	5.3729	5.34	13.66	21.05	25.12	22.48
60	5.3991	6.07	15.54	21.52	27.18	27.24
70	5.4290	7.00	17.66	21.64	29.15	31.58
83	5.4748	8.75	21.19	21.50	32.03	36.78

(ii) Values of  $V/V(0)$  as a function of  $p$  at  $77^\circ\text{K}$ .

$p$	2043	6000	8000	12000	16000	19000
$V/V(0)$	0.906	0.826	0.800	0.762	0.734	0.717

Solid krypton

(i) Zero pressure values of  $a_0$ ,  $\chi_T$ ,  $\beta$ ,  $C_V$ ,  $C_p$  and  $S$  as functions of  $T$ :

T	$a_0$	$\chi_T$	$\beta$	$C_V$	$C_p$	S
0	5.459	2.91	0	0	0	0
10	5.6464	2.93	1.42	1.033	1.037	0.25
20	5.6530	3.06	5.20	3.629	3.744	1.89
40	5.6793	3.50	8.21	5.118	5.626	5.21
60	5.7136	4.10	9.83	5.367	6.317	7.64
80	5.7543	4.93	11.49	5.371	6.840	9.53
100	5.8025	6.14	13.63	5.292	7.419	11.11
11578	5.8476	7.58	15.99	5.198	8.010	12.24

(ii) Values of  $V/V(0)$  as a function of  $p$  at  $77^\circ\text{K}$ .

$p$	200	400	600	1000	2000	3000	4000
$V/V(0)$	0.991	0.983	0.975	0.962	0.934	0.912	0.894

Solid xenon

(i) Zero pressure values of  $a_0$ ,  $\chi_T$ ,  $\beta$ ,  $C_V$ ,  $C_p$  and  $S$  as functions of  $T$ .

T	$a_0$	$\chi_T$	$\beta$	$C_V$	$C_p$	S
0	6.1310	2.90	0	0	0	0
10	6.1318	2.92	1.66	1.691	1.699	0.50
20	6.1381	3.02	4.26	4.210	4.310	2.63
40	6.1595	3.30	5.84	5.360	5.708	6.17
80	6.2137	4.06	7.21	5.563	6.446	10.39
115	6.2707	5.05	8.51	5.477	6.943	12.81
150	6.3397	6.61	10.41	5.338	7.593	14.74
160	6.3624	7.23	11.13	5.292	7.834	15.23

(ii) Values of  $V/V(0)$  as a function of  $p$  at  $150^\circ\text{K}$ .

$p$	2	5	8	14	20
$V/V(0)$	0.916	0.852	0.811	0.758	0.722

Appendix 7The Characterisation of an n Parameter Potential  
Function from Second Virial Data by Least Squares  
Refinement

Let us suppose that the potential function to be characterised contains n adjustable parameters  $P_i$  ( $i=1, \dots, n$ ) and that there are k different experimental values of the second virial coefficient available, where  $k > n$ . If the experimental values of the second virial coefficient are  $B_j^{\text{expt}}$  ( $j=1, \dots, k$ ), then the parameters which give the optimum least squares fit with experiment are those which minimise the quantity:

$$\sum_{j=1}^k (B_j^{\text{expt}} - B_j^{\text{calc}})^2 \quad (\text{A.7.1})$$

where  $B_j^{\text{calc}}$  are the calculated second virial coefficients. Let us assume a first approximation to  $P_i$  ( $i=1, \dots, n$ ) to be  $P_{i0}$  ( $i=1, \dots, n$ ) and that a better fit with experiment is given by  $P_{i0} + \delta P_i$  ( $i=1, \dots, n$ ). On expanding  $B_j^{\text{calc}}$  as a Taylor series in  $\delta P_i$  ( $i=1, \dots, n$ ) and truncating after linear terms, we obtain:

$$B_j^{\text{calc}} \approx B_{j0}^{\text{calc}} + \sum_{i=1}^n \delta P_i \left( \frac{\partial B_j^{\text{calc}}}{\partial P_i} \right)_0 \quad (j=1, \dots, k) \quad (\text{A.7.2})$$



where a zero subscript on a quantity denotes that quantity evaluated for  $P_i = P_{i0}$  ( $i=1, \dots, n$ ). On substituting (A.7.2) into (A.7.1) and minimising with respect to the quantities  $\delta P_i$  ( $i=1, \dots, n$ ) we obtain the so called normal equations, which may be written in matrix notation thus:

$$A = B \delta P \quad (\text{A.7.3})$$

where A is a column vector with elements:

$$a_i = \sum_{m=1}^k (B_m^{\text{expt}} - B_m^{\text{calc}}) \left( \frac{\partial B_m^{\text{calc}}}{\partial P_i} \right)_0 \quad (i=1, \dots, n)$$

B is a symmetric nxn matrix with elements:

$$b_{ij} = \sum_{m=1}^k \left( \frac{\partial B_m^{\text{calc}}}{\partial P_i} \right)_0 \left( \frac{\partial B_m^{\text{calc}}}{\partial P_j} \right)_0 \quad (i=1, \dots, n; j=1, \dots, n)$$

and  $\delta P$  is a column vector with elements  $\delta P_i$  ( $i=1, \dots, n$ ).

Replacing the partial derivatives by difference quotients evaluated by making a small (e.g. 1%) change in the differentiating variable, the set of equations (A.7.3) are straightforwardly solved for  $\delta P_i$  ( $i=1, \dots, n$ ). On adding these quantities to  $P_{i0}$  ( $i=1, \dots, n$ ), we obtain a better set of parameters, which, in turn, may be used to obtain an even better set. The procedure may be cycled until the shifts in the parameters are minimal.

Appendix 8Experimental and EXP-6 Calculated Values of the Second Virial Coefficients of Neon, Argon, Krypton and Xenon

In this appendix T stands for temperature and B(T) for the second virial coefficient at temperature T. T is expressed in °K and B(T) in cm<sup>3</sup> mole<sup>-1</sup>.

Neon

T	B(T) <sup>d)</sup>	B(T) <sup>b)</sup>	B(T) <sup>c)</sup>	B(T) <sup>d)</sup>
123.16	1.233 <sup>e)</sup>	1.265	1.847	1.303
131.94	2.915 <sup>f)</sup>	2.549	3.194	2.687
170.15	6.302 <sup>f)</sup>	6.408	7.237	6.841
173.16	6.750 <sup>e)</sup>	6.629	7.468	7.079
223.16	9.374 <sup>e)</sup>	9.310	10.026	9.958
273.16	10.767 <sup>g)</sup>	10.860	11.869	11.617
298.16	11.389 <sup>g)</sup>	11.400	12.425	12.193
323.16	11.822 <sup>g)</sup>	11.835	12.872	12.656
348.16	12.188 <sup>g)</sup>	12.190	13.234	13.033
373.16	12.481 <sup>g)</sup>	12.483	13.531	13.343
398.16	12.824 <sup>g)</sup>	12.725	13.776	13.599
423.16	13.079 <sup>g)</sup>	12.927	13.979	13.813
473.16	13.426 <sup>h)</sup>	13.241	14.289	14.141
573.16	13.695 <sup>h)</sup>	13.624	14.657	14.536
673.16	13.776 <sup>h)</sup>	13.817	14.829	14.728
773.16	13.736 <sup>h)</sup>	13.903	14.893	14.808
873.16	13.886 <sup>h)</sup>	13.928	14.895	14.822
973.16	13.982 <sup>h)</sup>	13.914	14.859	14.797

a) Experimental values

b) EXP-6 values calculated from the second virial parameters in Table 6 (p.161)

c) EXP-6 values calculated from the "pairwise additive" parameters in Table 2 (p.74)

- d) EXP-6 values calculated from the "triplet" parameters in Table 5 (p.148)
- e) Holborn and Otto (1925)
- f) Kamerlingh Onnes and Crommelin (1915);  
Kamerlingh Onnes, Crommelin and Martinez (1919)
- g) Michels, Wassenaar and Louwerse (1960)
- h) Nicholson and Schneider (1955).

Argon

T	B(T) <sup>a)</sup>	B(T) <sup>b)</sup>	B(T) <sup>c)</sup>	B(T) <sup>d)</sup>
81.948	-272.9 <sup>e)</sup>	-277.7	-239.0	-264.9
87.120	-245.9 <sup>e)</sup>	-245.8	-214.3	-237.3
92.777	-216.9 <sup>e)</sup>	-217.4	-191.8	-212.2
97.653	-194.85 <sup>e)</sup>	-197.0	-175.32	-193.83
102.081	-179.10 <sup>e)</sup>	-181.1	-162.22	-179.31
105.885	-167.82 <sup>e)</sup>	-168.96	-152.15	-168.18
108.073	-161.54 <sup>e)</sup>	-162.58	-146.80	-162.27
115.227	-144.85 <sup>e)</sup>	-144.14	-131.16	-145.06
119.997	-134.25 <sup>e)</sup>	-133.60	-122.10	-135.11
129.556	-114.93 <sup>e)</sup>	-115.72	-106.52	-118.05
133.16	-107.98 <sup>f)</sup>	-109.89	-101.38	-112.45
138.16	-100.88 <sup>f)</sup>	-102.50	-94.82	-105.30
143.16	-94.43 <sup>f)</sup>	-95.81	-88.84	-98.79
144.599	-93.18 <sup>e)</sup>	-94.00	-87.21	-97.02
146.047	-92.08 <sup>e)</sup>	-92.23	-85.62	-95.29
148.16	-88.45 <sup>f)</sup>	-89.72	-83.37	-92.83
150.66	-85.65 <sup>f)</sup>	-86.88	-80.80	-90.04
153.16	-82.97 <sup>f)</sup>	-84.16	-78.34	-87.37
157.411	-80.34 <sup>e)</sup>	-79.80	-74.37	-83.07
163.16	-73.25 <sup>f)</sup>	-74.37	-69.41	-77.69
173.16	-65.21 <sup>f)</sup>	-66.03	-61.74	-69.39
188.16	-54.83 <sup>f)</sup>	-55.61	-52.06	-58.94
190.519	-52.85 <sup>e)</sup>	-54.16	-50.71	-57.48

Argon (Cont.)

T	B(T) <sup>a)</sup>	B(T) <sup>b)</sup>	B(T) <sup>c)</sup>	B(T) <sup>d)</sup>
203.16	-46.52 <sup>f)</sup>	-47.10	-44.08	-50.34
223.16	-37.43 <sup>f)</sup>	-37.92	-35.40	-41.00
248.16	-28.57 <sup>f)</sup>	-28.94	-26.84	-31.80
273.16	-21.27 <sup>g)</sup>	-21.89	-20.08	-24.56
298.16	-15.76 <sup>g)</sup>	-16.24	-14.62	-18.71
323.16	-11.24 <sup>g)</sup>	-11.59	-10.13	43.90
348.16	-7.249 <sup>g)</sup>	-7.721	-6.382	-9.886
373.16	-3.999 <sup>g)</sup>	-4.446	-3.205	-6.485
398.16	-1.181 <sup>g)</sup>	-1.643	-0.484	-3.574
423.16	1.384 <sup>g)</sup>	0.782	1.867	-1.056
473.16	4.99 <sup>h)</sup>	4.76	5.72	3.07
573.16	10.77 <sup>h)</sup>	10.37	11.12	8.87
	9.8 <sup>i)</sup>			
673.16	15.74 <sup>h)</sup>	14.10	14.68	12.70
	13.1 <sup>i)</sup>			
773.16	17.76 <sup>h)</sup>	16.74	17.16	15.37
	16.0 <sup>i)</sup>			
873.16	19.48 <sup>h)</sup>	18.68	18.96	17.32
923.16	18.9 <sup>i)</sup>	19.47	19.68	18.10
1073	19.9 <sup>i)</sup>	21.31	21.13	19.89
1223.16	21.1 <sup>i)</sup>	22.60	22.43	21.13

a) Experimental values

b) EXP-6 values calculated from the second virial parameters in Table 6 (p.161)

c) EXP-6 values calculated from the "pairwise additive" solid state parameters in Table 2 (p.74)

d) EXP-6 values calculated from the "triplet" solid state parameters in Table 5 (p.148)

e) Weir, Wynne Jones, Rowlinson and Saville (1967 - but communicated to the author prior to publication)

- f) Michels, Levelt and de Graaf (1958)  
 g) Michels, Wijker and Wijker (1949)  
 h) Whalley and Schneider (1955)  
 i) Lecocq (1960).

Krypton

T	B(T) <sup>a)</sup>	B(T) <sup>b)</sup>	B(T) <sup>c)</sup>	B(T) <sup>d)</sup>
110.639	-370.5 <sup>e)</sup>	-368.2	-300.3	-341.1
112.417	-354.4 <sup>e)</sup>	-356.3	-291.7	-331.3
115.153	-334.1 <sup>e)</sup>	-339.4	-279.3	-316.9
118.138	-315.9 <sup>e)</sup>	-322.3	-266.8	-302.4
120.243	-307.4 <sup>e)</sup>	-311.2	-258.5	-292.8
127.788	-273.6 <sup>e)</sup>	-276.0	-231.9	-262.3
133.105	-251.44 <sup>e)</sup>	-255.01	-215.69	-243.84
142.810	-220.07 <sup>e)</sup>	-222.83	-190.41	-215.11
155.086	-188.73 <sup>e)</sup>	-190.63	-164.63	-185.85
168.550	-162.88 <sup>e)</sup>	-163.02	-141.76	-160.33
180.752	-142.84 <sup>e)</sup>	-142.96	-124.92	-141.52
200.590	-116.56 <sup>e)</sup>	-117.38	-103.04	-117.19
224.193	-95.46 <sup>e)</sup>	-94.66	-83.20	-95.26
273.16	-62.95 <sup>f)</sup>	-63.13	-55.03	-64.30
	-62.70 <sup>g)</sup>			
298.16	-52.35 <sup>f)</sup>	-51.94	-44.85	-53.16
323.16	-42.77 <sup>f)</sup>	-42.84	-36.51	-44.05
	-42.78 <sup>g)</sup>			
348.16	-35.21 <sup>f)</sup>	-35.32	-29.57	-36.48
373.16	-28.86 <sup>f)</sup>	-28.99	-23.70	-30.10
	-29.28 <sup>g)</sup>			
398.16	-23.47 <sup>f)</sup>	-23.60	-18.68	-24.64
423.16	-18.81 <sup>f)</sup>	-18.96	-14.35	-19.93
	-18.13 <sup>g)</sup>			

Krypton (Cont.)

T	B(T) <sup>a)</sup>	B(T) <sup>b)</sup>	B(T) <sup>c)</sup>	B(T) <sup>d)</sup>
448.16	-14.73 <sup>f)</sup>	-14.92	-10.57	-15.82
473.16	-11.11 <sup>f)</sup> -10.75 <sup>g)</sup>	-11.37	-7.25	-12.22
498.16	-8.402 <sup>f)</sup>	-8.239	-4.313	-9.030
523.16	-5.693 <sup>f)</sup>	-5.451	-1.698	-6.190
548.16	-3.167 <sup>f)</sup>	-2.957	0.644	-3.648
573.16	-1.115 <sup>f)</sup> 0.420 <sup>g)</sup>	-0.712	2.751	-1.360
673.16	7.240 <sup>g)</sup>	6.377	9.395	5.858
773.16	12.70 <sup>g)</sup>	11.40	14.08	10.96
873.16	17.19 <sup>g)</sup>	15.12	17.53	14.71

- a) Experimental values  
 b) EXP-6 values calculated from the second virial parameters in Table 6 (p.161)  
 c) EXP-6 values calculated from the "pairwise additive" solid state parameters in Table 2 (p.74)  
 d) EXP-6 values calculated from the "triplet" solid state parameters in Table 5 (p.148)  
 e) Weir, Wynne Jones, Rowlinson and Saville (1967)  
 f) Beattie, Barriault and Brierly (1952)  
 g) Whalley and Schneider (1955).

Xenon

T	B(T) <sup>a)</sup>	B(T) <sup>b)</sup>	B(T) <sup>c)</sup>	B(T) <sup>d)</sup>
273.16	-154.74 <sup>e)</sup>	-155.82	-149.18	-171.48
298.16	-130.27 <sup>e)</sup>	-131.44	-127.08	-146.72
323.16	-110.98 <sup>e)</sup>	-111.93	-109.15	-126.73
348.16	-95.10 <sup>e)</sup>	-95.97	-94.34	-110.26
373.16	-81.89 <sup>e)</sup>	-82.67	-81.90	-96.47
398.16	-70.62 <sup>e)</sup>	-71.44	-71.31	-84.76

Xenon (Cont.)

T	B(T) <sup>a)</sup>	B(T) <sup>b)</sup>	B(T) <sup>c)</sup>	B(T) <sup>d)</sup>
423.16	-61.02 <sup>e)</sup>	-61.83	-62.20	-74.70
448.20	-52.64 <sup>f)</sup>	-53.50	-54.27	-65.96
473.16	-47.36 <sup>g)</sup>	-46.25	-47.34	-58.33
473.21	-45.37 <sup>f)</sup>	-46.24	-47.33	-58.31
498.23	-39.05 <sup>f)</sup>	-39.84	-41.19	-51.57
523.25	-33.21 <sup>f)</sup>	-34.17	-35.74	-45.57
548.26	-28.02 <sup>f)</sup>	-29.11	-30.87	-40.22
573.16	-25.07 <sup>g)</sup>	-24.59	-26.50	-35.43
573.28	-23.55 <sup>f)</sup>	-24.57	-26.48	-35.41
673.16	-10.78 <sup>g)</sup>	-10.31	-12.66	-20.26
773.16	- 1.34 <sup>g)</sup>	- 0.22	- 2.89	- 9.54
873.16	7.95 <sup>g)</sup>	7.24	4.35	- 1.61
973.16	14.21 <sup>g)</sup>	12.97	9.88	4.47

- a) Experimental values
- b) EXP-6 values calculated from the second virial parameters in Table 6 (p.161)
- c) EXP-6 values calculated from the "pairwise additive" solid state parameters in Table 2 (p.74)
- d) EXP-6 values calculated from the "triplet" solid state parameters in Table 5 (p.148)
- e) Michels, Wassenaar and Louwerse (1954)
- f) Beattie, Barriault and Brierly (1951)
- g) Whalley, Lupien and Schneider (1955)